

**THEORETICAL AND EXPERIMENTAL STUDIES TO DETERMINE
COMPRESSIVE AND TENSILE STRENGTHS OF ROCKS,
USING MODIFIED POINT LOAD TESTING**

Mr. Prachya Tepnarong

**A Thesis Submitted in Partial Fulfillment of the Requirements
for the Degree of Master of Engineering in Geotechnology**

Suranaree University of Technology

Academic Year 2001

ISBN 974-533-055-8

การศึกษาด้านทฤษฎีและปฏิบัติเพื่อหาความต้านแรงกด
และแรงดึงของหินโดยใช้วิธีการทดสอบจุดกดแบบปรับเปลี่ยน

นายปรัชญา เทพณรงค์

วิทยานิพนธ์นี้เป็นส่วนหนึ่งของการศึกษาตามหลักสูตรปริญญาวิศวกรรมศาสตรมหาบัณฑิต

สาขาวิชาเทคโนโลยีธรณี

มหาวิทยาลัยเทคโนโลยีสุรนารี

ปีการศึกษา 2544

ISBN 974-533-055-8

Thesis title

**THEORETICAL AND EXPERIMENTAL STUDIES TO DETERMINE COMPRESSIVE
AND TENSILE STRENGTHS OF ROCKS, USING MODIFIED POINT LOAD TESTING**

Suranaree University of Technology Council has approved this thesis submitted in partial fulfillment of the requirement for a Master's Degree

Thesis Examining Committee


.....

(Assoc. Prof. Kittitep Fuenkajorn, Ph.D)

Chairman and Thesis Advisor


.....

(Dr. Chongpan Chonglakmani)

Member


.....

(Mr. Boonkarn Mangkonkarn)

Member


.....

(Assoc. Prof. Tawit Chitsomboon, Ph.D.)

Vice Rector for Academic Affairs


.....

(Assoc. Prof. Vorapot Khompis, Ph.D.)

Dean of Institute of Engineering

ปรัชญา เทพนรงค์ : การศึกษาด้านทฤษฎีและปฏิบัติเพื่อหาความต้านแรงกดและแรงดึง
ของหิน โดยใช้วิธีการทดสอบจุดกดแบบปรับเปลี่ยน (THEORETICAL AND
EXPERIMENTAL STUDIES TO DETERMINE COMPRESSIVE AND TENSILE
STRENGTHS OF ROCKS, USING MODIFIED POINT LOAD TESTING)

อ. ที่ปรึกษา : รศ.ดร.กิตติเทพ เฟื่องขจร, 150 หน้า. ISBN 974-533-055-8

การทดสอบจุดกดแบบปรับเปลี่ยนถูกพัฒนาในงานวิจัยนี้เพื่อหาค่าของความต้านแรงกดและ
ความต้านแรงดึงของหินที่ปราศจากรอยแตก จุดประสงค์หลักของงานวิจัยคือการพัฒนาการทดสอบ
หินที่มีความรวดเร็ว ราคาถูก น่าเชื่อถือ และสามารถนำมาปฏิบัติในภาคสนามและในห้องปฏิบัติการ
เครื่องมือที่ใช้ในการทดสอบจุดกดแบบปรับเปลี่ยนจะคล้ายคลึงกับการทดสอบจุดกดแบบดั้งเดิม ยก
เว้นแต่ในส่วนของหัวกดที่มีลักษณะตัดเรียบทำให้พื้นที่หน้าตัดเป็นรูปร่างกลมแทนที่จะเป็นรูปครึ่งทรง
กลมตามแบบดั้งเดิม งานวิจัยนี้ได้สร้างแบบจำลองทางคอมพิวเตอร์และการทดสอบในห้องปฏิบัติการ
เพื่อค้นหาสูตรแบบใหม่ที่จะนำมาใช้ในการคำนวณผลของการทดสอบจุดกดแบบปรับเปลี่ยน ผลที่ได้
จากแบบจำลองทางคอมพิวเตอร์ชี้ให้เห็นว่า ความเค้นที่จะทำให้ตัวอย่างหินแตกได้จะมีค่าสูงขึ้นถ้าตัว
อย่างหินมีขนาดความหนาและเส้นผ่าศูนย์กลางเพิ่มมากขึ้น ค่าความเค้นดึงสูงสุดจะเกิดขึ้นใกล้กับหัว
กดอยู่ที่ความลึกประมาณเท่ากับเส้นผ่าศูนย์กลางของหัวกด ข้อสรุปนี้ได้นำมาช่วยในการวิเคราะห์ผลที่
ได้จากการทดสอบในห้องปฏิบัติการ การทดลองในห้องปฏิบัติการประกอบด้วย การทดสอบจุดกดทั้ง
แบบดั้งเดิมและแบบปรับเปลี่ยน และมีการทดสอบเพื่อหาแรงกดสูงสุดและแรงดึงสูงสุดตามวิธีแบบ
มาตรฐาน โดยใช้ตัวอย่างหินอ่อนจากจังหวัดสระบุรีซึ่งจัดเตรียมและทำการทดสอบมากกว่า 500 ตัว
อย่าง ผลการทดสอบแรงกดสูงสุดในแกนเดียวระบุว่าค่าแรงกดสูงสุดที่หินวิบัติได้จะมีค่าลดลงถ้าอัตรา
ส่วนของความยาวต่อเส้นผ่าศูนย์กลางของตัวอย่างหินมีค่ามากขึ้น ซึ่งสรุปได้ว่าค่าที่ได้จากการทดสอบ
จุดกดแบบปรับเปลี่ยนของหินที่บางครั้งจะนำมาสัมพันธ์กับความต้านแรงกดสูงสุดของหิน และค่าที่
ได้จากตัวอย่างหินที่มีความหนาบางครั้งจะมาใช้เป็นดัชนีที่เกี่ยวข้องกับความต้านแรงดึงสูงสุดของหิน
การเปรียบเทียบผลระบุว่า การทดสอบจุดกดแบบปรับเปลี่ยนสามารถคาดคะเนค่าแรงกดสูงสุดของตัว
อย่างหินได้ดีกว่าการทดสอบจุดกดแบบดั้งเดิม ส่วนค่าแรงดึงสูงสุดที่ถูกคาดคะเนโดยการทดสอบจุด
กดแบบปรับเปลี่ยนมีความสอดคล้องกับค่าแรงดึงสูงสุดที่ได้จากการทดสอบแบบบราซิล

สาขาวิชาเทคโนโลยีธรณี

ปีการศึกษา 2544

ลายมือชื่อนักศึกษา.....P. Tepramong.....

ลายมือชื่ออาจารย์ที่ปรึกษา.....K. C. M.....

PRACHYA TEPNARONG : THEORETICAL AND EXPERIMENTAL STUDIES TO DETERMINE COMPRESSIVE AND TENSILE STRENGTHS OF ROCKS, USING MODIFIED POINT LOAD TESTING THESIS ADVISOR : ASSOC.PROF. KITTITEP FUENKAJORN, Ph.D. 150 PP. ISBN 974-533-055-8

COMPRESSIVE STRENGTH / TENSILE STRENGTH / SIZE EFFECT / POINT LOAD / ROCK

A modified point load (MPL) testing technique is proposed to correlate the results with the uniaxial compressive strength (UCS) and tensile strength of intact rock. The primary objective is to develop an inexpensive and reliable rock testing method for use in the field and in the laboratory. The test apparatus is similar to that of the conventional point load (CPL), except that the loading points are cut flat to have a circular cross-sectional area instead of using a half-spherical shape. To derive a new solution, finite element analyses and laboratory experiments have been carried out. The simulation results suggest that the applied stress required to fail the MPL specimen increases logarithmically as the specimen thickness or diameter increases. The maximum tensile stress occurs directly below the loading area with a distance approximately equal to the loading diameter. The MPL tests, CPL tests, UCS tests, and Brazilian tension tests have been performed on Saraburi marble under a variety of sizes and shapes. Over 500 specimens have been prepared and tested. The UCS test results indicate that the strengths decrease with increasing length-to-diameter ratio. The test results can be postulated that the MPL strength can be correlated with the compressive strength when the MPL specimens are relatively thin, and should be an indicator of the tensile strength when the specimens are significantly larger than the diameter of the loading points. Predictive capability of the MPL and CPL techniques has been assessed and compared. Extrapolation of the test results suggests that the MPL results predict the UCS of the rock specimens better than does the CPL testing. The tensile strength predicted by the MPL also agrees reasonably well with the Brazilian tensile strength of the rock.

สาขาวิชาเทคโนโลยีธรณี
ปีการศึกษา 2544

ลายมือชื่อนักศึกษา.....*P. Tepnarong*.....
ลายมือชื่ออาจารย์ที่ปรึกษา.....*K. C. J.*.....

TABLE OF CONTENTS

	PAGE
ABSTRACT (ENGLISH).....	I
ABSTRACT (THAI).....	II
ACKNOWLEDGMENTS.....	III
TABLE OF CONTENTS.....	IV
LIST OF TABLES.....	VII
LIST OF FIGURES.....	IX
LIST OF ABBREVIATIONS.....	XVI
CHAPTER	
I INTRODUCTION.....	1
1.1 Rationale and Background.....	1
1.2 Objectives.....	1
1.3 Proposed Concept.....	2
1.4 Methodology.....	2
1.5 Scope and Limitations of the Study.....	5
1.6 Thesis Contents.....	6
II LITERATURE REVIEW.....	7
III LABORATORY EXPERIMENTS.....	11
3.1 Introduction.....	11
3.2 Sample Collection and Preparation.....	11
3.3 Modified Point Load Tests on Saraburi Marble.....	14
3.3.1 Objective.....	14
3.3.2 Specimen Specification.....	14
3.3.3 Test Procedure.....	22

TABLE OF CONTENTS (Continued)

	PAGE
3.3.4 Results and Analysis.....	22
3.3.5 Discussions.....	29
3.4 Characterization Tests on Saraburi Marble.....	29
3.4.1 Uniaxial Compressive Strength Tests.....	29
3.4.2 Brazilian Tensile Strength Tests.....	39
3.4.3 Triaxial Compressive Strength Tests.....	42
3.4.4 Conventional Point Load Tests.....	47
3.5 Tension Tests on Saraburi Marble.....	54
3.5.1 Specific Objective.....	54
3.5.2 Ring Tension Tests.....	54
3.5.3 Four Point-Bending.....	57
3.6 Verification Tests on Other Rock Types.....	57
3.6.1 Objective.....	57
3.6.2 Uniaxial Compressive Strength Tests.....	57
3.6.3 Brazilian Tensile Strength Tests.....	60
3.6.4 Conventional Point Load Tests.....	60
3.6.5 Modified Point Load Tests.....	60
3.7 Discussions.....	68
IV FINITE ELEMENT ANALYSES.....	68
4.1 Objectives.....	68
4.2 Finite Element Mesh.....	68
4.3 Model Parameters.....	68
4.4 Modeling Results and Discussions.....	87
4.4.1 Effects of Thickness.....	87
4.4.2 Effects of the Poisson's ratio.....	87
4.4.3 Effects of Diameter (Width).....	93

TABLE OF CONTENTS (Continued)

	PAGE
4.4.4 Effects of t/d and D/d on P/σ_2	93
4.4.5 Effects of the Friction on Loading Platens.....	99
V COMPRESSIVE AND TENSILE STRENGTH PREDICTIONS.....	100
5.1 Modified Point Load Predictions.....	100
5.1.1 Compressive Strength Predictions.....	100
5.1.2 Tensile Strength Predictions.....	100
5.2 Conventional Point Load Predictions.....	100
5.3 Comparisons and Verifications.....	101
VI DISCUSSIONS.....	104
VII CONCLUSIONS AND FUTURE RESEARCH NEEDS.....	108
7.1 Conclusions.....	108
7.2 Future research needs and recommendations.....	109
REFERENCES.....	110
APPENDIX	
APPENDIX A. Summary of the Laboratory Experimental Results.....	115
APPENDIX B. Rock Sample designation coding system.....	148
CURRICULUM VITAE.....	150

LIST OF TABLES

TABLE	PAGE
3.1 Results of modified point load tests on circular disks of Saraburi marble.....	23
3.2 Results of modified point load tests on square disks on Saraburi marble.....	24
3.3 Results of uniaxial compressive strength tests to determine size and shape effects of Saraburi marble specimens.....	33
3.4 Results of Brazilian tensile strength tests on Saraburi marble.....	41
3.5 Results of triaxial compressive strength tests on Saraburi marble.....	44
3.6 Results of conventional point load tests on Saraburi marble.....	50
3.7 Results of ring tensile strength tests on Saraburi marble.....	56
3.8 Results of four-point bending tests on Saraburi marble.....	59
3.9 Uniaxial compressive strength test results from different rock types.....	61
3.10 Brazilian tensile strength test results from different rock types.....	61
3.11 Conventional point load test results from different rock types.....	62
3.12 Modified point load test results from different rock types.....	63
4.1 Characteristics of 57 finite element models constructed to study the effects of the specimen diameter and thickness.....	70
4.2 Constants in logarithmic relations between $-P/\sigma_2$ and t/d , computed from finite elements analysis.....	98
4.3 Constants in logarithmic relations between $-P/\sigma_2$ and D/d , computed from finite elements analysis.....	98
5.1 Comparisons of the compressive strength and tensile strength results.....	102
5.2 Comparisons of the tensile strength results of Saraburi marble for different test methods.....	102
6.1 Comparisons of the investment costs between UCS test and MPL test.....	107

LIST OF TABLES (Continued)

TABLE	PAGE
6.2	Comparisons of the operating costs between UCS test and MPL test..... 107
6.3	Comparisons of the estimate unit costs between UCS test and MPL test..... 107
A.1	Summary results of modified point load tests on the circular disk of Saraburi marble..... 116
A.2	Summary results of modified point load tests on the square disk of Saraburi marble..... 120
A.3	Summary results of uniaxial compressive strength tests of Saraburi marble..... 125
A.4	Summary results of Brazilian tensile strength tests on Saraburi marble.....135
A.5	Summary results of triaxial compressive strength tests on Saraburi marble..... 136
A.6	Summary results of conventional point load tests on Saraburi marble..... 137
A.7	Summary results of Ring tensile strength tests on Saraburi marble..... 139
A.8	Summary results of Four point bending tests on Saraburi marble.....140
A.9	Summary verification results of uniaxial compressive strength tests on different rock types.....141
A.10	Summary verification results of Brazilian tensile strength tests on different rock types..... 142
A.11	Summary verification results of conventional point load tests on different rock types.....143
A.12	Summary verification results of modified point load tests on different rock types.....145

LIST OF FIGURES

FIGURE	PAGE
1.1	Research plan and related activities and variables.....3
2.1	Loading system of the conventional point load (CPL) tester.....8
2.2	Standard loading platen shape for the conventional point load testing (ISRM suggested method and ASTM D5731-95).....8
3.1	Laboratory experimental program planned in the research.....12
3.2	Saraburi marble blocks with nominal size of 25 cm x 30 cm x 30 cm are collected from a quarry in Saraburi province.....13
3.3	Laboratory core drilling. The core drilling machine (model SBEL 1150) is used to drill core specimens using diamond impregnated bit with diameters varying from 22.5 to 92.5 cm.....15
3.4	A 54 mm impregnated diamond bit (NX size) is used to drill cores from a block of Saraburi marble.....16
3.5	A core specimen of Saraburi marble is cut to produce appropriate rock specimen for each test by a cutting machine..... 17
3.6	A 92.5 cm diameter core specimen of Saraburi marble is ground to meet the ASTM (D4543-85) specifications.....17
3.7	Some Saraburi marble specimens prepared for testing with various sizes and shapes....18
3.8	Comparison of the conventional and modified loading points. The modified loading points are cut flat to have a curricular cross section area..... 19
3.9	Modified loading points, with diameters varying from 5, 10, 15, 20, 25, to 30 mm.....19
3.10	Test arrangement of circular disk specimen used in the modified point load testing. Point load tester model SBEL PLT-75, capacity of 350 kN, is used to load the rock specimen along its axis. Deformation between the loading points is measured with displacement dial gages.....20

LIST OF FIGURES (Continued)

FIGURE	PAGE
3.11	A square disk specimen is tested by the modified point load using 10 mm diameter loading platen.....21
3.12	The 67.4 mm-diameter Saraburi marble specimens failed by modified point load tests using various sizes of the loading diameter.....25
3.13	The various sizes of Saraburi marble specimens failed by modified point load tests using a 10 mm loading diameter.....25
3.14	Post-tested specimens, the compressive shear failure is usually predominant under the loading point.....26
3.15	Modified point load test results for the circular disk specimens with $D/d = 6.74$27
3.16	Modified point load test results for the square disk specimens with various t/d ratios...28
3.17	Saraburi marble specimens diameters varying from 22.5, 38.5, 54.0, to 67.4 mm. They are prepared for uniaxial compressive strength tests.....31
3.18	Uniaxial compressive strength test on 67.4 mm diameter specimen of Saraburi marble with $L/D = 2.5$. The specimen is loaded axially in compression machine model ELE-ADR2000.....32
3.19	A 67.4 mm diameter specimen of Saraburi marble with $L/D = 2.5$ failed by uniaxial compressive strength test. Arrows indicate the extension fracture.....34
3.20	The extension fractures occurs along core specimen axis by uniaxial compressive strength test. ($D = 67.5$ mm and $L/D = 2.0$).....35
3.21	Specimen of Saraburi marble failed under the shear failure mode by uniaxial compressive strength test. The shear failure plane is about 30 degrees from specimen axis. ($D = 67.5$ mm and $L/D = 2.5$).....36
3.22	Specimen of Saraburi marble failed under the compressive shear failure mode (conical shape) by uniaxial compressive strength test. ($D = 67.5$ mm and $L/D = 1.0$)...37
3.23	Shape effect on uniaxial compressive strength of Saraburi marble. Experimental results and curve fitted using power law.....38

LIST OF FIGURES (Continued)

FIGURE	PAGE
3.24	Saraburi marble specimens with diameters varying from 22.5, 38.5, 54.0, to 67.4 mm with L/D = 2.5 for Brazilian tensile strength tests.....40
3.25	Brazilian test on 67.4 mm diameter specimen of Saraburi marble. The specimen is loaded along the diameter in ELE-ADR2000 compression machine.....40
3.26	The 22.5, 38.5, 54.0, and 67.4 mm diameter specimens of Saraburi marble failed along the loading diameter in the Brazilian tests.....41
3.27	Experimental results and curve fitted of Brazilian test results. Evans' power law, $\sigma_B = A(D)^{-B}$43
3.28	A 54 mm diameter specimen of Saraburi marble with L/D = 2.0 failed by triaxial compressive strength test at confining pressure (σ_3) 20.7 MPa (Sample No. MB-26-12-TR-3).....45
3.29	Mohr's circle representing the triaxial compressive strength test results.....46
3.30	Point load tester model SBEL PLT-75 for the conventional point load tests, with maximum loading capacity of 350 kN.....48
3.31	The conventional point load testing on Saraburi marble specimen with D = 67.4 mm and t = 30.2 mm.....49
3.32	The 67.4 mm diameter specimens of Saraburi marble failed by the conventional point load tests.....51
3.33	Conventional point load test results of the Saraburi marble for D/d = 6.74, using the relationship $I_s = P/t^2$52
3.34	Conventional point load test results of the Saraburi marble for D/d = 6.74, using the relationship $I_s = P/(D.t)$53
3.35	A 92.4 mm external diameter and 30.5 mm internal diameter specimen of Saraburi marble used in the ring tension test.....55
3.36	The Saraburi marble specimens failed by ring tension tests along the loading diameter.....55

LIST OF FIGURES (Continued)

FIGURE	PAGE
3.37	A 100x350x13 mm ³ rectangular beam specimen of Saraburi marble is used in the four-point bending test.....58
3.38	Saraburi marble rectangular beam specimen failed by four-point bending. The specimens failed in the middle of the beam.....58
3.39	Modified point load test results for Saraburi limestone disk specimens with various D/d ratios.....64
3.40	Modified point load test results of Khoa Somphoat limestone irregular lumps for various D/d ratios.....65
3.41	Modified point load test results for Khok Kruat Sandstone disk specimens with various D/d ratios.....66
4.1	Boundary and loading conditions of finite element model used to study the stress distribution within MPL specimen. Due to the presence of two symmetry planes, only one quarter of the specimen needs to be analyzed.....69
4.2	Mesh and boundary conditions used in finite element analysis of modified point load test specimen (Model No. 1). It represents 2.5 mm thick specimen with t/d = 0.5 and D/d = 15.....72
4.3	Mesh and boundary conditions used in finite element analysis of modified point load test specimen (Model No. 2). It represents 5.0 mm thick specimen with t/d = 1 and D/d = 15.....73
4.4	Mesh and boundary conditions used in finite element analysis of modified point load test specimen (Model No. 3). It represents 10 mm thick specimen with t/d = 2 and D/d =15.....74
4.5	Mesh and boundary conditions used in finite element analysis of modified point load test specimen (Model No. 4) It represents 15 mm thick specimen with t/d = 3 and D/d = 15.....75

LIST OF FIGURES (Continued)

FIGURE	PAGE
4.6	Mesh and boundary conditions used in finite element analysis of modified point load test specimen (Model No. 5). It represents 20 mm thick specimen with $t/d = 4$ and $D/d = 15$76
4.7	Mesh and boundary conditions used in finite element analysis of modified point load test specimen (Model No. 6). It represents 30 mm thick specimen with $t/d = 6$ and $D/d = 15$77
4.8	Mesh and boundary conditions used in finite element analysis of modified point load test specimen (Model No. 7). It represents 40 mm thick specimen with $t/d = 8$ and $D/d = 15$78
4.9	Mesh and boundary conditions used in finite element analysis of modified point load test specimen (Model No. 8). It represents 100 mm thick specimen with $t/d = 20$ and $D/d = 15$79
4.10	Mesh and boundary conditions used in finite element analysis of modified point load test specimen (Model No. 9). It represents 5 mm diameter specimen with $t/d = 2.5$ and $D/d = 1$ 80
4.11	Mesh and boundary conditions used in finite element analysis of modified point load test specimen (Model No. 10). It represents 10 mm diameter specimen with $t/d = 2.5$ and $D/d = 2$ 81
4.12	Mesh and boundary conditions used in finite element analysis of modified point load test specimen (Model No. 11). It represents 15 mm diameter specimen with $t/d = 2.5$ and $D/d = 3$ 82
4.13	Mesh and boundary conditions used in finite element analysis of modified point load test specimen (Model No. 12). It represents 25 mm diameter specimen with $t/d = 2.5$ and $D/d = 5$ 83

LIST OF FIGURES (Continued)

FIGURE	PAGE
4.14	Mesh and boundary conditions used in finite element analysis of modified point load test specimen (Model No. 13). It represents 50 mm diameter specimen with $t/d = 2.5$ and $D/d = 10$84
4.15	Mesh and boundary conditions used in finite element analysis of modified point load test specimen (Model No. 14). It represents 75 mm diameter specimen with $t/d = 2.5$ and $D/d = 15$85
4.16	Mesh and boundary conditions used in finite element analysis of modified point load test specimen (Model No. 15) It represents 100 mm diameter specimen with $t/d = 2.5$ and $D/d = 20$86
4.17	Distribution of the maximum principal (σ_1/P) stresses along the loaded axis of MPL specimens obtained form finite elements analysis (Model No. 2 through 8). The t/d varies from 1, 2, 3, 4, 6, 8 to 20 with a constant $D/d = 15$ 88
4.18	Distribution of the minimum principal (σ_2/P) stresses along the loaded axis of MPL specimens obtained form finite elements analysis (Model No. 2-8). The t/d varies from 1, 2, 3, 4, 6, 8 to 20 with a constant $D/d = 15$ 89
4.19	Distribution of the difference of the maximum and minimum principal stresses ($\sigma_1/P - \sigma_2/P$) along the loaded axis of MPL specimens obtained form finite elements analysis (Model No. 2-8). The t/d varies from 1, 2, 3, 4, 6, 8 to 20 with a constant $D/d = 15$ 90
4.20	Distribution of the maximum principal stresses (σ_1/P) or vertical stresses (σ_x/P) along the loaded axis of MPL specimens using Model No. 5 with $D/d = 15$ and $t/d = 4$. The Poisson's ratio varies from 0 to 0.5. The effects of Poisson's ratio have not been obtained from the simulations..... 91

LIST OF FIGURES (Continued)

FIGURE	PAGE
4.21	Distribution of the minimum principal stresses (σ_2/P) or horizontal stresses (σ_y/P) along the loaded axis of MPL specimens using Model No. 5 with $D/d = 15$ and $t/d = 4$. The Poisson's ratio varies from 0 to 0.5. The effects of Poisson's ratio have been obtained from the simulations.....92
4.22	Distribution of the maximum principal stresses (σ_1/P) along the loaded axis of MPL specimens obtained from finite elements analysis (Model No. 9-15). The D/d varies from 1, 2, 3, 5, 10, 15 to 20 with a constant $t/d = 2.5$94
4.23	Distribution of the minimum principal stresses (σ_2) along the loaded axis of MPL specimens obtained from finite elements analysis (Model No. 9-15). The D/d varies from 1, 2, 3, 5, 10, 15 to 20 with a constant $t/d = 2.5$95
4.24	Normalized failure stress as a function of t/d , obtained from 57 models.....96
4.25	Normalized failure stress as a function of D/d , obtained from 57 models.....97
B.1	Rock Sample designation coding system..... 149

LIST OF ABBREVIATIONS

b	=	Width of Rectangular Beam Specimen
c	=	Cohesion
CPL	=	Conventional Point Load
d	=	Diameter of Loading Point
I_s	=	Conventional Point Load Strength Index
K	=	Stress Concentration Factor
l	=	Spacing between the Loading Point
L/D	=	Length-to-Diameter Ratio
MPL	=	Modified Point Load
P	=	Applied Stress (Applied Pressure)
r'	=	Relative Hole Radius (Hole Radius/Disk Radius)
x	=	Horizontal Distance from Loading Point
y	=	Vertical Distance from Loading Point
α	=	Coefficient of the Stress
β	=	Coefficient of the Shape
ϕ	=	Angle of Internal Friction (Shearing Resistance)
ν	=	Poisson's Ratio
σ_1	=	Maximum Principal Stress (Vertical Stress)
σ_2	=	Minimum Principal Stress (Horizontal Stress)
σ_{bending}	=	Four Point Bending Tensile Strength
σ_B	=	Brazilian Tensile Strength
σ_C	=	Uniaxial Compressive Strength (UCS)
σ_n	=	Normal Stress
σ_R	=	Ring Tensile Strength
τ	=	Shear Stress

CHAPTER I

INTRODUCTION

1.1 Rationale and Background

In geological exploration, mechanical rock properties are one of the most important parameters that will be later used in the analysis and design of any engineering structures in rock mass. To obtain these properties, the rock from the site is extracted normally by means of core drilling, and then transported the cores to the laboratory where the mechanical testing can be conducted. Laboratory test machine is normally huge and can not be transported to the site. On-site testing of the rocks may be carried out by other technique, but only on a very limited scale. This method is called point load strength testing. This test however provides unreliable results, and lacks theoretical supports. Its results may imply to other important properties (e.g., compressive and tensile strengths), but only based on an empirical formula, which usually poses a high degree of uncertainty.

To save cost and energy that are consumed by drilling processes, rock core transportation, and laboratory testing, a new method for on-site testing is needed. The researcher proposes to modify the currently used point load testing machine to be able to yield the compressive and tensile strengths of the rock specimens with irregular shapes. The new technique which is thereafter called “modified point load (MPL) testing,” will be backed by solid theoretical ground. The testing machine will also remain small and will be easy to operate on-site. If the new technique can be invented successfully, it may significantly reduce the cost, time and energy that have been consumed by the convention methods.

1.2 Objectives

The objective of the present research is to develop a new testing technique, called modified point load test, to obtain a better indicator of the compressive and tensile strengths of intact rock. The new technique is intended to be easy to operate both in the field (on-site testing) and in the laboratory testing. The related strength calculation will be relied on the engineering

mechanics theories. This new method will improve the level of confidence in the analysis and design. Being capable of operating in the field, it will allow on-site testing, and hence will save energy that is consumed by the old processes of rock drilling, sample preparation, rock core transportation, and testing.

1.3 Proposed Concept

Several researchers have correlated the point load index with the uniaxial compressive strength of the rocks (e.g. Miller, 1965; Reichmuth, 1968; Beiniawski, 1975; Pells, 1975; Jaeger and Cook, 1979; Turk and Dearman, 1986; Kaczynski, 1986 and Chau and Wong, 1996). Brook (1977, 1985, 1993) has also established a relation between the point load strength with the uniaxial compressive strength of intact rocks. It is however recognized here that the tensile failure is the dominant mode of failure for the point load specimen. As a result, the point load strength should be related to the tensile strength of the rock rather than the compressive strength. Strictly speaking, the dominant mode of failure for the point load specimens is governed by the size or the distance the loading points. For small specimens, the failure should be in biaxial or polyaxial compression modes. For a large specimen, the biaxial tension will be predominant mode of failure. Recognizing this phenomena, an attempt is made here to distinguish between the compressive and tensile failures under a wide range of specimen sizes. Theoretical derivation and numerical simulation may be used to assist in describing the stress and strain distribution between the loading points for various specimen sizes. Relationships between the point load index and the compressive and tensile strength may therefore be established. The final goal is that one can conduct point load testing on various specimen sizes, and use the results as an indicator of compressive and tensile strengths of the intact rocks.

1.4 Methodology

This research consists of two main tasks. One is the laboratory experiment. The second is the computer simulation. Their results are correlated and verified. The work plan is illustrated in Figure 1.1. The research activities are divided into six tasks.

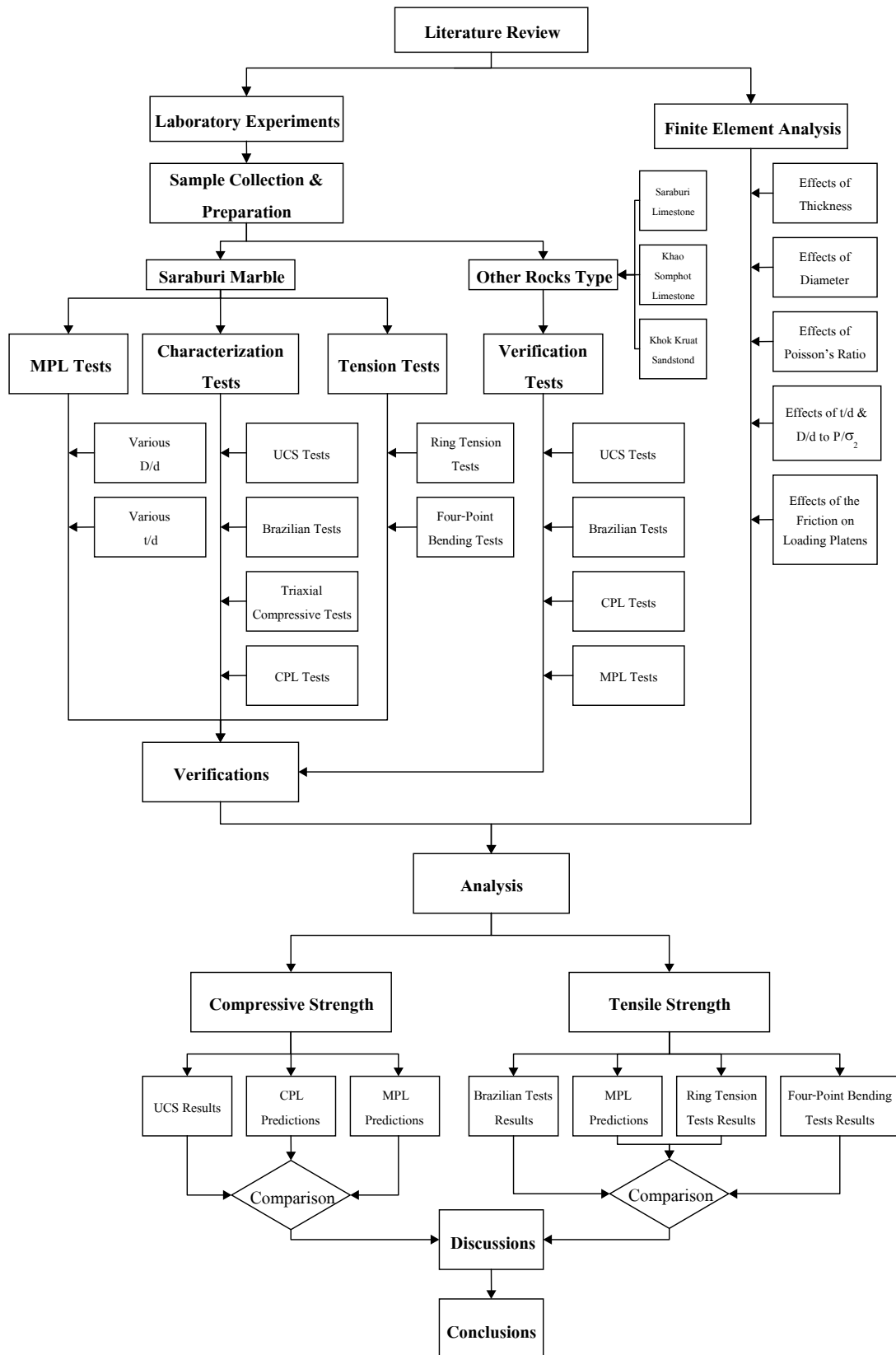


Figure 1.1 Research plan and related activities and variables.

1.4.1 Literature Review

Literature review has been carried out to study the state-of-the-art of point loading technique, including theories, test procedures, results, analysis and applications. The sources of information are from journals, technical reports and conference papers. A summary of the literature review is given in this thesis. Discussions have also been made on the advantages and disadvantages of the testing, the validity of the test results when correlating with the uniaxial compressive strength of the rock, and on the failure mechanism the specimens.

1.4.2 Sample Collection and Preparation

Rock samples have been collected from the site. The selection criteria are that the rock should be homogeneous as much as possible, and that the sample collection should be convenient and repeatable. Saraburi marble has been selected as a prime candidate for testing. Other rock samples used in the verification process include Saraburi limestone, Khao Somphot limestone and Koak Kruat sandstone. Sample preparation has been carried out in the laboratory at the Suranaree University of Technology.

1.4.3 Theoretical Study of the Rock Failure Mechanisms

The theoretical work primarily involves numerical analyses on the MPL specimens under various sizes and shapes. Failure mechanisms of the modified point load test specimens have been analyzed in terms of stress distributions along loaded axis. The finite element code GEO will be used (Fuenkajorn and Serata, 1993 and Serata and Fuenkajorn, 1992) in the simulation. The effects of Poisson's ratio and the effects of friction at the interface between the loading platen and the rock surface. The mathematical solution is derived to correlate the MPL strength results with the uniaxial compressive strength and tensile strength of the rock specimens.

1.4.4 Experimental Work

The laboratory testing is divided into four main groups as shown in the diagram (Figure 1.1). The testing includes a series of 1) the modified point load tests, 2) the characterization tests (conventional point load index tests, the uniaxial compressive strength tests, the Brazilian tensile strength tests and the triaxial compressive strength tests), 3) the tension tests (the ring tensile

strength tests and the four-point bending tests), and 4) the verification tests of the different rock types. The characterization tests yield data basis for use in the comparison. Saraburi marble has been used as main rock specimens to develop the concept and solutions. Other rock types have been used to evaluate the predictive capability of the theory (or equation) developed. These rocks include Saraburi limestone, Khao Somphot limestone and Khok Kruat sandstone. All tests have been conducted on a variety of specimen sizes and shapes. Size and shape effects on the strength results have been assessed.

1.4.5 Analysis

A series of finite element analyses have been performed to investigate the induced stress as a function of the applied load, the sample size and shape, and the size of loading point. The results have been used to interpret the experimental results. The analytical and/or empirical solutions have been developed to correlate the point load results with the uniaxial compressive strength and tensile strength of the rock specimens. The size and shape effects of rock specimens have been determined. The predictability of the methods and discrepancy of the results have been identified.

1.4.6 Thesis Writing and Presentation

All aspects of the theoretical and experimental studies mentioned have been documented and incorporated into the thesis. The thesis also discusses the validity and potential applications of the results.

1.5 Scope and Limitations of the Study

Saraburi marble has been selected as a prime candidate for use in the experiment. In the verification process, the testing has been carried out on Saraburi limestone, Khao Somphot limestone and Khok Kruat sandstone. The analytical and experimental work assumes linearly elastic, homogeneous and isotropic conditions. The largest specimen size is 92 mm in diameter. The effects of loading rate and temperature are not considered, i.e. the loading rate is maintained constant (Costin, 1987). The investigation of failure mode is on macroscopic scale. Microscopic phenomena during failure are not considered (Horii and Nemat-Nasser, 1985; Nimick, 1988).

The finite element analyses is made in axisymmetric and assumed under linearly elastic, homogeneous and isotropic conditions. All tests are performed at room temperatures. The effect of the elevated temperatures is not considered.

1.6 Thesis Contents

This first chapter introduces the thesis, by briefly describing the rationale and background, and identifying the objectives of the work. The third section describes the proposed concept of the new testing technique. The fourth section describes the research methodology. The fifth section identifies the scope and limitations of the study. The sixth section gives a chapter by chapter overview of the contents of this thesis.

The second chapter describes the literature review. A detailed description applications and the limitations of the point load testing are provided. Relevant literatures including those in journals, proceedings, and reports have been reviewed.

Chapter three describes the methods and results of the laboratory experiments. The method and results of finite element analyses are described in Chapter four. Chapter five presents the correlation between the MPL results and the UCS results.

The discussions on the effects of size and shape of specimens, the effects of Poisson's ratio, the effects the friction at loading interface, and on the reliability of MPL are presented in Chapter six.

Chapter seven provides the conclusions and recommendations for future studies.

Comprehensive results of laboratory experiments are given in Appendix A. The coding system used to identify individual rock samples is explained in Appendix B.

CHAPTER II

LITERATURE REVIEW

Conventional point load (CPL) testing is intended as an index test for the strength classification of rock material. It has long been practiced to obtain an indicator of the uniaxial compressive strength (UCS) of intact rocks. The testing equipment (Figure 2.1) is essentially a loading system comprising a loading frame, hydraulic oil pump, ram and loading platens. The geometry of the loading platen is standardized (Figure 2.2) having 60 degrees angle of the cone with 5 mm radius of curvature at the cone tip. It is made of hardened steel. The CPL test method has been widely employed because the test procedure and sample preparation are simple, quick and inexpensive as, compared with such conventional tests as the unconfined compressive strength test. Starting with a simple method to obtain a rock property index, the International Society for Rock Mechanics (ISRM) commissions on testing methods have issued a recommended procedure for the point load testing (ISRM, 1985). The test has also been established as a standard test method by the American Society for Testing and Materials in 1995 (ASTM D5731-95). Although the point load test has been studied extensively (e.g. Broch and Franklin, 1972; Bieniawski, 1974 and 1975; Wijk, 1980; Brook, 1985), the theoretical solutions for the test results remain rare. Several attempts have been made to truly understand the failure mechanisms and the impact of the specimen size on the point load strength results. It is commonly agreed that tensile failure is induced along the axis between loading points (Evans, 1961; Hiramatsu, 1966; Wijk, 1978,1980). The most commonly accepted formula relating the CPL index and the UCS is proposed by Broch and Franklin (1972). The UCS (or σ_c) can be estimated as about 24 times the point load strength index (I_s) of rock specimens with a diameter-to-length ratio of 0.5. The I_s value should also be corrected to a value equivalent to the specimen diameter of 50 mm. The factor of 24 can sometimes lead to an error in the prediction of the UCS. Most previous studied have been done experimentally, but rare theoretical attempt has been made to study the validity of Broch and Franklin formula.

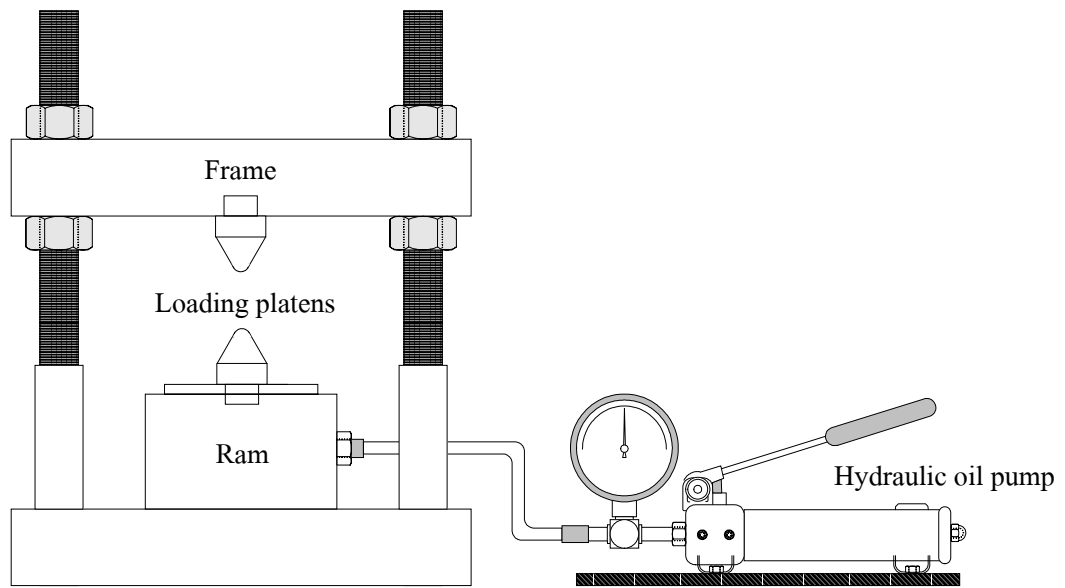


Figure 2.1 Loading system of the conventional point load (CPL) tester.

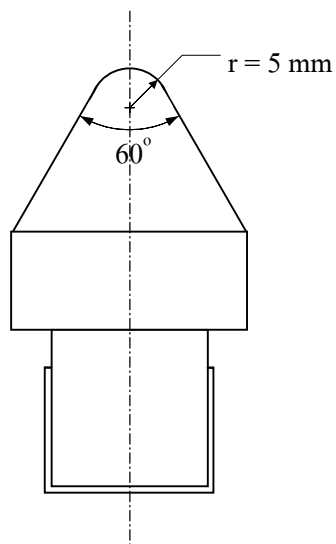


Figure 2.2 Standard loading platen shape for the conventional point load testing (ISRM suggested method and ASTM D5731-95).

The CPL testing has been performed using a variety of sizes and shapes of rock specimen (Wijk, 1980; Forster, 1983; Panek and Fannon, 1992; Chau and Wong, 1996; Butenuth, 1997). This is to determine the most suitable specimen sizes and to correlate the index results among different specimen sizes. These investigators have proposed empirical relations between the I_s and the σ_c to be universally applicable to various rock types. However, some uncertainty of these relations remains.

Panek and Fannon (1992) show the results of the CPL tests, USC tests and Brazilian tension tests that are performed on three hard rocks (iron-formation, metadiabase, and ophitic basalt). The CPL strength is analyzed in term of the size and shape effects. More than 500 irregular lumps were tested in the field. The shape effect exponents for compression have been found to be varied with rock types. The shape effect exponents in CPL tests are constant for the three rocks. Panek and Fannon (1992) recommend that the monitoring of the compressive and tensile strengths should have various sizes and shapes of specimen to obtain the certain properties.

Chau and Wong (1996) study analytically the conversion factor relating between σ_c and I_s . A wide range of the ratios of the uniaxial compressive strength to the point load index has been observed among various rock types. It has been found that the USC of rocks can vary from 6.2 (Nevada test site tuff) to 105 (Flaming Gorge shale) times the I_s , depending on the rock type. The conversion factor relating σ_c to be I_s depends on the compressive and tensile strengths, the Poisson's ratio, and the length and diameter of the specimen. The conversion factor of 24 (Broch and Franklin, 1972) falls within this range but it is by no mean universal.

Butenuth, (1997) discusses the CPL test results from the sandstone, marble and granite that are published by other researchers. The comparison of the results is based on the force at failure and the initial geometrical area of failure rather than upon the ratio of force and area. It is different from those observe elsewhere. The failure force (or load) has been linearly related with the failure area for various specimen sizes. However, this study does not have the relationship between the CPL results or the estimation of the compressive and tensile strengths.

Wei et al. (1999) and Chau and Wei (1999) investigate analytically the stress distribution of a finite solid circular cylinder, which provides an improved analytical solution for the CPL test. The numerical results show that the tensile stress profiles along the load diameter is not uniform.

The tensile stress at the center of the cylinders is not the largest, as previously understood. The maximum tensile stresses are developed near the loading platens. They conclude that the stress distribution depends on the Poisson's ratio, the size of contact surface, and the degree of anisotropy of the specimens. The contact between the conical surface of loading point and the rock surface tends to increase as the load increases for very soft rocks. This causes the tensile strength to decrease. The definition of a singular loading point as used in the principle is therefore not strictly valid. In addition the compressive shear zone under the load platens suggests that the failure should be in biaxial or polyaxial compression modes more rather uniaxial compression (Wiebols et al., 1968). The applicability of the results therefore becomes questionable.

CHAPTER III

LABORATORY EXPERIMENTS

3.1 Introduction

The primary objectives of the laboratory experiments are to modify the current point load testing technique, to determine basic mechanical rock properties, and to verify the proposed method. The laboratory test program is divided into four main groups; 1) modified point load (MPL) tests on Saraburi marble, 2) characterization tests on Saraburi marble, 3) tension tests on Saraburi marble, and 4) verification tests on different rock types. These tasks are shown in Figure 3.1. The results from the group 1) through 3) are used to develop the new theory and the appropriate procedure for the MPL testing. In group 4), the results from the additional tests on different rock types are used in the verification of the proposed method.

3.2 Sample Collection and Preparation

Rock samples have been collected from the field site where they occur. The selection criteria are that the rock should be homogeneous as much as possible, and that the sample collection should be convenient and repeatable. Under these criteria Saraburi marble has been selected as a prime candidate for testing (Figure 3.2).

Saraburi marble was collected from a quarry in Saraburi province. The rock exposes along the edge of the Korat Plateau (DMR, 1983). It is classified as the Saraburi Group. It is a Middle to Earlier Permian age. This rock is medium-to-coarse grained, composed mainly of calcite. The grained size ranges between 3 and 5 mm. Saraburi marble has a white with impure light to medium gray bands.

Other rock types used in the verification tests include Saraburi limestone, Khao Somphot limestone and Khok Kruat sandstone.

Gray to bluish gray bedded to massive Saraburi limestone is taken from the Khum-Ngern Khum-Tong quarry, Pakchong district, Nakhon Ratchasima province. Most of the limestone has fine to medium grained texture. It belongs to the Permian Saraburi Group.

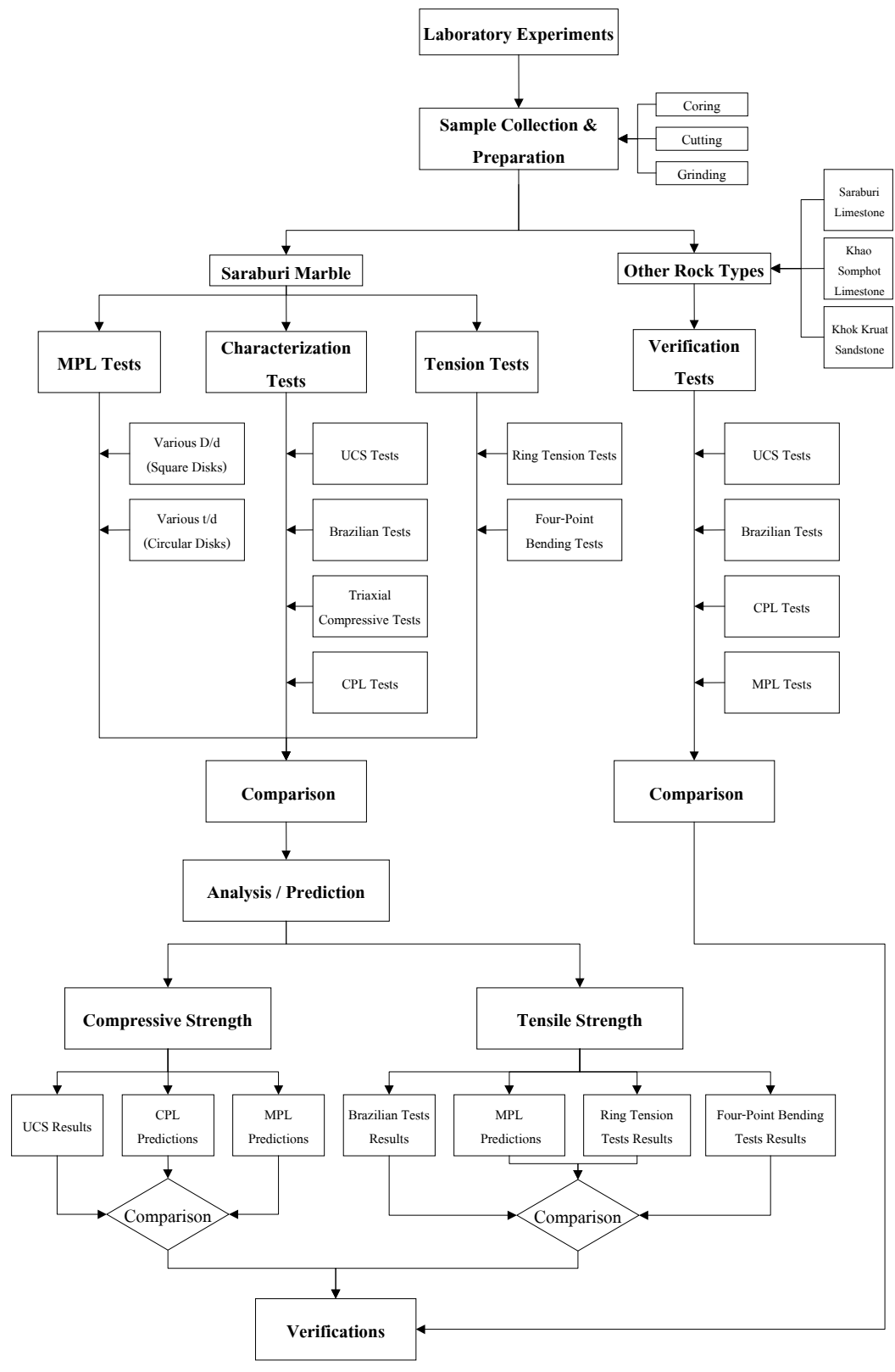


Figure 3.1 Laboratory experimental program planned in the research.



Figure 3.2 Saraburi marble blocks with nominal size of 25 cm x 30 cm x 30 cm are collected from a quarry in Saraburi province.

Khao Somphot limestone is collected from Lopburi province. It is light gray. It has a medium to fine grained texture. The age of Khao Somphot limestone is in the upper middle Permian.

Khok Kruat sandstone is a fine to medium grained rock. It is collected from Nakhon Ratchasima province. The rock is a unit of Khok Kruat formation in the Korat group. The age of sandstone is between the upper and middle Jurassic. The color is reddish brown.

Sample preparation has been carried out for a series for testing under different sample sizes. It is conducted in the laboratory facility at the Suranaree University of Technology. The process includes coring, cutting and grinding (Figures 3.3 through 3.7). Preparation of these samples follows the ASTM standards (ASTM D4543-85). Details of the sample specifications (size and shape) will be described later along with the corresponding tests. The rock sample coding system is explained in Appendix B.

3.3 Modified Point Load Tests on Saraburi Marble

3.3.1 Objective

The primary objective of the modified point load (MPL) tests on Saraburi marble is to produce the strength results for various size and shape. They will later be compiled and evaluated to determine the mathematical relationship, which may be useful to predict the UCS of the rock.

The test configurations for the proposed MPL testing are similar to those of the conventional point load (CPL) test, except that the loading points are cut flat to have a circular cross-sectional area instead of using a half-spherical shape. Figure 3.8 compares the conventional loading point with the modified loading points having the diameters of 5 and 10 mm. Several sizes of the loading point (platen) have been built in this research, i.e., loading diameters varying from 5, 10, 15, 20, 25, to 30 mm (Figure 3.9).

3.3.2 Specimen Specifications

The MPL specimens are taken as circular and square disks. Figures 3.10 and 3.11 show the test arrangement for both specimen shapes. The circular specimen thickness (t) is varied from 5 mm to 40 mm with a constant diameter (D) of 67.4 mm. This test series is to determine the thickness effects and to predict the tensile strength of the rock. The square specimen width (D)



Figure 3.3 Laboratory core drilling. The core drilling machine (model SBEL 1150) is used to drill core specimens using diamond impregnated bit with diameters varying from 22.5 to 92.5 cm.

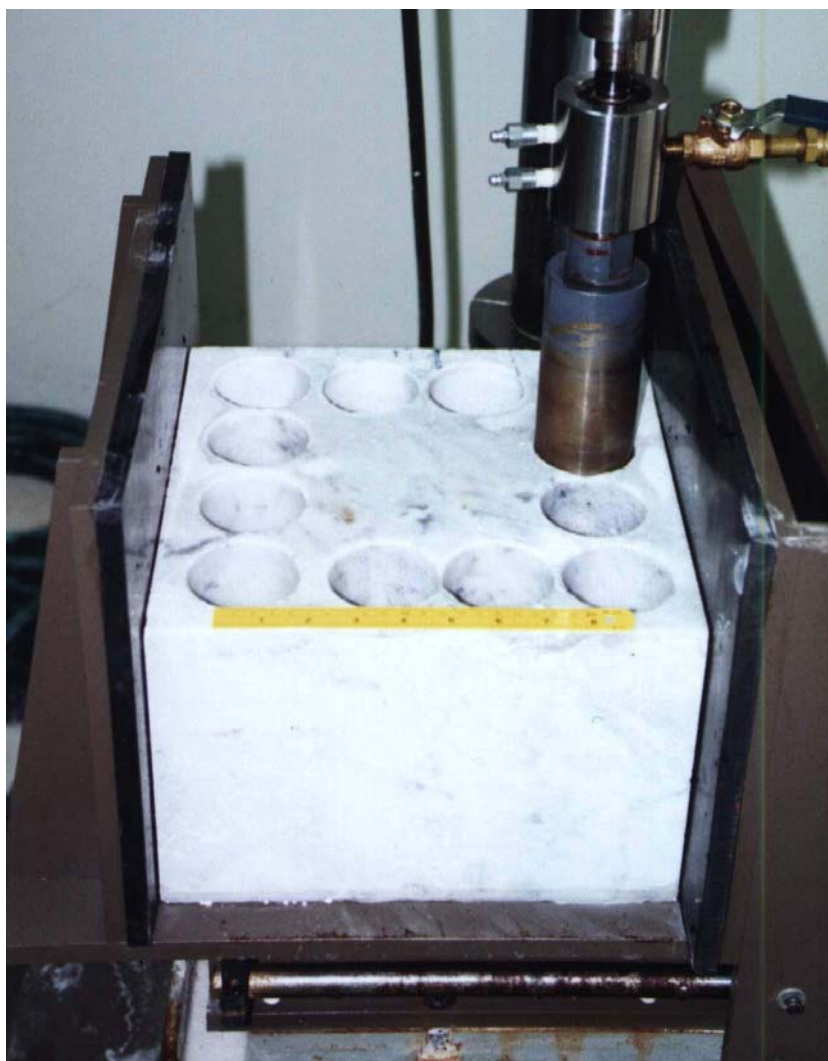


Figure 3.4 A 54 mm impregnated diamond bit (NX size) is used to drill cores from a block of Saraburi marble.

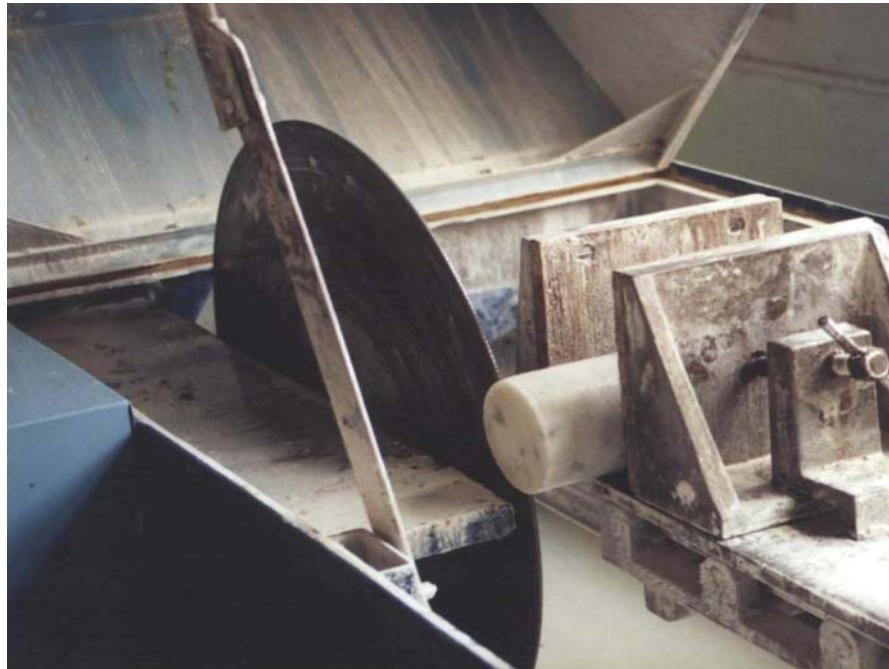


Figure 3.5 A core specimen of Saraburi marble is cut to produce appropriate rock specimen for each test by a cutting machine.

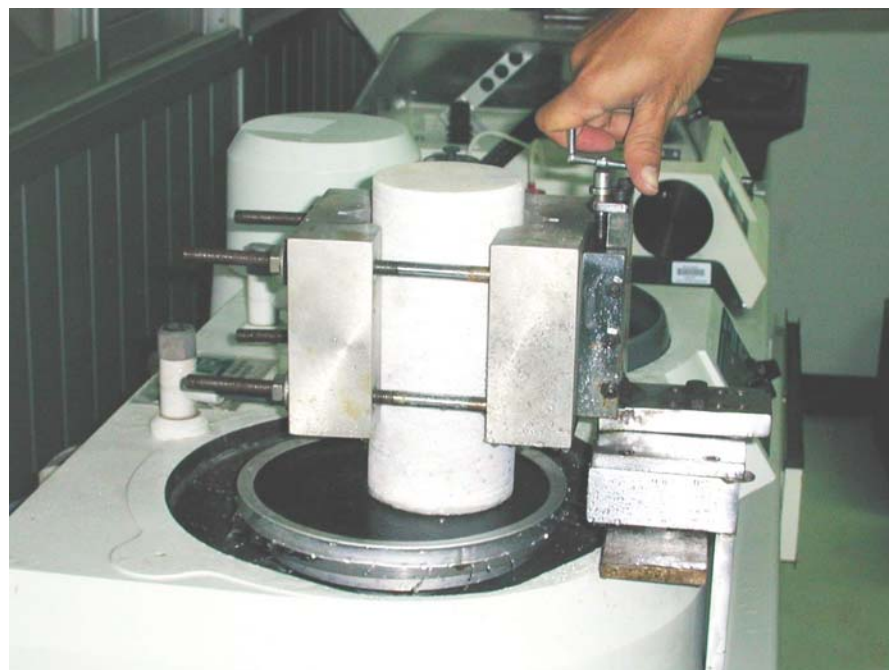


Figure 3.6 A 92.5 cm diameter core specimen of Saraburi marble is ground to meet the ASTM (D4543-85) specifications.



Figure 3.7 Some Saraburi marble specimens prepared for testing with various sizes and shapes.

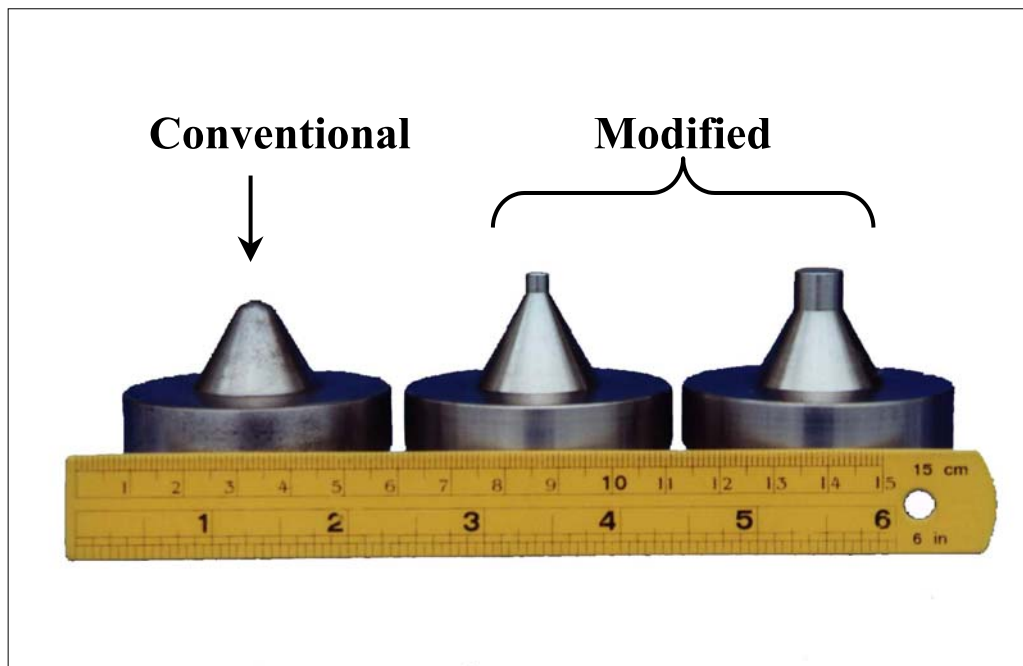


Figure 3.8 Comparison of the conventional and modified loading points. The modified loading points are cut flat to have a circular cross section area.

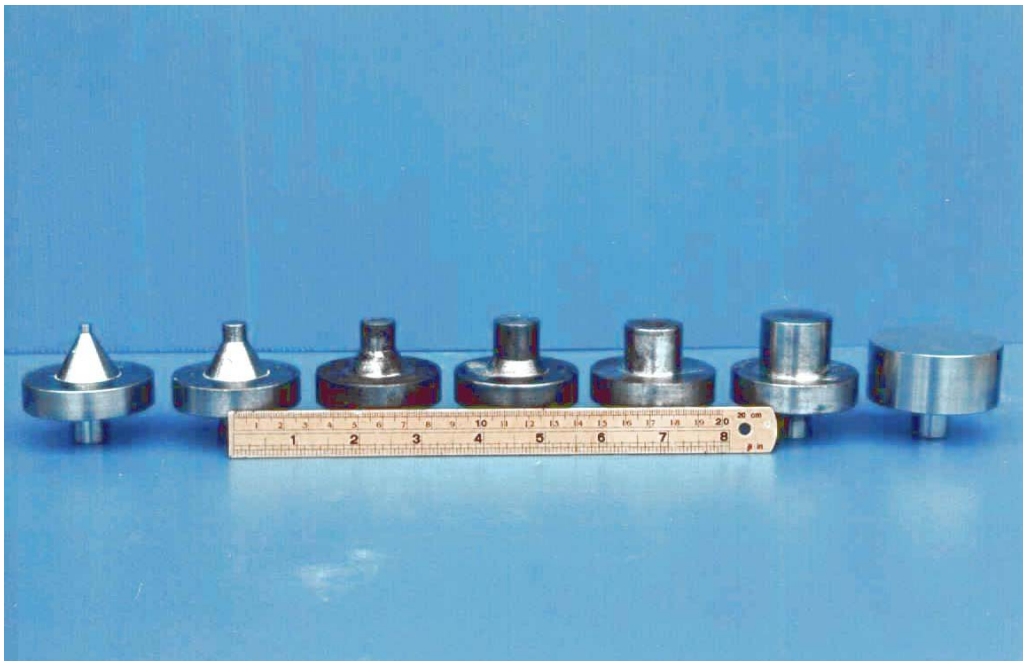


Figure 3.9 Modified loading points, with diameters varying from 5, 10, 15, 20, 25, to 30 mm.

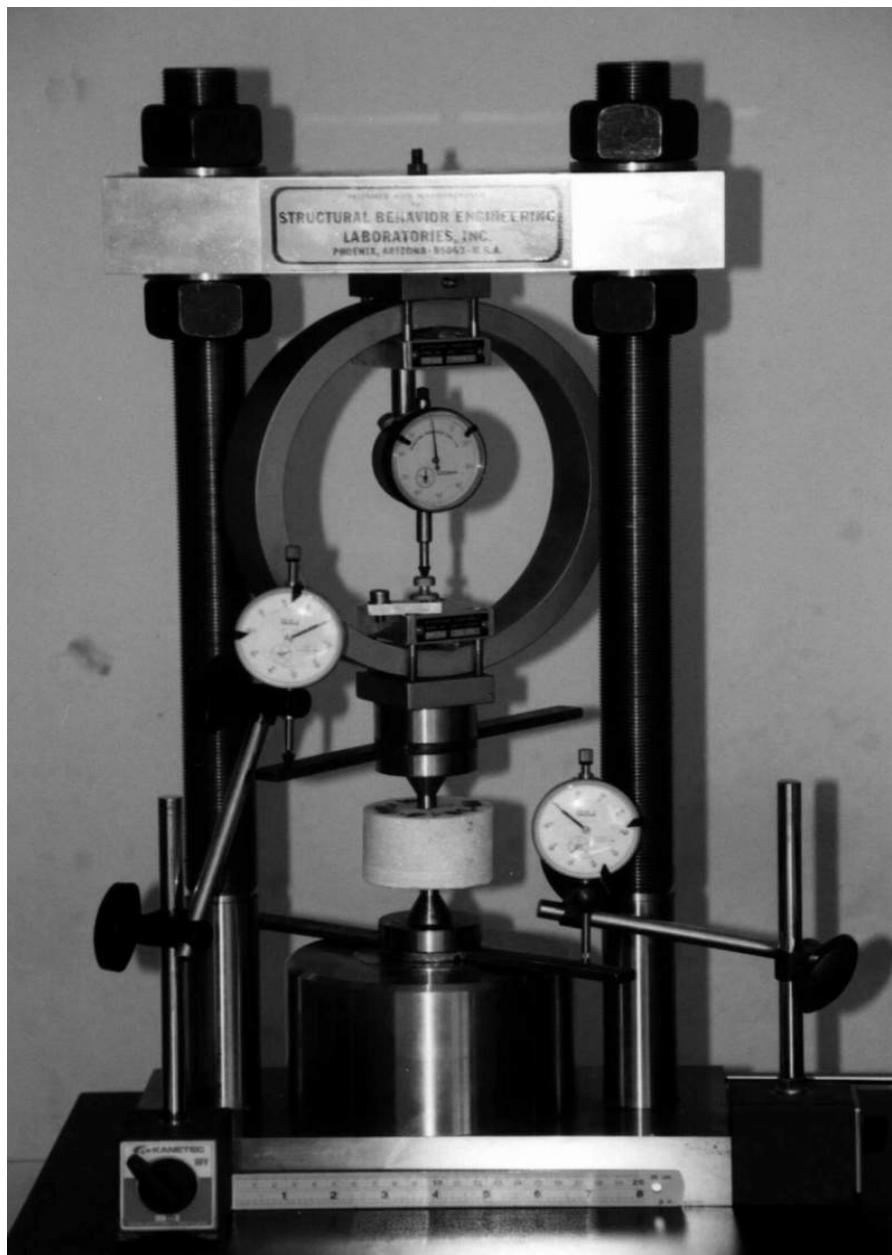


Figure 3.10 Test arrangement of circular disk specimen used in the modified point load testing. Point load tester model SBEL PLT-75, capacity of 350 kN, is used to load the rock specimen along its axis. Deformation between the loading points is measured with displacement dial gages.



Figure 3.11 A square disk specimen is tested by the modified point load using 10 mm diameter loading platen.

varies from 20 mm to 150 mm with a constant thickness (t) of 18 mm. It is performed to determine the diameter (width) effects and estimate the UCS of the rock.

3.3.3 Test Procedure

The apparatus used in this experiment is the point load tester model SBEL PLT-75 with maximum load capacity of 350 kN. The displacement gauges with a precision up to 0.001 mm are used to monitor the deformation of the rock between the loading points as the load increases. This is primarily to detect the development of compressive failure (initiation of micro-cracks) underneath the loading points, as well as the corresponding applied stress. The load is applied along the specimen axis, and is increased until the failure occurs. Post-failure characteristics are observed and recorded. Photographs are taken of the failed specimens.

3.3.4 Test Results and Analysis

The results of the modified point load tests are shown in Tables 3.1 and 3.2. The failure strengths are calculated by dividing the failure load by the contact area;

$$P = \frac{F}{\pi d^2 / 4} \quad (3.1)$$

where P is the modified point load strength, F is the applied load at failure, and d is the modified loading point diameter. All specimens failed along the loading axis, as shown in Figures 3.12 and 3.13. The thin specimens (less than twice the loading diameter) failed under compressive shear failure mode, while the thick specimens (thicker than three times the loading diameter) are failed in the extension failure mode. Figure 3.14 shows the compressive shear failure and extension failure that are occurred under the loading point.

Figures 3.15 and 3.16 show two sets of MPL test results by plotting the failure stresses P (in MPa) as a function of specimen thickness and diameter, respectively. To isolate the effect of the loading diameter, the specimen diameter and thickness are normalized by the diameter of loading point (d), as shown in the figures. The stress P increases exponentially as t/d increases, which can be expressed by a power equation.

Table 3.1 Results of modified point load tests on circular disks of Saraburi marble.

Average Diameter, D (mm)	Average Thickness, t (mm)	t/d	D/d	Loading Point Diameter, d (mm)	Number of Specimens	Average Density (g/cm³)	Mean MPL Strength, P (MPa)	Standard Deviation (%)
67.44	40.12	4.0	6.7	10	10	2.46	294.2	±29.9
67.39	29.88	3.0	6.7	10	10	2.67	227.0	±19.2
67.45	20.16	2.0	6.7	10	10	2.65	171.5	±22.4
67.47	15.06	1.5	6.8	10	10	2.65	144.5	±21.5
67.42	10.11	1.0	6.7	10	10	2.64	137.6	±30.6
67.44	7.42	0.7	6.7	10	10	2.62	143.9	±36.1
67.36	5.55	0.6	6.7	10	10	2.70	94.9	±25.8
67.42	39.01	7.8	13.5	5	7	2.69	666.1	±7.9
67.39	39.34	3.9	6.7	10	9	2.71	320.9	±19.9
67.40	39.43	2.6	4.5	15	10	2.68	168.7	±17.5
67.40	39.18	2.0	3.4	20	8	2.69	87.8	±45.8
67.38	39.44	1.6	2.7	25	6	2.69	78.9	±29.1
67.38	38.84	1.3	2.3	30	6	2.68	42.0	±13.8

Table 3.2 Results of modified point load tests on square disks on Saraburi marble.

Average Diameter, D (mm)	Average Thickness, t (mm)	t/d	D/d	Loading Point Diameter, d (mm)	Number of Specimens	Average Density (g/cm ³)	Mean MPL Strength, P (MPa)	Standard Deviation (%)
23.20	18.19	3.6	4.6	5	5	2.82	348.4	±8.4
48.00	18.19	3.6	9.6	5	5	2.77	394.2	±8.7
74.40	18.19	3.6	14.9	5	5	2.27	556.2	±2.4
99.20	18.19	3.6	19.8	5	5	2.75	591.8	±7.6
135.00	18.19	3.6	27.0	5	5	2.65	675.3	±26.6
150.00	18.19	3.6	30.0	5	5	2.57	653.9	±14.1
16.23	17.94	2.5	2.2	7.28	5	2.51	127.8	±12.9
22.70	18.15	2.5	3.1	7.28	5	2.85	213.8	±17.2
36.04	17.87	2.5	5.0	7.28	5	2.62	283.5	±3.1
50.51	18.08	2.5	6.9	7.28	10	2.64	309.3	±20.1
70.90	18.23	2.5	9.7	7.28	5	2.74	310.9	±22.9
99.10	18.10	2.5	13.6	7.28	5	2.61	360.8	±16.7
151.80	18.16	2.5	20.9	7.28	5	2.57	428.1	±15.3
23.80	18.19	1.8	2.4	10	5	2.84	106.2	±9.1
48.20	18.19	1.8	4.8	10	5	2.71	202.9	±11.3
73.40	18.19	1.8	7.3	10	5	2.71	236.6	±12.0
98.20	18.19	1.8	9.8	10	5	2.76	281.4	±9.3
124.40	18.19	1.8	12.4	10	5	2.72	233.5	±10.7
150.40	18.19	1.8	15.0	10	5	2.80	267.1	±14.0
22.40	18.19	0.9	1.1	20	5	2.90	86.0	±20.7
48.00	18.19	0.9	2.4	20	5	2.72	93.5	±26.6
73.00	18.19	0.9	3.7	20	5	2.71	114.6	±18.6
99.00	18.19	0.9	5.0	20	5	2.71	87.2	±27.1
127.80	18.19	0.9	6.4	20	5	2.95	96.9	±24.1
150.40	18.19	0.9	7.5	20	5	2.65	136.6	±33.3



Figure 3.12 The 67.4 mm-diameter Saraburi marble specimens failed by modified point load tests using various sizes of the loading diameter.

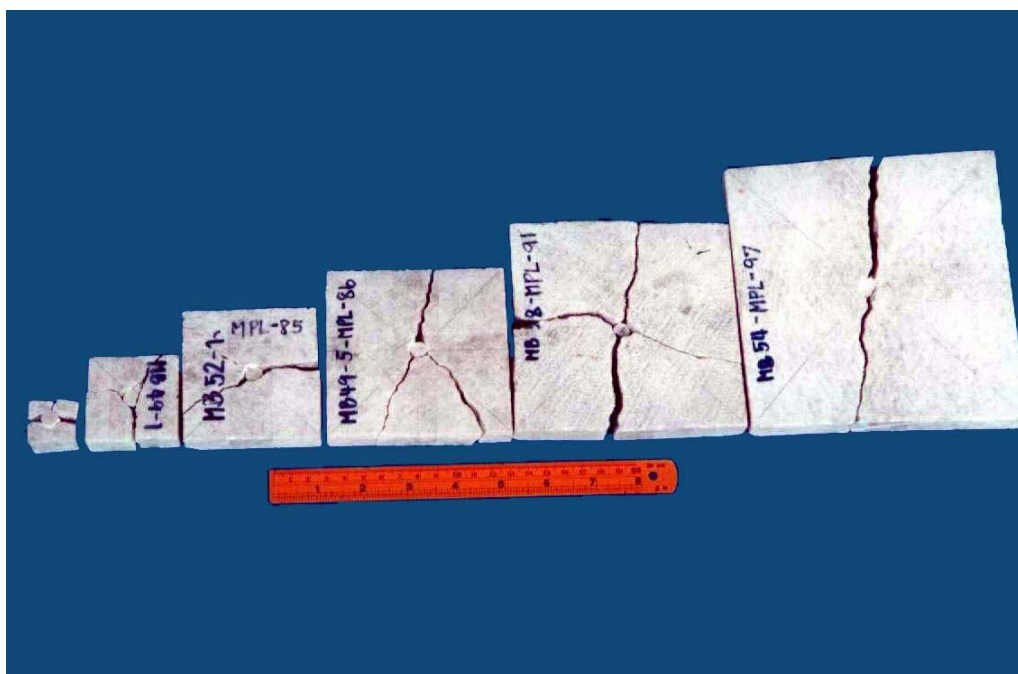


Figure 3.13 The various sizes of Saraburi marble specimens failed by modified point load tests using a 10 mm loading diameter.

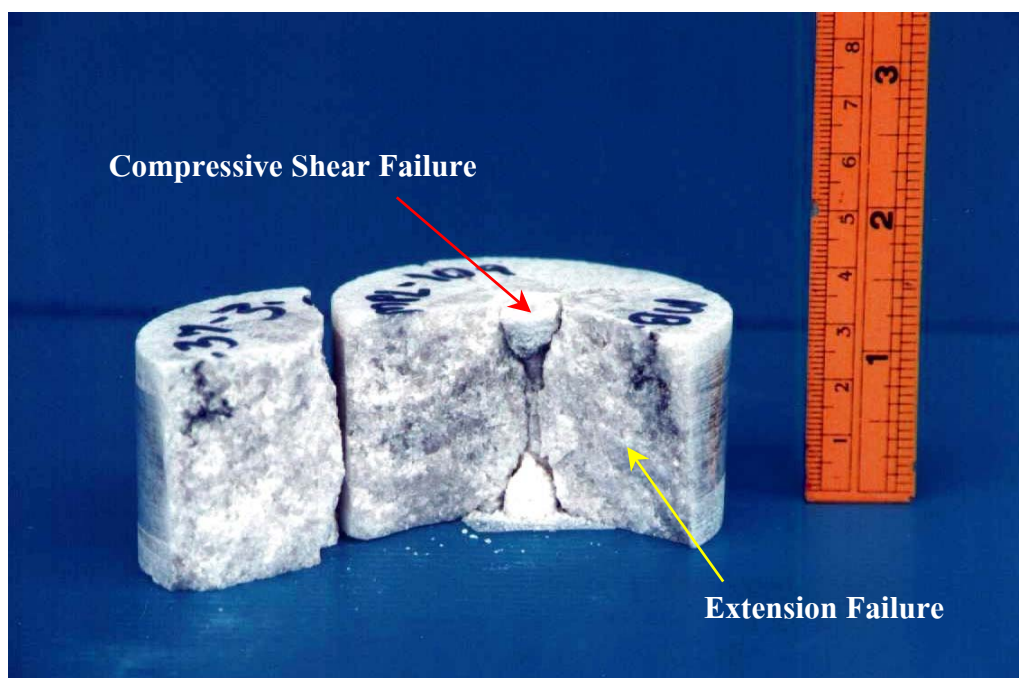


Figure 3.14 Post-tested specimens, the compressive shear failure is usually predominant under the loading point.

Modified Point Load Strength of Saraburi Marble

$D/d = 6.74, t/d = 0.5, 0.75, 1.0, 1.5, 2.0, 3.0, 4.0$

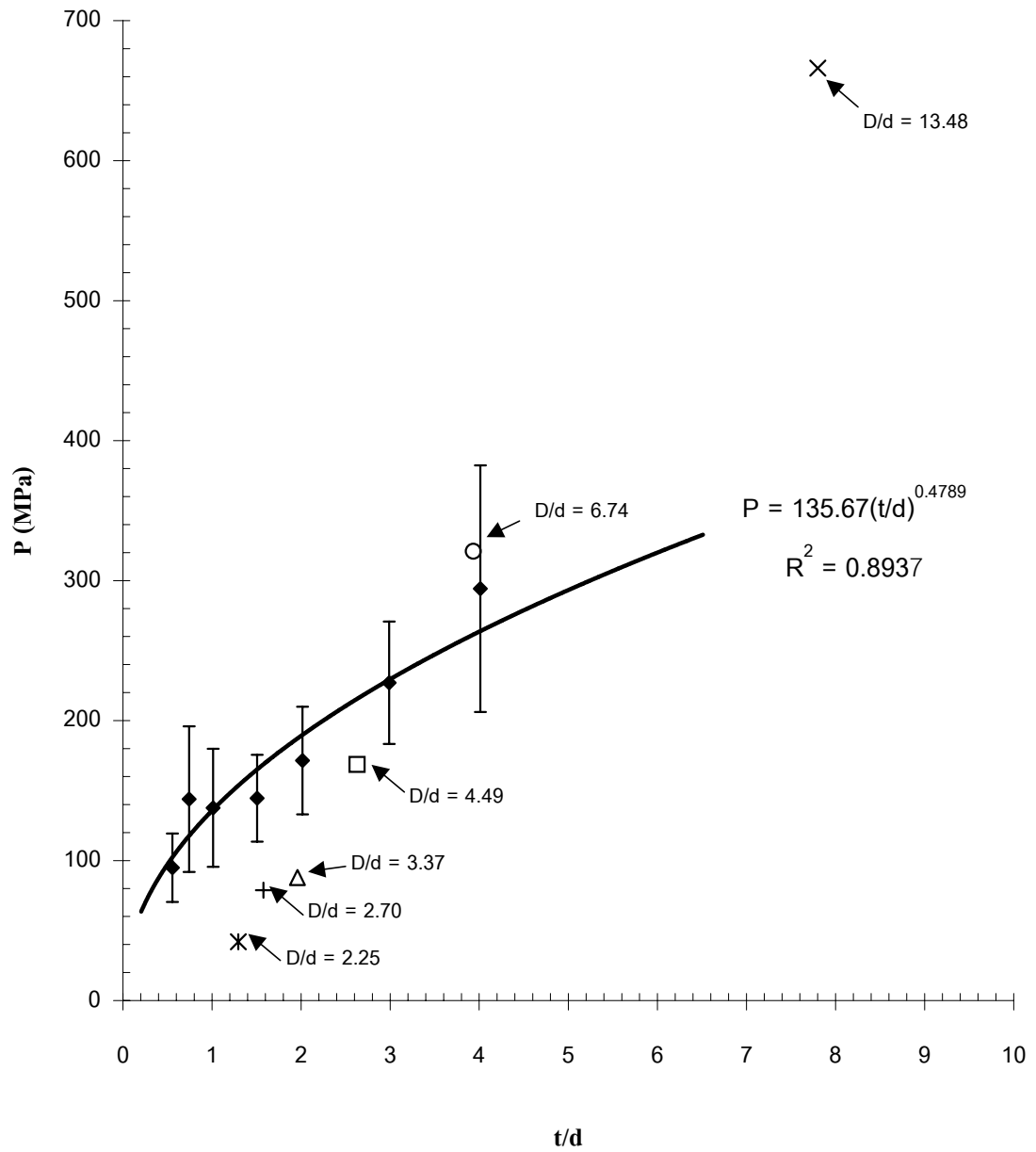


Figure 3.15 Modified point load test results for the circular disk specimens with $D/d = 6.74$.

Modified Point Load Strength of Saraburi Marble

$t/d = 0.91, 1.82, 2.5, 3.64$

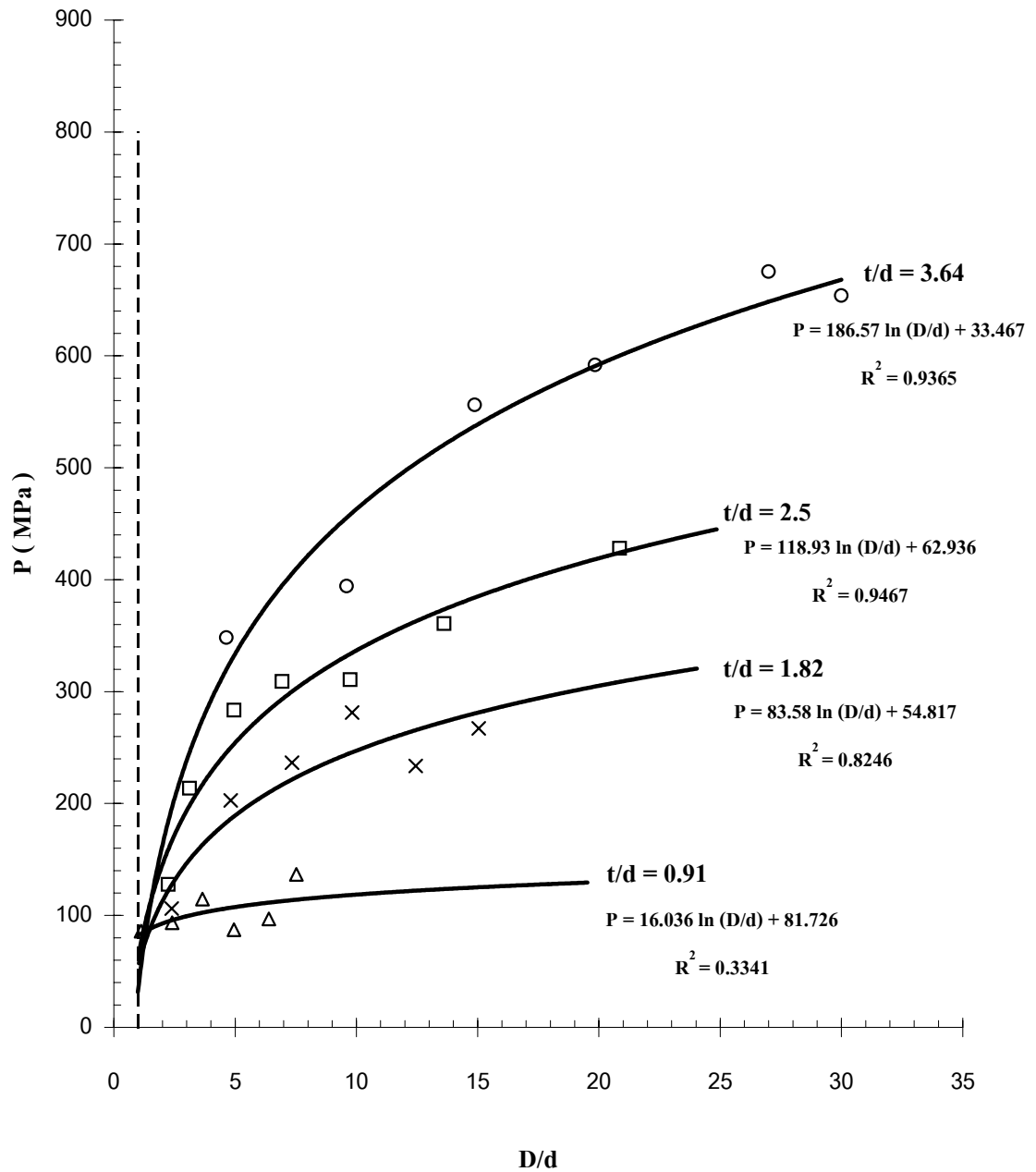


Figure 3.16 Modified point load test results for the square disk specimens with various t/d ratios.

$$P = A(t/d)^B \quad (3.2)$$

where P is the MPL strength (in MPa), t/d is the specimen thickness-to-loading platens diameter ratio, A and B are constants depending upon the rock specimen thickness (t/d). For Saraburi marble, A = 135.7 MPa and B = 0.48.

The MPL strength P tends to increase with the ratio D/d, which can be expressed by a logarithmic equation.

$$P = A \ln(D/d) + B \quad (3.3)$$

where P is the MPL strength (in MPa), D/d is the specimen diameter-to-loading platens diameter ratio, A and B are constants depending upon the rock specimen diameter (D/d). For Saraburi marble at t/d = 2.5, A = 118.9 MPa and B = 62.9 MPa. The standard deviation for each specimen size is about 10-25%. Comprehensive results of all MPL tests are described in Appendix A (Tables A1 and A2).

3.3.5 Discussions

Post-tested observations on the specimens also suggest that shear failure is predominant when the specimen thickness is less than twice the loading diameter while extension failure is predominant when the specimens are thicker than three times the loading diameter. This implies that the MPL strength should be correlated with the compressive strength when the MPL specimens are relatively thin, and should be an indicator of the tensile strength when the specimens are significantly larger than the diameter of the loading points. Applications of the MPL test results will be discussed in Chapter five.

3.4 Characterization Tests on Saraburi Marble

3.4.1 Uniaxial Compressive Strength Tests

The objectives are to develop a data basis to compare with the MPL results via a new governing equation and to study the size and shape effects of the specimen on the uniaxial compressive strength.

A series of uniaxial compressive strength (UCS) tests have been conducted on Saraburi marble. The sample preparation and test procedure follow the applicable ASTM standard (ASTM D2938-86) and the ISRM suggested method (Brown, 1981), as much as practical. A total of 280 specimens have been tested under various sizes and shapes. The specimen diameter is varied from 22.5, 38.5, 54.0, to 67.4 mm as shown in Figure 3.17. The length-to-diameter ratio (L/D) varies from 0.25, 0.50, 0.75, 1.0, 1.5, 2.0, to 2.5. The loading device used in this experiment is the compression machine model ELE-ARD2000, with capacity of 2000 kN. All specimens are loaded to failure under a constant loading rate such that failures occur within 5-10 minute of loading (Figure 3.18). Post-failure characteristics are observed.

The uniaxial compressive strength of the specimen is calculated by dividing the maximum load by the original cross-sectional area. The results of the uniaxial compressive strength tests are shown in Table 3.3. The specimens are failed under various modes of failure, including the extension failure mode (Figures 3.19 and 3.20), the shear failure mode (Figure 3.21) and the compressive shear failure mode (Figure 3.22). Figure 3.23 plots the compressive strength as a function of L/D ratio. The strength decreases as the L/D increases. The relationship can be best represented by a power equation;

$$\sigma_c = \alpha(L/D)^{-\beta} \quad (3.2)$$

where σ_c is the uniaxial compressive strength, L/D is the length-to-diameter ratio, α is coefficient of the stress, and β is coefficient of the shape. By using least square fitting, a mathematical relationship between the strength and shape of specimen for Saraburi marble can be obtained, as $\alpha = 66.3$ MPa and $\beta = 0.53$. This strength-shape equation can be used to isolate the effect of shape from the strength result, in order to predict the UCS of a specimen with arbitrary L/D. The UCS of Saraburi marble is averaged as 46.8 MPa (at L/D = 2.5). Details of the results are presented in Appendix A (Table A3).

The results clearly show the end effects of the specimen on the strength values. The larger the L/D ratio, the lower the strength. The strength results however show no effect of the specimen size. This is probably due to the fact that the size effect pronounces more in tensile



Figure 3.17 Saraburi marble specimens with diameters varying from 22.5, 38.5, 54.0, to 67.4 mm. They are prepared for uniaxial compressive strength tests.

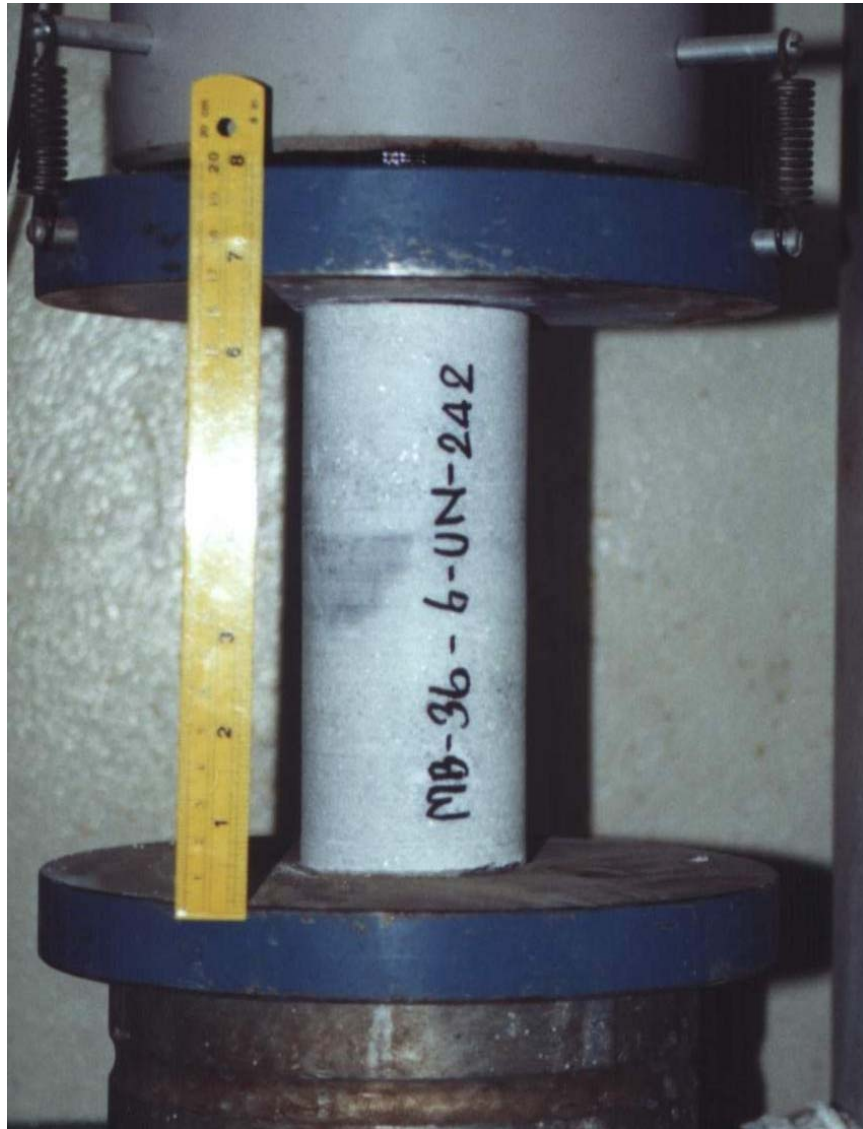


Figure 3.18 Uniaxial compressive strength test on 67.4 mm diameter specimen of Saraburi marble with $L/D = 2.5$. The specimen is loaded axially in compression machine model ELE-ADR2000.

Table 3.3 Results of uniaxial compressive strength tests to determine size and shape effects of Saraburi marble specimens.

Average Diameter, D (mm)	Average Length, L (mm)	L/D	Number of Specimens	Average Density (g/cm ³)	Mean Compressive Strength, σ_c (MPa)	Standard Deviation (%)
22.64	5.46	0.2	10	2.58	184.9	±23.4
22.44	11.41	0.5	10	2.62	101.5	±25.6
22.43	16.89	0.8	10	2.65	81.7	±35.3
22.44	22.49	1.0	10	2.63	49.8	±28.6
22.39	33.29	1.5	10	2.68	52.1	±47.0
22.51	44.26	2.0	10	2.67	45.0	±26.0
22.59	54.69	2.4	10	2.68	36.5	±22.9
38.51	11.27	0.3	10	2.68	237.9	±21.9
38.52	23.12	0.6	10	2.63	122.1	±27.7
38.51	35.86	0.9	10	2.62	62.2	±53.6
38.51	49.02	1.3	10	2.64	89.2	±30.9
38.52	61.83	1.6	10	2.66	60.1	±33.5
38.54	77.92	2.0	10	2.69	83.6	±46.7
38.55	96.46	2.5	10	2.69	36.8	±57.9
53.93	13.82	0.3	10	2.61	96.7	±12.8
53.93	28.02	0.5	10	2.67	61.7	±43.9
53.96	40.37	0.8	10	2.68	35.4	±19.8
53.94	54.39	1.0	10	2.70	42.9	±22.0
53.94	81.07	1.5	10	2.50	50.0	±32.2
53.95	100.99	1.9	10	2.69	51.1	±34.1
53.98	128.94	2.4	10	2.71	61.4	±20.3
67.43	17.71	0.3	10	2.66	227.6	±20.4
67.37	33.37	0.5	10	2.69	80.3	±17.3
67.48	50.36	0.8	10	2.69	45.2	±18.7
67.42	66.11	1.0	10	2.69	53.7	±29.6
67.35	99.91	1.5	10	2.70	55.3	±24.0
67.41	132.77	2.0	10	2.73	43.9	±29.4
67.44	166.78	2.5	10	2.73	52.5	±27.9

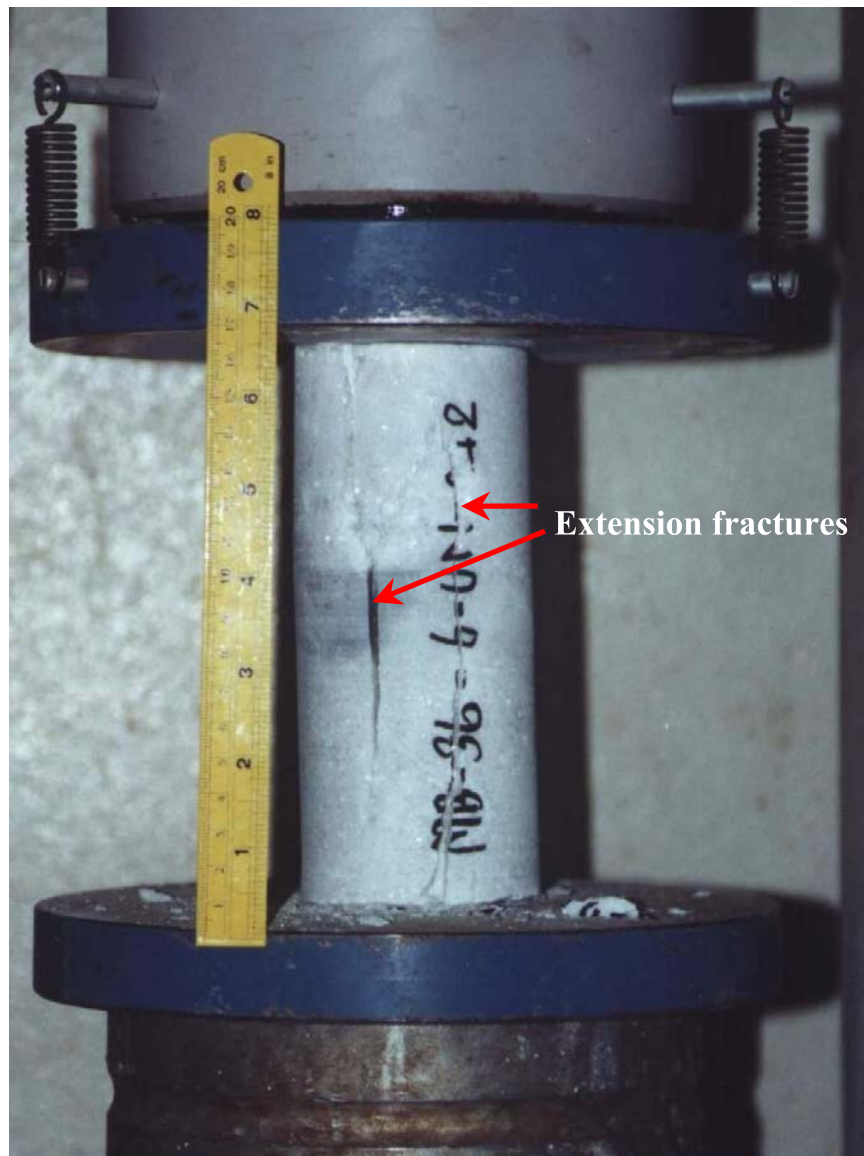


Figure 3.19 A 67.4 mm diameter specimen of Saraburi marble with $L/D = 2.5$ failed by uniaxial compressive strength test. Arrows indicate the extension fracture.



Figure 3.20 The extension fractures occurs along core specimen axis by uniaxial compressive strength test. ($D = 67.5$ mm and $L/D = 2.0$)



Figure 3.21 Specimen of Saraburi marble failed under the shear failure mode by uniaxial compressive strength test. The shear failure plane is about 30 degrees from specimen axis. ($D = 67.5$ mm and $L/D = 2.5$)



Figure 3.22 Specimen of Saraburi marble failed under the compressive shear failure mode (conical shape) by uniaxial compressive strength test. ($D = 67.5$ mm and $L/D = 1.0$)

Uniaxial Compressive Strength of Saraburi Marble

L/D = 0.25, 0.5, 0.75, 1.0, 1.5, 2.0, 2.5

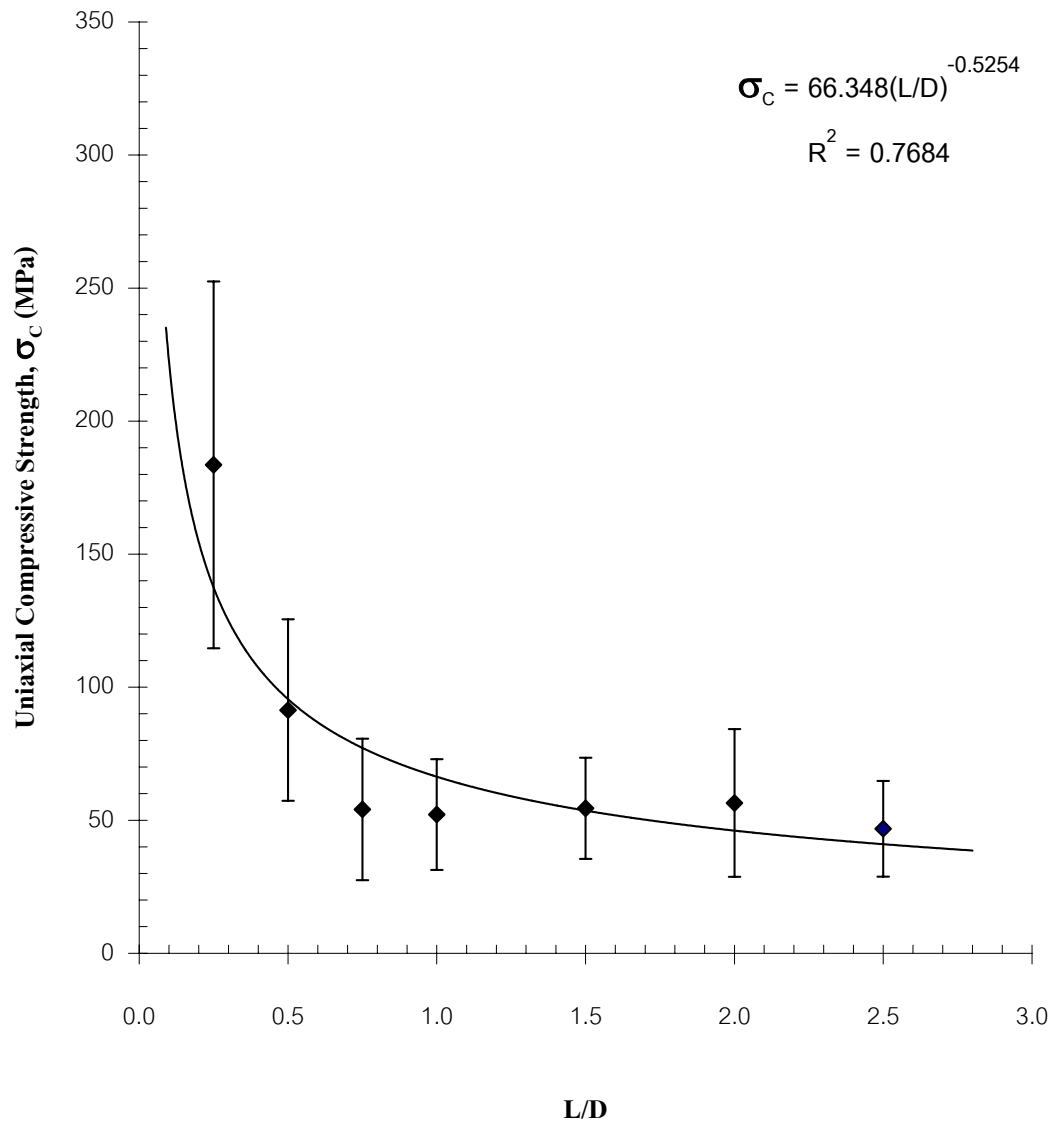


Figure 3.23 Shape effect on uniaxial compressive strength of Saraburi marble. Experimental results and curve fitted using power law.

failure than does in compressive shear failure. Short specimens (L/D lower than two) tend to fail under the compressive shear failure mode. Extension failure dominates when the L/D ratios are larger than two. In general this finding agrees reasonably well with similar experiments obtained elsewhere (Ghosh et al., 1995).

3.4.2 Brazilian Tensile Strength Tests

The objective of the Brazilian tensile strength test is to determine the relationship between the MPL strength and the rock tensile strength, and the comparison of the results with the other tension test methods. A series of Brazilian (indirect) tension tests have been performed on the Saraburi marble. The sample preparation and test procedure have followed the applicable ASTM standards (ASTM D3967-81) and ISRM suggested method (Brown, 1981). Forty specimens have been tested. They have a constant L/D ratio = 0.5, while the specimen diameters vary from 22.5, 38.5, 54.0, to 67.4 mm as shown in Figure 3.24. Each disk is diametrically load to failure (Figure 3.25). The loading rate is controlled at approximately 200 N/s. Post-failure characteristics are observed.

The results of the Brazilian tensile strength tests are shown in Table 3.4. The tensile strength is calculated using the equation (Jaeger and Cook, 1979);

$$\sigma_B = \frac{2P}{\pi Dt} \quad (3.3)$$

where σ_B is the Brazilian test tensile strength, P is the failure load, D is the disk diameter, and t is the disk thickness. All of specimens failed along the loading diameter (Figure 3.26). The tensile strength tends to decrease as the specimen size (diameter) increases, and can be expressed by a power equation (Evans, 1961);

$$\sigma_B = A(D)^{-B} \quad (3.4)$$

where σ_B is the Brazilian tensile strength, D is the diameter of the specimen, A and B are constants depending upon the nature of the rock.



Figure 3.24 Saraburi marble specimens with diameters varying from 22.5, 38.5, 54.0, to 67.4 mm with $L/D = 2.5$ for Brazilian tensile strength tests.



Figure 3.25 Brazilian test on 67.4 mm diameter specimen of Saraburi marble. The specimen is loaded along the diameter in ELE-ADR2000 compression machine.

Table 3.4 Results of Brazilian tensile strength tests on Saraburi marble.

Average Disk Diameter, D (mm)	Average Thickness, t (mm)	t/D	Number of Specimens	Average Density (g/cm ³)	Mean Tensile Strength, σ_B (MPa)	Standard Deviation (%)
22.43	11.19	0.5	10	2.64	5.1	±22.6
38.51	19.07	0.5	10	2.65	4.9	±21.2
53.96	27.48	0.5	10	2.65	3.6	±22.4
67.39	34.09	0.5	10	2.66	3.6	±21.5

**Figure 3.26** The 22.5, 38.5, 54.0, and 67.4 mm diameter specimens of Saraburi marble failed along the loading diameter in the Brazilian tests.

By using least square fitting, a mathematical relationship between the strength and diameters of the specimen can be obtained as shown in Figure 3.27. For Saraburi marble, $A = 16.7$ MPa/mm and $B = 0.37$. This strength-size equation can be used to isolate the effect of size (diameter) from strength result, in order to predict the tensile strength of a Brazilian disk sample with arbitrary diameter. The Brazilian tensile strength of Saraburi marble is averaged as 4 MPa for 50 mm diameter specimens.

The Brazilian tensile strengths decrease with increasing specimen diameter. This finding agrees with those obtained from similar experiments (Fuenkajorn and Daemen, 1986). The uses of Evans' power law in determining a mathematical relationship between the strength and size of specimen seem appropriate. The value A relates to the strength of rock material. It increases as the rock strength increases. The value of B expresses the decrease in rock strength as the specimen size (diameter) increases.

3.4.3 Triaxial Compressive Strength Tests

The objective of the triaxial compressive strength test is to determine the compressive strengths of Saraburi marble under various confining pressures. The sample preparation and test procedure follow the applicable ASTM (ASTM D2664-86) and ISRM suggested method (Brown, 1981), as much as practical. A total of 5 specimens have been tested under various confining pressures. The L/D of the specimen equals 2.0. The equipment used in this experiment includes the pressure controlling device (model WF 40070), the triaxial compression chamber (Hoek-Franklin), and the axial loading device. All specimens are loaded to failure under a constant loading rate such that failures occur within 5-10 minute of loading under each confining pressure. The confining pressures used here are 1.7, 3.4, 6.9, 13.8 and 20.7 MPa. Post-failure characteristics are observed.

The results of the triaxial compressive strength tests are shown in Table 3.5. Figures 3.28 shows the shear failure by triaxial loading at confining pressure (σ_3) equal to 20.7 MPa. Figure 3.29 is shows the Mohr stress circles of the results with shear stresses as ordinates and normal stress as abscissas. The relationship can be represented by (Hoek, 1990);

$$\tau = c + \sigma_n \tan \phi \quad (3.5)$$

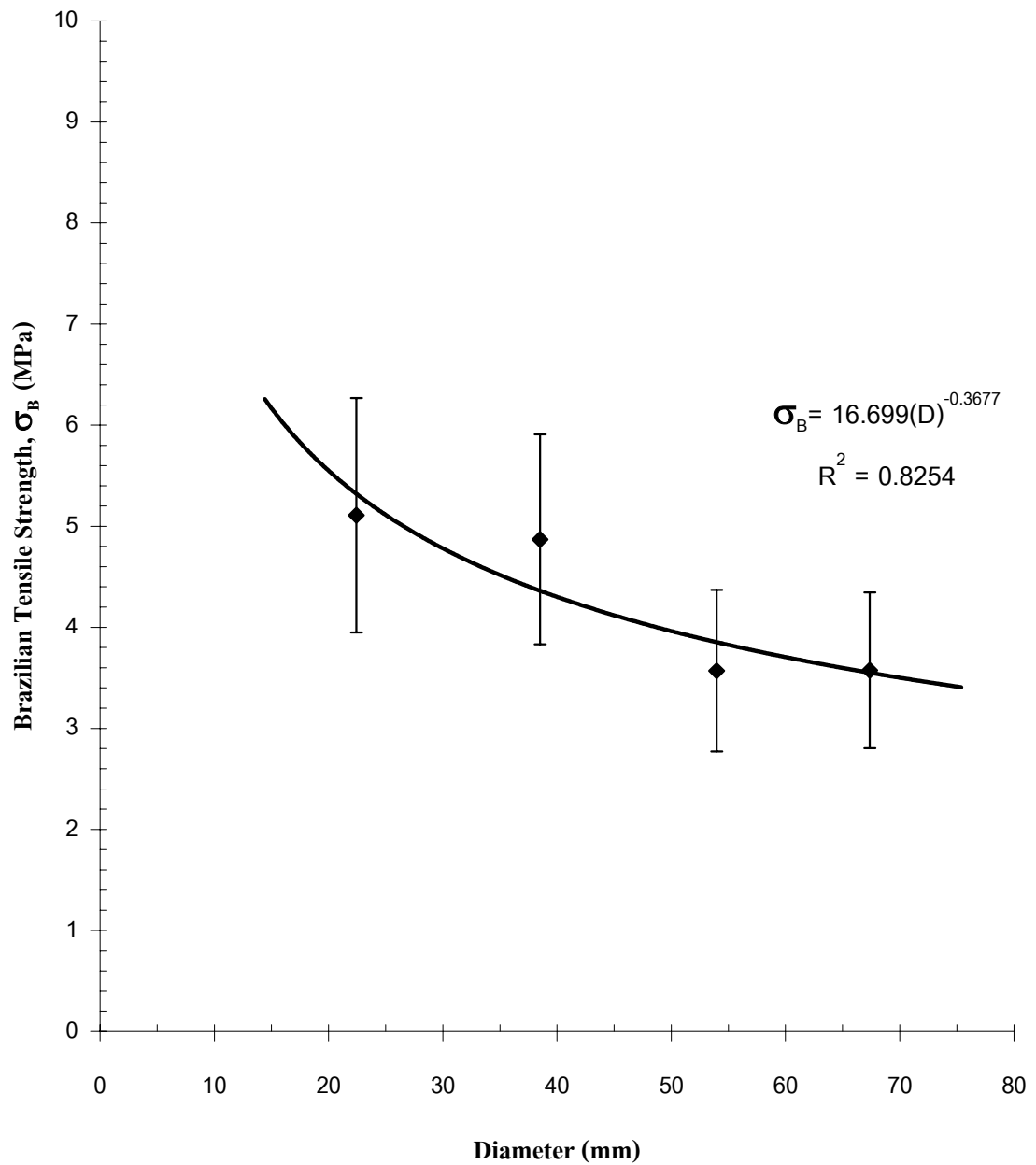
Brazilian Tensile Strength of Saraburi Marble $D = 22.5, 38.5, 54.0, 67.4 \text{ mm}, L/D = 0.5$ 

Figure 3.27 Experimental results and curve fitted of Brazilian test results. Evans' power law,

$$\sigma_B = A(D)^{-B}.$$

Table 3.5 Results of triaxial compressive strength tests on Saraburi marble.

Sample No.	Diameter (mm)	Length (mm)	Load at Failure (kN)	Confining Pressure, σ_3 (MPa)	Axial Stress at Failure, σ_1 (MPa)
MB-25-8-TR-6	53.9	100.7	174	1.7	76.2
MB-26-11-TR-1	53.9	100.8	250	3.4	109.5
MB-26-7-TR-4	54.1	100.1	274	6.9	119.8
MB-25-10-TR-5	54.0	102.8	284	13.8	124.4
MB-26-12-TR-3	54.0	100.3	386	20.7	169.1



Figure 3.28 A 54 mm diameter specimen of Saraburi marble with $L/D = 2.0$ failed by triaxial compressive strength test at confining pressure (σ_3) 20.7 MPa (Sample No. MB-26-12-TR-3).

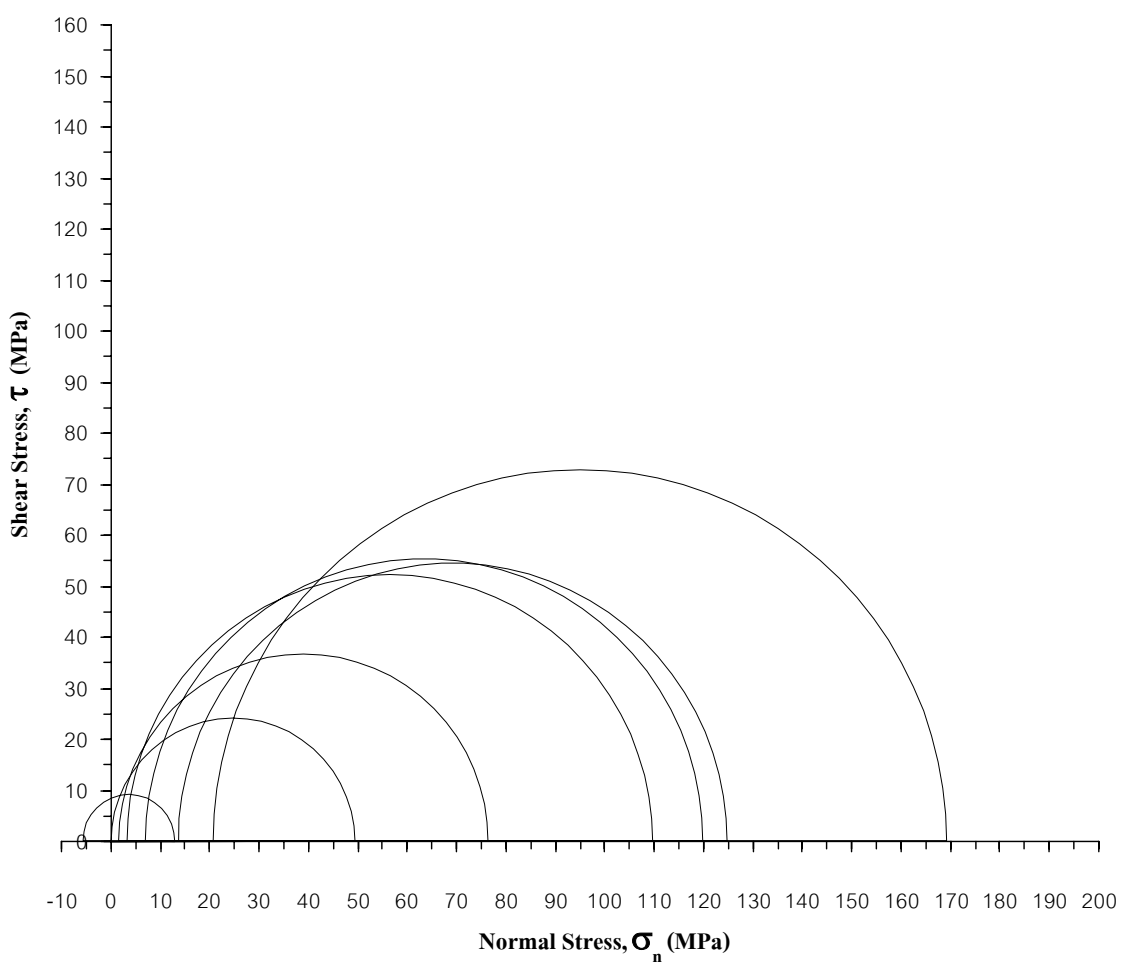


Figure 3.29 Mohr's circle representing the triaxial compressive strength test results.

where τ is the shear stress, c is the cohesion, σ_n is the normal stress, and ϕ is the angle of internal friction (shearing resistance). For the marble, the internal friction angle and the cohesion equal 40 degrees and 14 MPa, respectively.

The results show the axial stresses (σ_1) increase with increasing the confining pressure (σ_3). This finding agrees with other researchers obtained from similar experiments (e.g. Hoek and Brown, 1980).

3.4.4 Conventional Point Load Tests

The objective of this test is to determine of the CPL strength index for use in the comparison in term of the predictive capability with that of the MPL test.

The test procedure follows the applicable ASTM standard (ASTM D5731-95) and ISRM suggested method (ISRM, 1985). The main equipment are used in this experiment is the point load tester (model SBEL PLT-75 capacity 350 kN) (Figure 3.30). The specimen diameter is maintained constant at 67.4 mm. The specimen thickness varies from 5.0 to 40.0 mm. A total of 70 specimens have been tested. A 67.4 mm diameter of core specimen is loaded along its axis, as shown in Figure 3.31. Each sample is loaded to failure at a constant rate. Post-failure characteristics are observed.

Table 3.6 shows the results. The calculations of CPL strength index use two different formulas,

$$I_S = \frac{P}{t^2} \quad (3.6)$$

and
$$I_S = \frac{P}{Dt} \quad (3.7)$$

where I_S is the CPL strength index, P is the load at failure, D is the diameter of specimen, and t is the thickness of specimen (or the distance between two loading point). The specimens are failed along loading direction as shown in Figures 3.32. Figures 3.33 and 3.34 plot the relationship between the I_S and the distance between two loading points for both method of calculation.

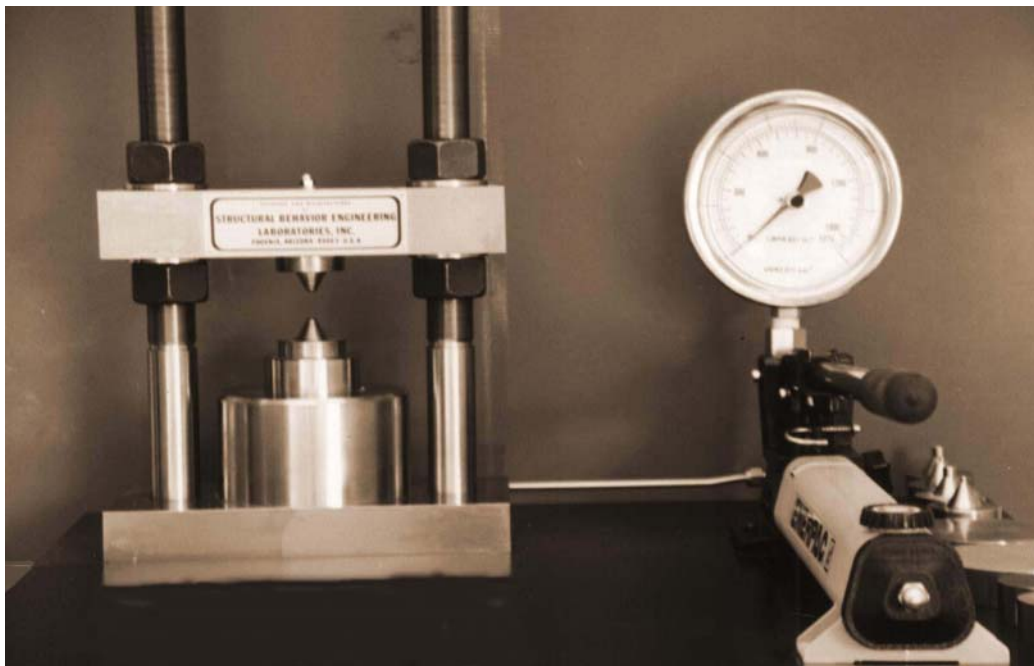


Figure 3.30 Point load tester model SBEL PLT-75 for the conventional point load tests, with maximum loading capacity of 350 kN.

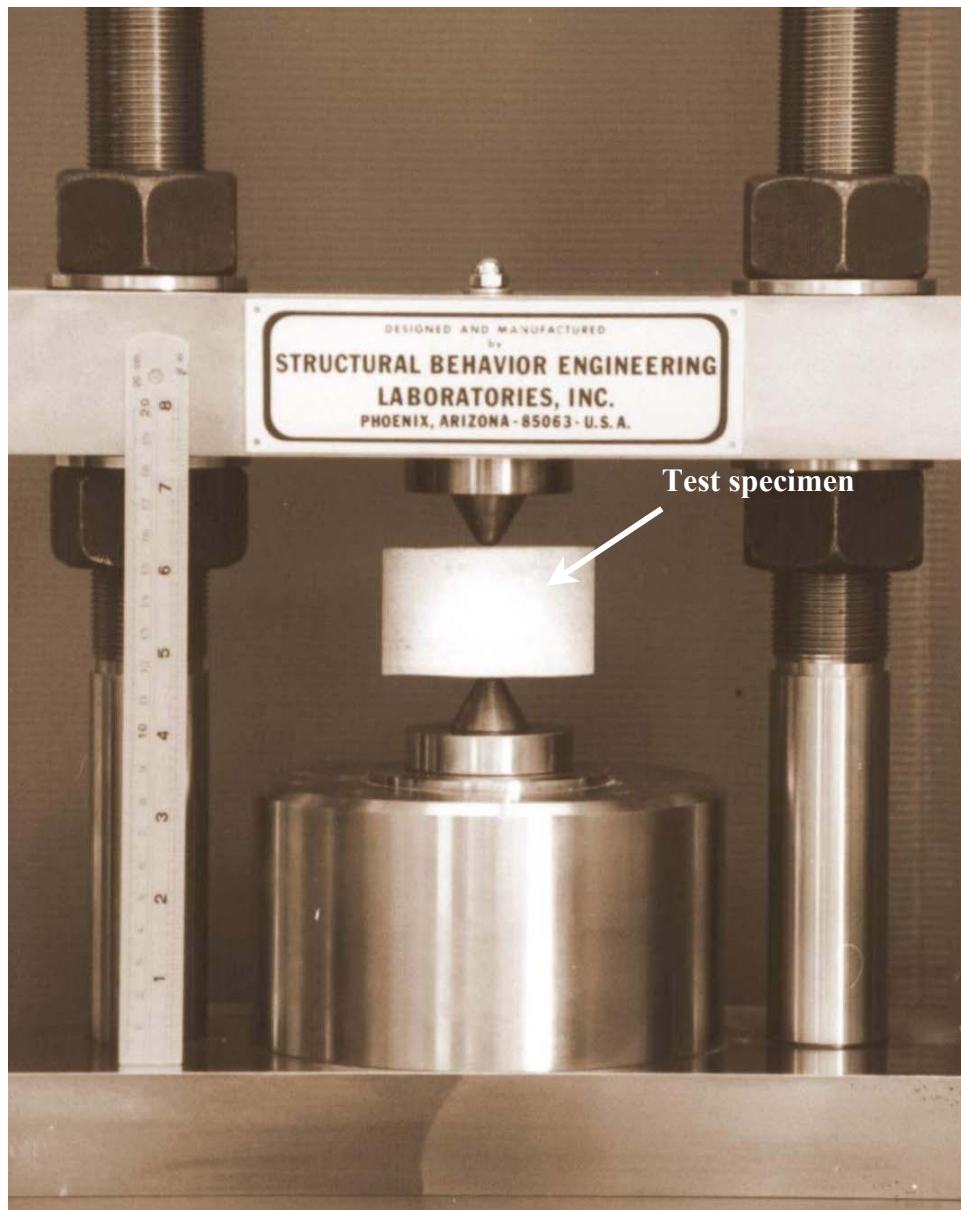


Figure 3.31 The conventional point load testing on Saraburi marble specimen with $D = 67.4$ mm and $t = 30.2$ mm.

Table 3.6 Results of conventional point load tests on Saraburi marble.

Average Diameter,	Average Thickness,	t/D	Number of Specimens	Average Density (g/cm ³)	Mean Point Load Index, $I_s = P/t^2$ (MPa)	Standard Deviation (%)	Mean Point Load Index, $I_s = P/Dt$ (MPa)	Standard Deviation (%)
67.36	5.69	0.1	10	2.61	53.7	±10.7	4.5	±12.5
67.44	7.88	0.1	10	2.59	38.5	±19.1	4.5	±17.4
67.44	10.66	0.2	10	2.63	28.5	±15.3	4.5	±12.4
67.47	15.89	0.2	10	2.61	19.1	±24.7	4.5	±20.3
67.40	19.63	0.3	10	2.69	14.3	±14.4	4.1	±9.1
67.37	30.20	0.5	10	2.70	9.9	±17.5	4.5	±21.1
67.39	39.38	0.6	10	2.69	7.4	±14.7	4.3	±13.7



Figure 3.32 The 67.4 mm diameter specimens of Saraburi marble failed by the conventional point load tests.

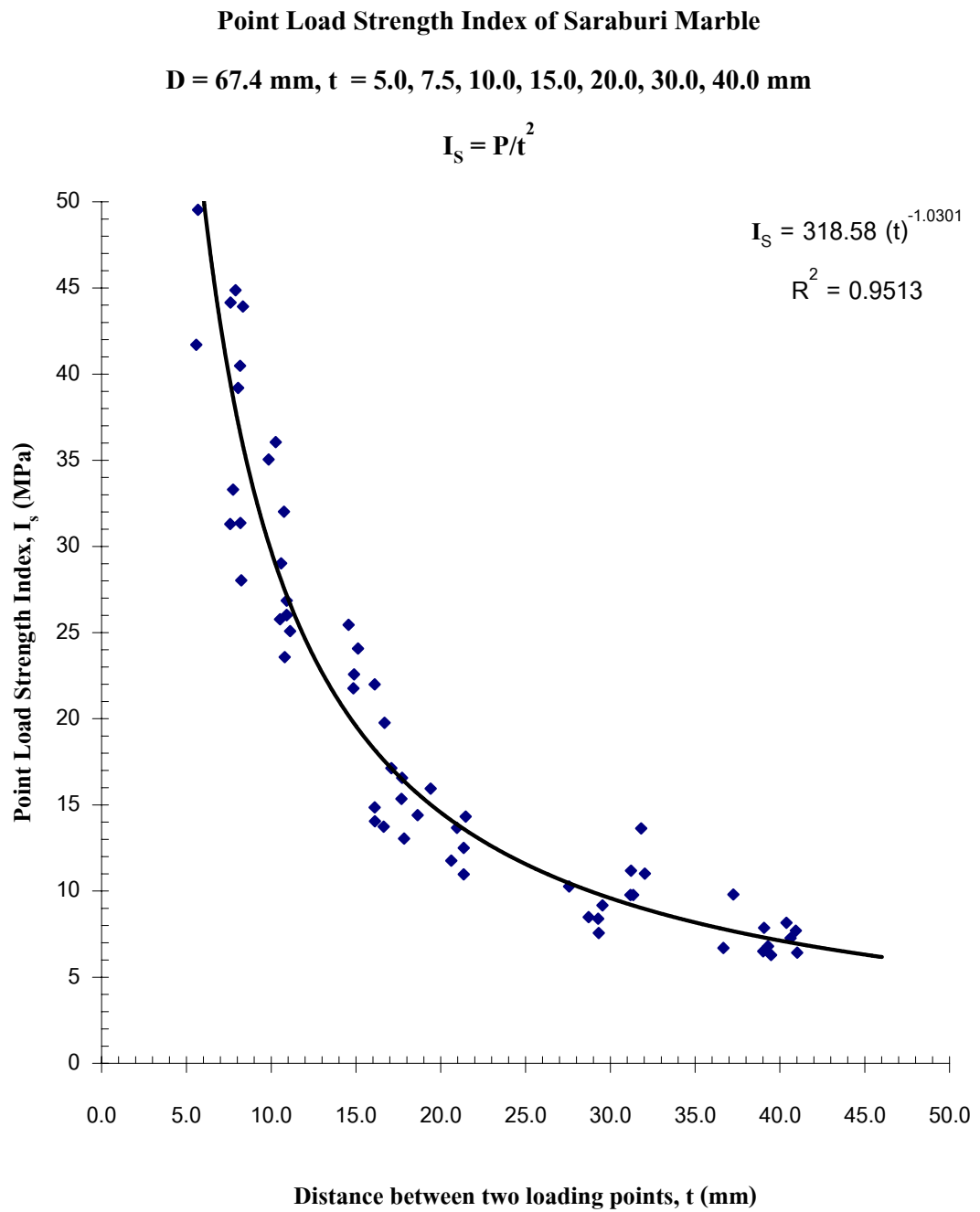


Figure 3.33 Conventional point load test results of the Saraburi marble for $D/d = 6.74$, using the relationship $I_s = P/t^2$.

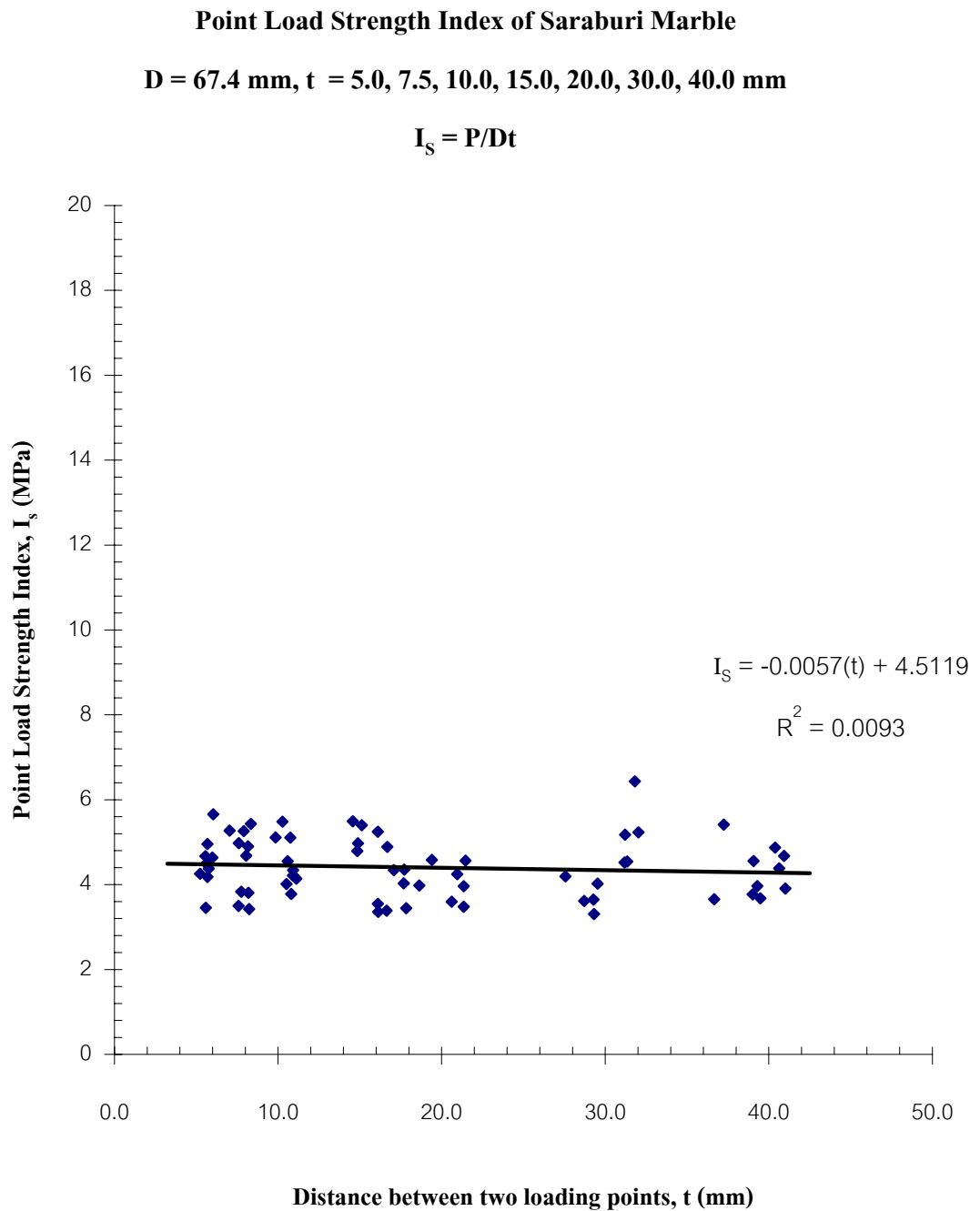


Figure 3.34 Conventional point load test results of the Saraburi marble for $D/d = 6.74$, using the relationship $I_s = P/(D.t)$.

The CPL strength index is calculated by dividing the failure load by the cross section of the splitting area (equation 3.7). It seems to be independent of the specimen dimensions. The point load strength index is averaged as 4.5 MPa.

3.5 Tension Tests on Saraburi Marble

3.5.1 Specific Objective

The objective of these additional tension tests is to determine the effect of stress gradients on the tensile strength of Saraburi marble. The ring tension test and the four-point bending test are used to obtain the tensile under different stress gradient on the incipient failure plane.

3.5.2 Ring Tension Tests

The ring tension test is designed to measure the tensile strength of rock disks with a center hole. The rock samples of Saraburi marble are drilled to produce rock cylinders with 92.4 mm external diameter and 30.5 mm internal diameter. The specimen thickness is maintained constant at 46.4 mm. Each disk is placed in a compression machine and load diametrically until failure (Figure 3.35). The loading rate is approximate 200 N/s. The load at failure is recorded.

The results of the ring tensions tests on Saraburi marble are shown in Table 3.7. The ring tensile strength can be calculated by (Ripperger and Davids, 1947);

$$\sigma_R = \frac{2PK}{\pi Dt} \quad (3.8)$$

where σ_R is the ring tensile strength, P is load at failure, D is the disk diameter, t is the disk thickness, K is the stress concentration factor ($K = 6 + 38 (r')^2$), and r' is relative hole radius (hole radius/disk radius). All ring specimens failed along the loading diameter (Figure 3.36). Even though secondary crack (Hobbs, 1965) are observed in some specimens, these cracks have no effect on the failure loads (Addinall and Hackett, 1964). The ring tensile strength is obtained from Saraburi marble are averaged as 14.5 ± 0.8 MPa.

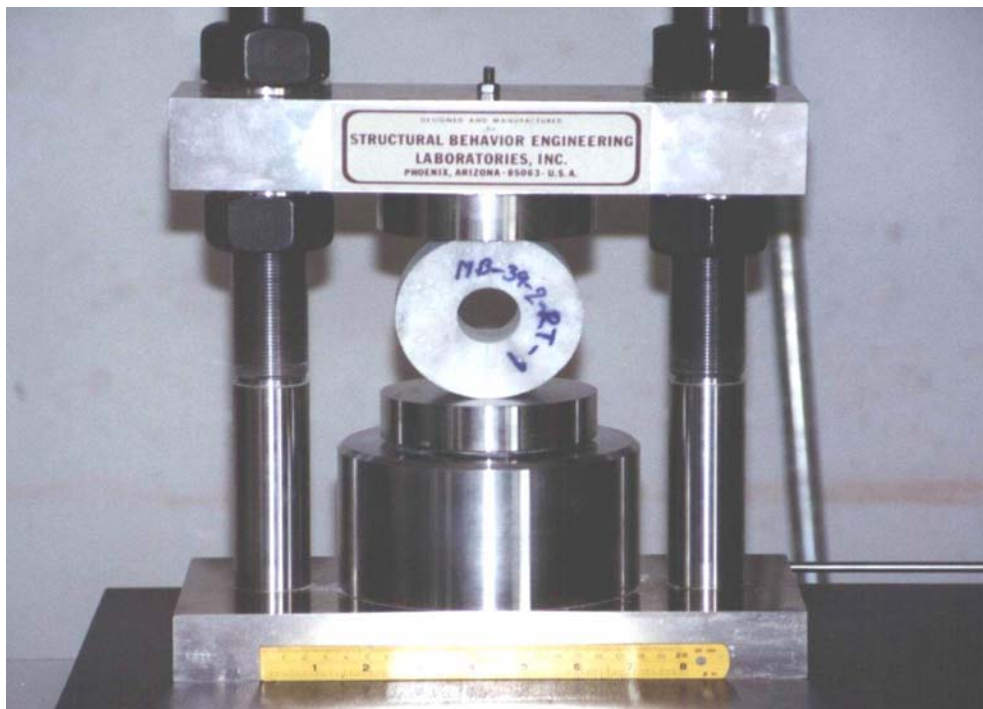


Figure 3.35 A 92.4 mm external diameter and 30.5 mm internal diameter specimen of Saraburi marble used in the ring tension test.



Figure 3.36 The Saraburi marble specimens failed by ring tension test along the loading diameter.

Table 3.7 Results of ring tensile strength tests on Saraburi marble.

Sample No.	External Diameter, D₁ (mm)	Internal Diameter, D₂ (mm)	Thickness, t (mm)	Failure Load, P (kN)	σ_R (MPa)
MB-39-2-RT-1	92.5	30.9	45.7	9.1	14.1
MB-39-2-RT-2	92.6	30.1	46.4	9.5	14.1
MB-39-1-RT-3	92.4	30.4	45.2	9.8	15.2
MB-39-1-RT-4	92.4	29.9	48.1	11.0	15.8
MB-39-1-RT-5	92.3	30.9	47.9	9.2	13.6
			Average	9.7	14.5
			S.D.	±0.8	±0.8

3.5.3 Four-Point Bending Tests

The four-point bending test (Brook, 1993) is conducted on the rectangular beam of Saraburi marble. A 100x350x13 mm³ of rectangular beam specimens are prepared in the laboratory (Figure 3.37). The specimen is loaded until failure along four loading points with a constant spacing of 8 cm. The load at failure is recorded.

The results of the four-point bending tests on Saraburi marble are shown in Table 3.8. The four point bending tensile strength is calculated using an equation (Brook, 1993);

$$\sigma_{\text{bending}} = \frac{3Fl}{2bh^2} \quad (3.9)$$

where σ_{bending} is the four-point bending tensile strength, F is the load at failure, l is the spacing between the loading points, b is the width of rectangular beam specimen, and h is the thickness of specimen. All rectangular beam specimens are failed in the middle as shown in Figure 3.38.

The four-point bending tensile strength of Saraburi marble is averaged as 7.5 MPa with 1 MPa of the standard deviation.

All tension test results will be discussed and compared with MPL results in Chapter five.

3.6 Verification Tests on Other Different Rock Types

3.6.1 Objective

The specific objective is to determine the compressive and tensile strengths of different rock types and use the results to verify the theory and the experiments that have been developed from the Saraburi marble testing. Uniaxial compressive strength tests (UCS), Brazilian tension tests, conventional point load (CPL) tests and modified point load (MPL) tests have been carried out on Saraburi limestone, Khao Somphot limestone and Khok Kruat sandstone.

3.6.2 Uniaxial Compressive Strength Tests

The sample preparation and test procedure follow the applicable ASTM standard (ASTM D2938-86) and ISRM suggested method (Brown, 1981). The L/D equals 2.5. All specimens are loaded to failure under a constant loading rate. Post-failure characteristics are observed.

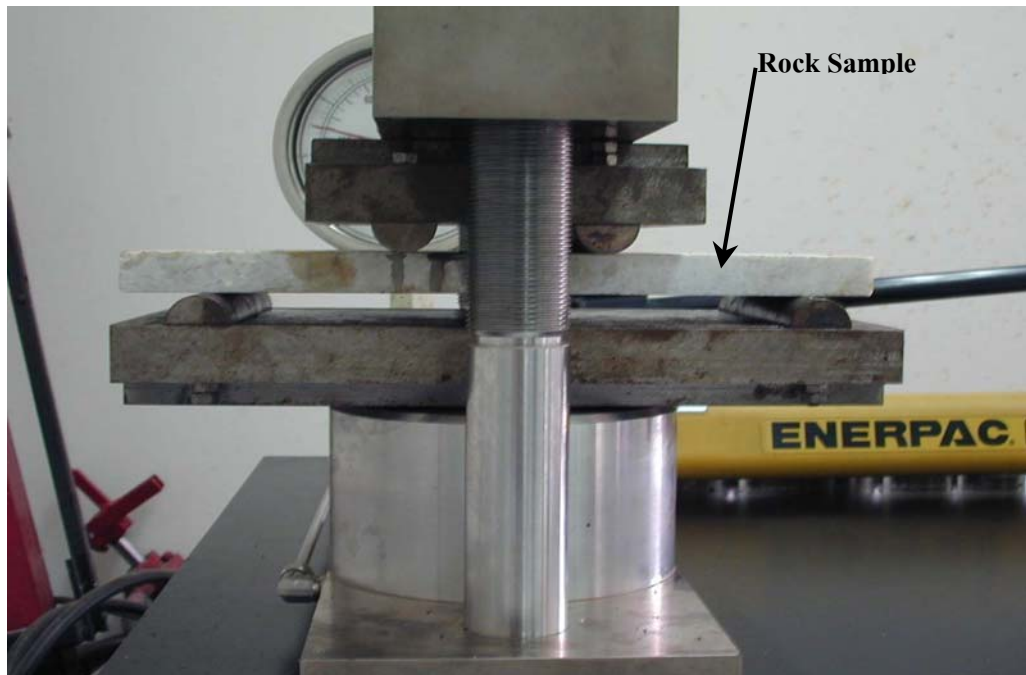


Figure 3.37 A $100 \times 350 \times 13 \text{ mm}^3$ of rectangular beam specimen of Saraburi marble are prepared using in the four-point bending test.

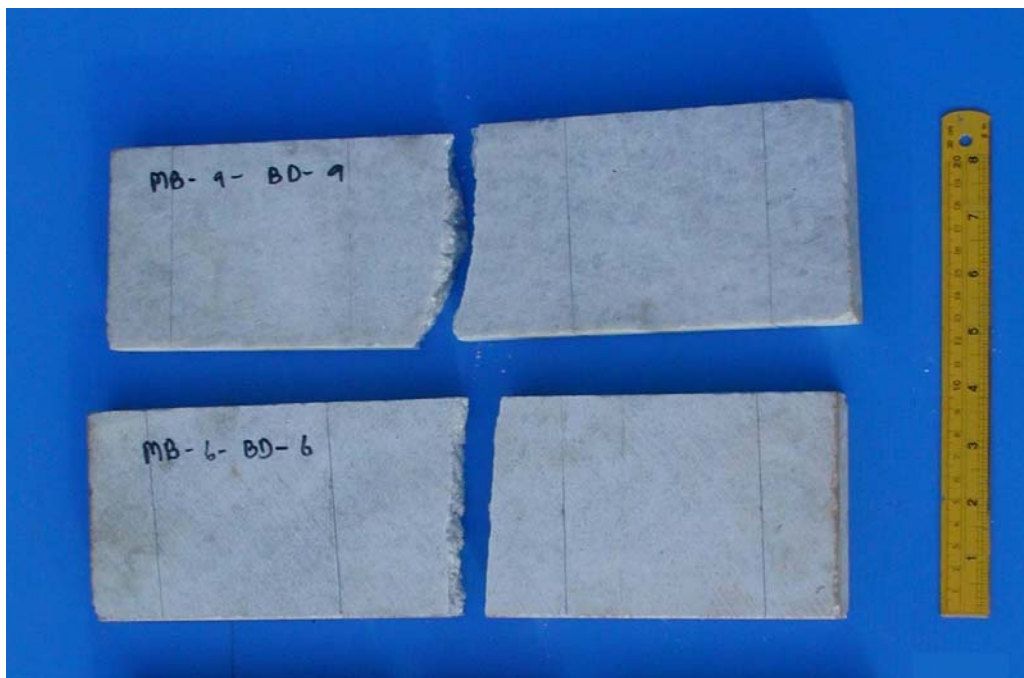


Figure 3.38 Saraburi marble rectangular beam specimen failed by four-point bending tests. The specimens failed in the middle of the beam.

Table 3.8 Results of four-point bending tests on Saraburi marble.

Sample No.	Width, b (mm)	Thickness, h(mm)	Length, L (mm)	Spacing, l (mm)	Failure Load F (kN)	σ_{bending} (MPa)
MB-1-BD-1	100.3	18.2	320	80.0	1.97	7.1
MB-2-BD-2	101.4	18.6	310	80.0	2.12	7.2
MB-3-BD-3	102.3	18.4	290	80.0	1.42	4.9
MB-4-BD-4	101.0	17.9	300	80.0	2.27	8.4
MB-5-BD-5	100.5	18.2	305	80.0	2.17	7.8
MB-6-BD-6	102.0	18.4	300	80.0	2.15	7.5
MB-7-BD-7	101.4	17.3	305	80.0	1.97	7.8
MB-8-BD-8	101.6	18.2	300	80.0	2.15	7.7
MB-9-BD-9	99.8	18.1	300	80.0	2.47	9.1
MB-10-BD-10	100.4	18.0	302	80.0	2.17	7.7
Average					2.01	7.5
S.D.					± 0.27	± 1.1

The UCS test results for each rock type are summarized in Table 3.9. The average UCS of Saraburi limestone, Khao Somphot limestone and Khok Kruat sandstone are 49.3, 43.2 and 21.8 MPa, respectively. The brittle extension fractures (longitudinal splitting) are dominant with some shearing fractures.

3.6.3 Brazilian Tensile Strength Tests

The sample preparation and test procedures have followed the applicable ASTM standards (ASTM D3967-81) and ISRM suggested method (Brown, 1981). All specimens have a constant L/D ratio = 0.5. Each disk is diametrically loaded to failure. An extension fracture usually occurs (failed long the loading diameter). The Brazilian test results for each rock type are given in Table 3.10. The average Brazilian tensile strengths of Saraburi limestone, Khao Somphot limestone and Khok Kruat sandstone are 8.5, 7.8 and 1.5 MPa, respectively.

3.6.4 Conventional Point Load Tests

The test method follows the applicable ASTM standard (ASTM D5731-95) and ISRM suggested method (Brown, 1981). The rock specimens are circular disks for Saraburi limestone and Khok Kruat sandstone, and are irregular lumps for Khao Somphot limestone. Each specimen is axially loaded to failure. Table 3.11 shows the CPL test results for each rock type. The CPL strength index (I_s) is calculated by equation 3.7 and using the relationship $\sigma_c = 24 I_s$ recommended by ASTM D5731-95. The calculated UCS for Saraburi limestone, Khao Somphot limestone and Khok Kruat sandstone are 76.8, 124.8 and 24 MPa, respectively.

3.6.5 Modified Point Load Tests

The rock specimens are the circular disk specimens for Saraburi limestone and Khok Kruat sandstone, and the irregular lumps for Khao Somphot limestone. The irregular shape specimens are carefully selected to allow flat and parallel surfaces for loading. The specimen diameter-to-the loading diameter ratio (D/d) is varied from 2.3 to 11. The thickness-to-the loading diameter ratio (t/d) is varied from 2.5 to 3. Table 3.12 gives a summary of the MPL test results. Figures 3.38 through 3.40 plot the failure stresses (P) as a function of D/d for Saraburi limestone, Khao Somphot limestone and Khok Kruat sandstone, respectively.

Table 3.9 Uniaxial compressive strength test results from different rock types.

Rock Type	Average	Average	L/D	Number	Average	Mean	Standard
	Diameter,	Length,			Density		
	D (mm)	L (mm)		of	(g/cm ³)	Strength, σ_c	(MPa)
				Specimens		(MPa)	(MPa)
Saraburi Limestone	38.23	102.56	2.6	8	2.74	49.3	±18.2
Khao Somphoat Limestone	53.41	126.83	2.4	10	2.77	43.2	±22.2
Khok Kraut Sandstone	53.80	127.40	2.4	7	2.35	21.8	±6.8

Table 3.10 Brazilian tensile strength test results from different rock types.

Rock Type	Average	Average	L/D	Number	Average	Mean Brazilian	Standard
	Diameter,	Thickness,			Density		
	D (mm)	t (mm)		of	(g/cc)	Strength, σ_B	(MPa)
				Specimens		(MPa)	(MPa)
Saraburi Limestone	53.93	25.49	0.5	10	2.66	8.5	±2.5
Khao Somphot Limestone	53.89	25.68	0.5	10	2.68	7.8	±1.0
Khok Kraut Sandstone	53.93	25.50	0.5	5	2.31	1.4	±0.3

Table 3.11 Conventional point load test results from different rock types.

Rock Type	Average Diameter, D (mm)	Average Thickness, t (mm)	t/D	Number of Specimens	Mean Point Load Index, $I_s = P/Dt$ (MPa)	Standard Deviation (MPa)	Prediction of Compressive Strength, $\sigma_c = 24I_s$ (MPa)
Saraburi Limestone	61.75	28.28	0.3	30	3.2	±1.52	76.8
Khao Somphot Limestone	70.66	26.48	0.4	30	5.2	±2.23	124.8
Khok Kraut Sandstone	53.84	25.13	0.5	5	1.0	±0.49	24.0

Table 3.12 Modified point load test results from different rock types.

Rock Type	Average Diameter, D (mm)	Average Thickness, t (mm)	D/d	t/d	Number of Specimens	Mean MPL Strength, P (MPa)	Standard Deviation (MPa)
Saraburi	22.28	57.49	1.1	2.9	4	59.1	±12.5
Limestone	23.47	24.75	2.4	2.5	5	139.8	±27.3
	38.42	26.43	3.8	2.6	5	211.9	±42.4
	53.94	25.77	5.4	2.6	5	301.3	±105.9
	67.05	25.50	6.7	2.6	4	311.3	±114.4
	92.49	27.08	9.3	2.7	4	358.1	±71.9
Khao	50.76	52.61	2.5	2.6	2	96.8	±32.0
Somphot	46.10	39.13	3.6	3.1	2	120.1	±6.6
Limestone	79.75	45.25	5.4	3.3	2	185.0	±95.0
	80.98	41.96	6.1	3.2	3	158.3	±38.0
	83.35	37.06	6.7	3.0	2	179.2	±137.4
	91.30	35.85	7.3	2.9	2	211.8	±42.6
	101.20	34.86	8.1	2.8	2	123.5	±86.6
	55.60	12.76	11.1	2.6	2	196.1	±61.2
Khok Kraut	22.98	25.61	2.3	2.6	5	25.2	±7.7
Sandstone	54.09	27.23	5.4	2.7	5	62.1	±8.0
	67.42	25.00	6.7	2.5	5	98.8	±15.4
	92.84	26.56	9.3	2.7	5	112.1	±11.0

**Modified Point Load Strength
of Saraburi Limestone (t/d=2.5)**

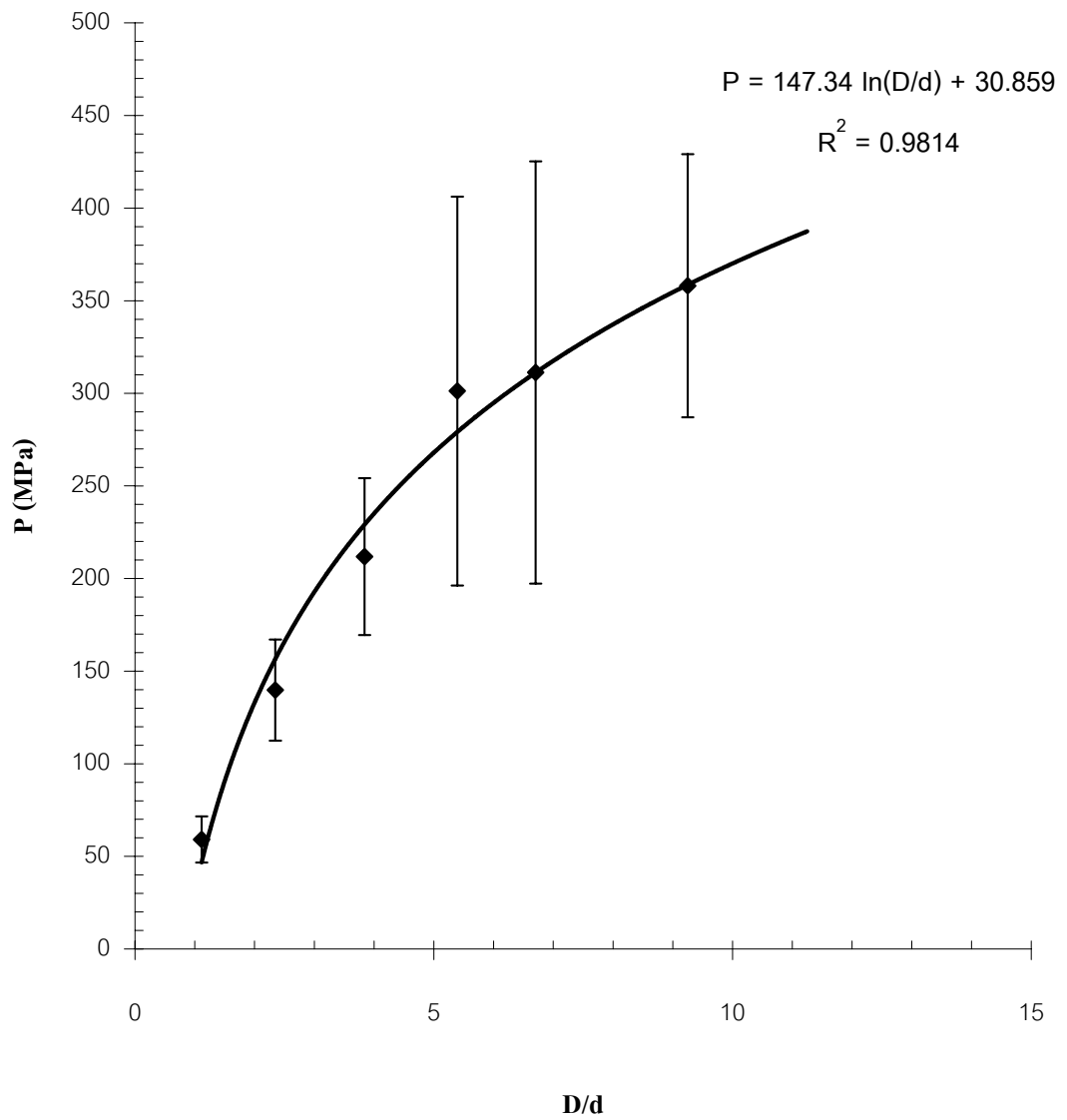


Figure 3.39 Modified point load test results for Saraburi limestone disk specimens with various D/d ratios.

**Modified Point Load Strength on Irregular Shape
of Khao Somphot Limestone (t/d=2.5-3)**

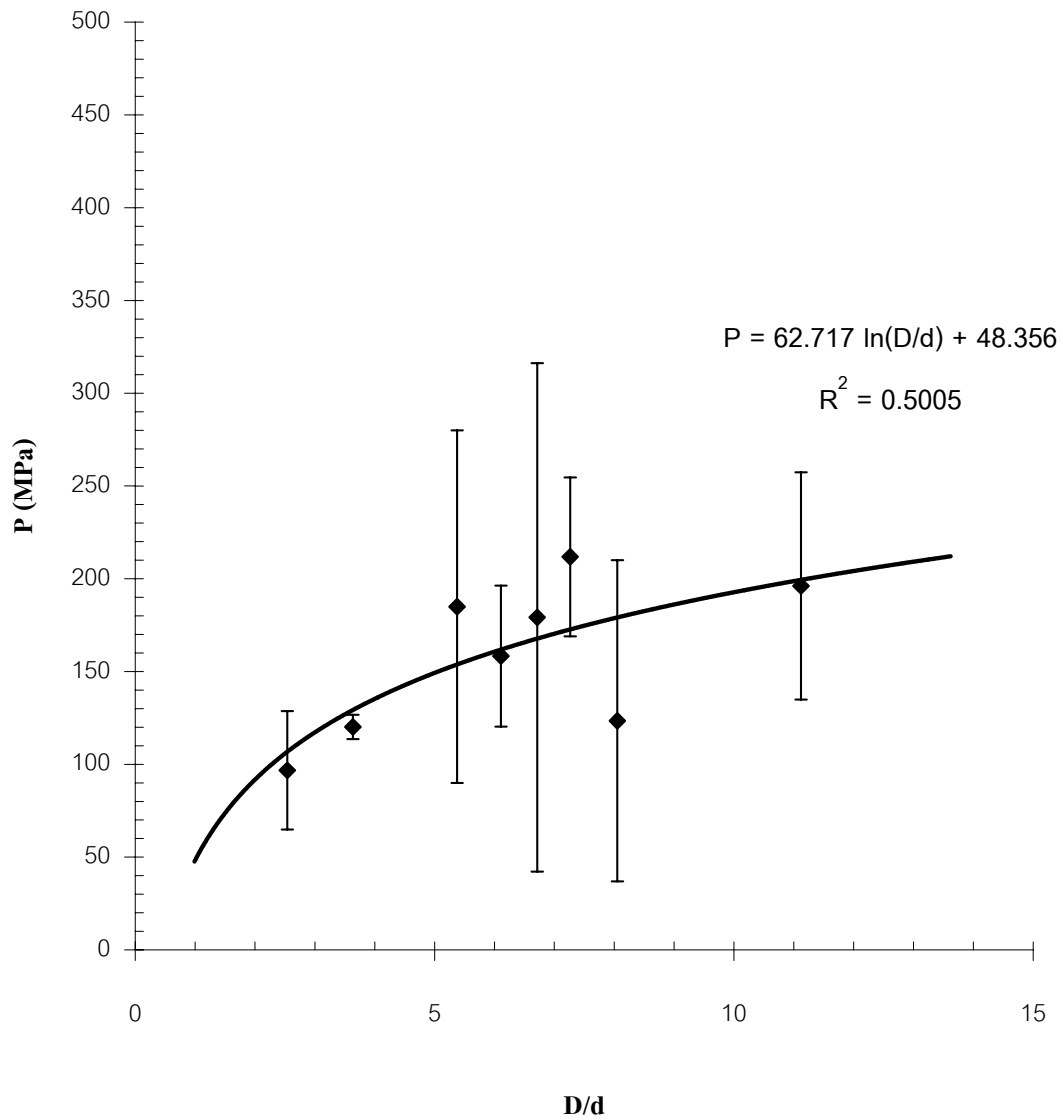


Figure 3.40 Modified point load test results of Khoa Somphoat limestone irregular lumps for various D/d ratios.

**Modified Point Load Strength
of Khok Kruat Sandstone (t/d=2.5)**

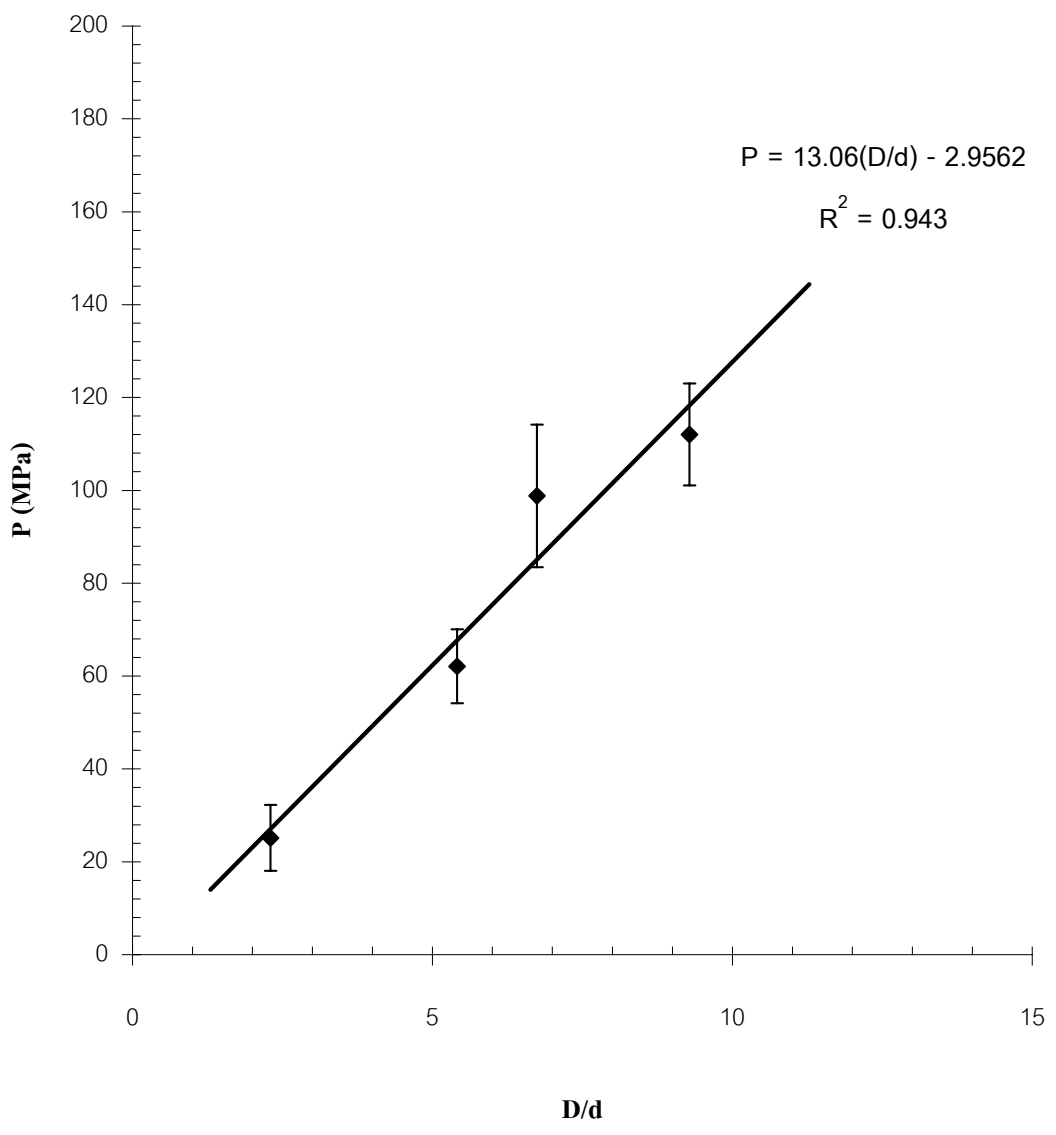


Figure 3.41 Modified point load test results for Khok Kruat Sandstone disk specimens with various D/d ratios.

The results of Saraburi limestone and Khao Somphot limestone can be expressed by a logarithmic equation.

$$P = A \ln(D/d) + B \quad (3.10)$$

where P is the MPL strength (in MPa), D/d is the specimen diameter-to-loading platens diameter ratio, and A and B are constants depending upon the rock specimen diameter (D/d). For Saraburi limestone, A = 147.3 MPa and B = 30.9 MPa. The values of constant A = 62.7 MPa and B = 48.4 MPa for Khao Somphot limestone.

The linear equation is used to fit the test results from Khok Kruat sandstone.

$$P = A(D/d) + B \quad (3.11)$$

where P is the MPL strength (in MPa), D/d is the specimen diameter-to-loading platens diameter ratio, and A and B are constants depending upon the rock specimen diameter (D/d). For Khok Kruat sandstone, A = 13.1 MPa and B = -3.0 MPa.

The MPL predictions of the compressive and tensile strengths are presented in Chapter five.

3.7 Discussions

The UCS results from the various sizes (diameter) have not shown the effects of the size on the compressive strengths. The end effects (shape effects) on the strength values of the specimens can be notably observed. From this investigation, the thin specimens tend to fail under the compression. The extension failure dominates when the specimens are thicker. These effects of L/D agree well with the Brazilian tension test results, which fail in tension mode. The Brazilian tensile strengths decrease with increasing specimen diameter (distance between loading platens).

All results have relatively high standard deviations. Even though the rocks appear to be uniform and homogeneous, the variability might be caused by the inclusions in the marble and the large grain sizes (about 0.3-0.5 cm) of the rock.

CHAPTER IV

FINITE ELEMENT ANALYSES

4.1 Objectives

The main objective of the finite element analyses is to determine the stress distribution along the loaded axis of MPL specimens as affected by the specimen diameter and thickness. The results will be used to correlate between the MPL strength with the compressive and tensile strengths of the rock specimens. The analysis is made in axisymmetric, assuming that the material is linearly elastic, homogeneous and isotropic. A finite element code GEO (Serata and Fuenkajorn, 1992a; Fuenkajorn and Serata, 1993) is used in the simulations.

4.2 Finite Element Mesh

Due to the presence two symmetry planes (horizontal and vertical) across a center of specimen, only one quarter of the specimen has been modeled (Figure 4.1). A total of 57 finite element meshes are constructed for this study. Table 5.1 lists the characteristics of finite element mesh showing that the specimen diameter and thickness have been varied. The smallest elements have an area of approximately 0.25 mm x 0.25 mm. Small elements are used near the loading point boundary, where it will be subjected to high intensity of stress and strain gradients. The finite element mesh and boundary conditions are designed for studying of the thickness effects with a constant diameter as shown in Figures 4.2 through 4.9 (Model Nos. 1-8). Figures 4.10 through 4.16 show the meshes and boundary conditions used for studying the diameter (width) effects (Model Nos. 9-15). The last series of the meshes (Model Nos. 16-57) are used to obtain both thickness and diameter effects and to determine the effects of friction caused by the point load platens.

4.3 Model Parameters

For all models the elastic parameters of the marble are maintained constant. They are obtained from the uniaxial compression test. The elastic modulus is defined as 6.75 GPa, and the

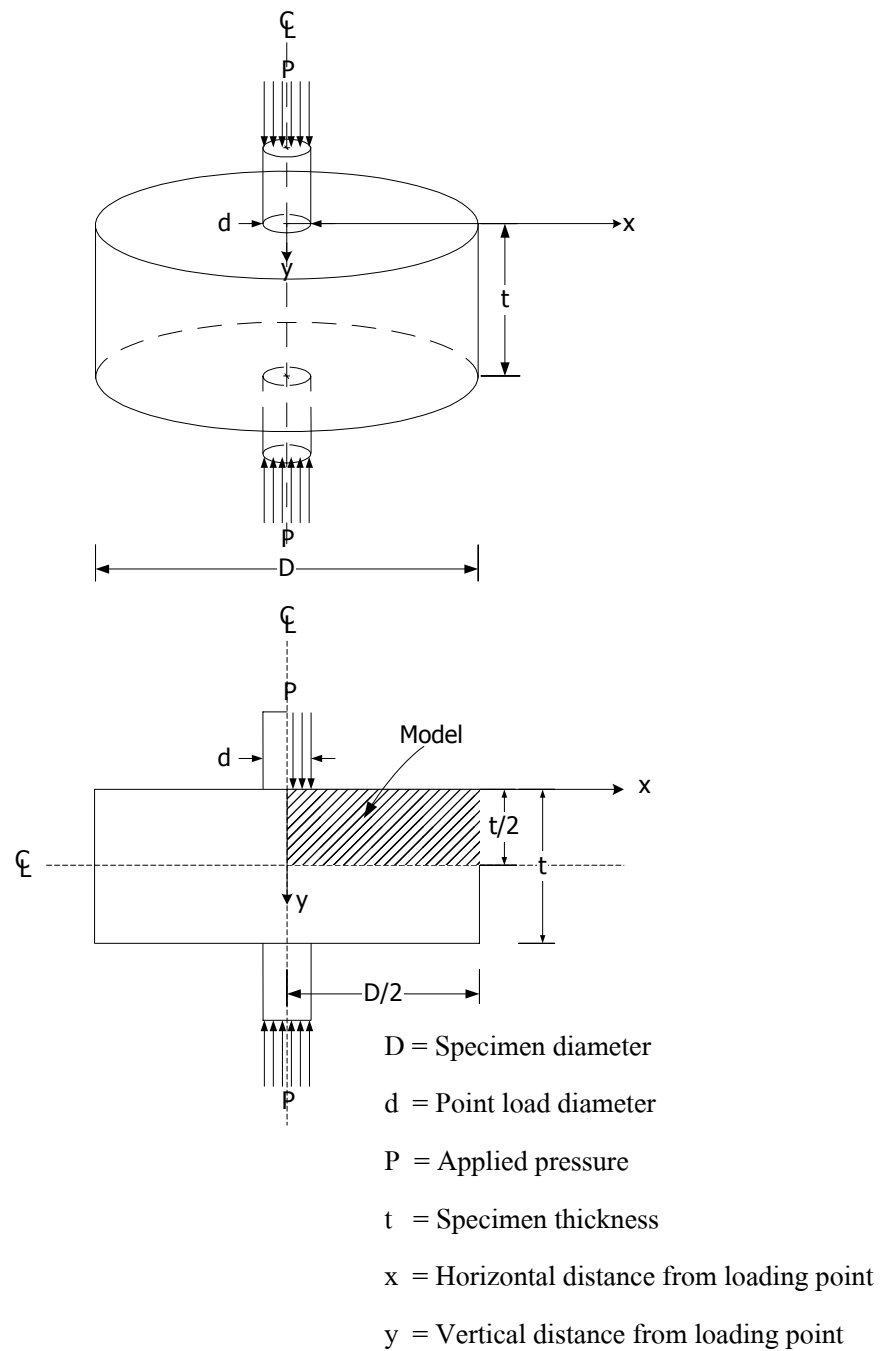


Figure 4.1 Boundary and loading conditions of finite element model used to study the stress distribution within MPL specimen. Due to the presence of two symmetry planes, only one quarter of the specimen needs to be analyzed.

Table 4.1 Characteristics of 57 finite element models constructed to study the effects of the specimen diameter and thickness.

Model No.	Number of Nodes	Number of Elements	D/d	t/d
1	201	158	15	0.5
2	350	306	15	1
3	662	612	15	2
4	972	917	15	3
5	1294	1232	15	4
6	1916	1843	15	6
7	2449	2366	15	8
8	2891	2801	15	20
9	264	230	1	2.5
10	504	460	2	2.5
11	744	690	3	2.5
12	1104	1035	5	2.5
13	1246	1170	10	2.5
14	1276	1196	15	2.5
15	1292	1208	20	2.5
16	231	230	1	2
17	341	300	1	3
18	561	500	1	5
19	649	577	1	10
20	694	613	1	15
21	742	637	1	20
22	441	100	2	2
23	651	600	2	3
24	1071	1000	2	5
25	1223	1144	2	10
26	1295	1207	2	15
27	1343	1249	2	20

Table 4.1 Characteristics of 57 finite element models constructed to study the effects of specimen diameter and thickness (continued).

Model No.	Number of Nodes	Number of Elements	D/d	t/d
28	651	600	3	2
29	961	900	3	3
30	1581	1500	3	5
31	1795	1710	3	10
32	1894	1800	3	15
33	1960	1860	3	20
34	707	660	5	2
35	1044	991	5	3
36	1717	1652	5	5
37	1968	1905	5	10
38	2091	2022	5	15
39	2173	2100	5	20
40	722	670	10	2
41	1062	1005	10	3
42	1752	1682	10	5
43	2023	1955	10	10
44	2161	2087	10	15
45	2253	2175	10	20
46	731	676	15	2
47	1074	1014	15	3
48	1773	1700	15	5
49	2056	1985	15	10
50	2203	2126	15	15
51	2310	2220	15	20
52	738	681	20	2
53	1082	1020	20	3
54	1787	1712	20	5
55	2078	2005	20	10
56	2231	2152	20	15
57	2333	2250	20	20

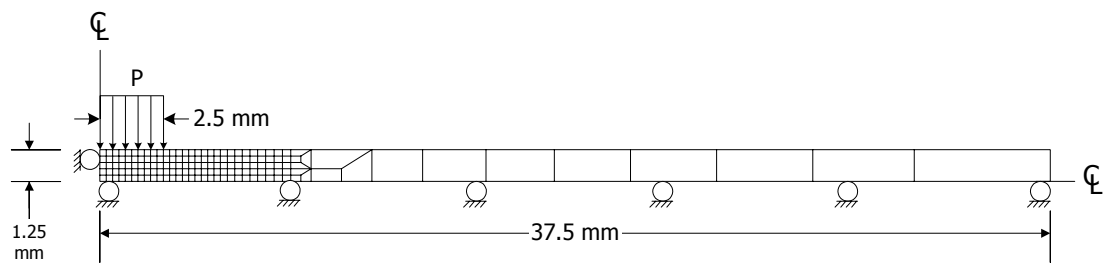


Figure 4.2 Mesh and boundary conditions used in finite element analysis of modified point load test specimen (Model No. 1). It represents 2.5 mm thick specimen with $t/d = 0.5$ and $D/d = 15$.

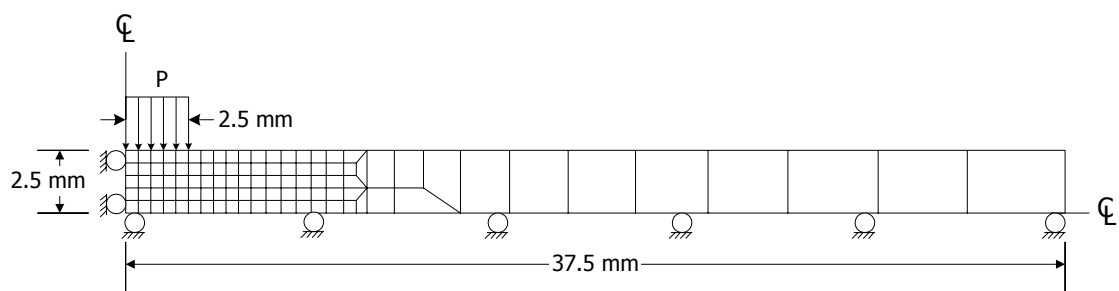


Figure 4.3 Mesh and boundary conditions used in finite element analysis of modified point load test specimen (Model No. 2). It represents 5.0 mm thick specimen with $t/d = 1$ and $D/d = 15$

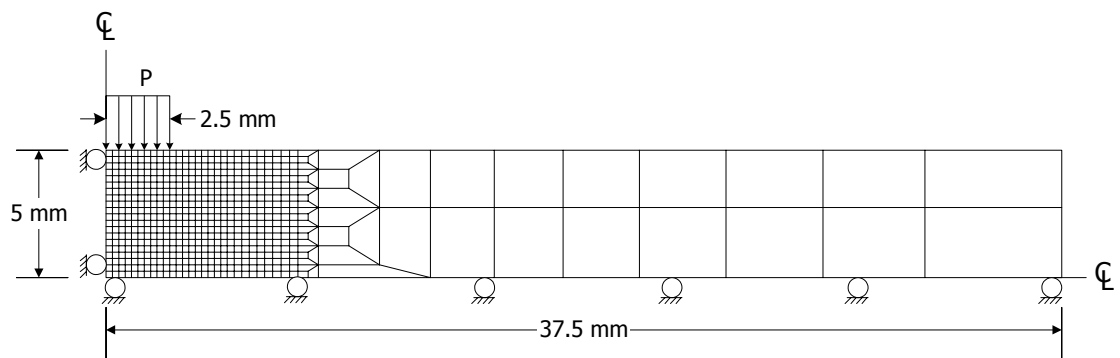


Figure 4.4 Mesh and boundary conditions used in finite element analysis of modified point load test specimen (Model No. 3). It represents 10 mm thick specimen with $t/d = 2$ and $D/d = 15$.

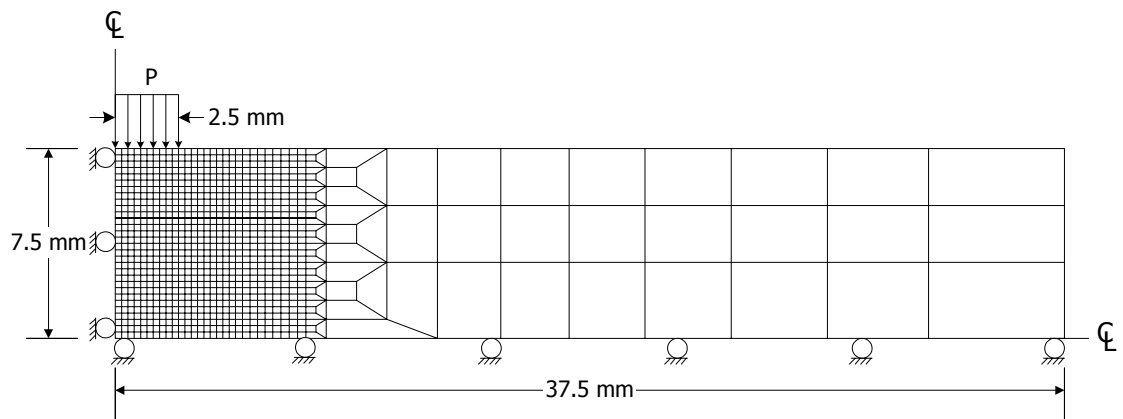


Figure 4.5 Mesh and boundary conditions used in finite element analysis of modified point load test specimen (Model No. 4). It represents 15 mm thick specimen with $t/d = 3$ and $D/d = 15$.

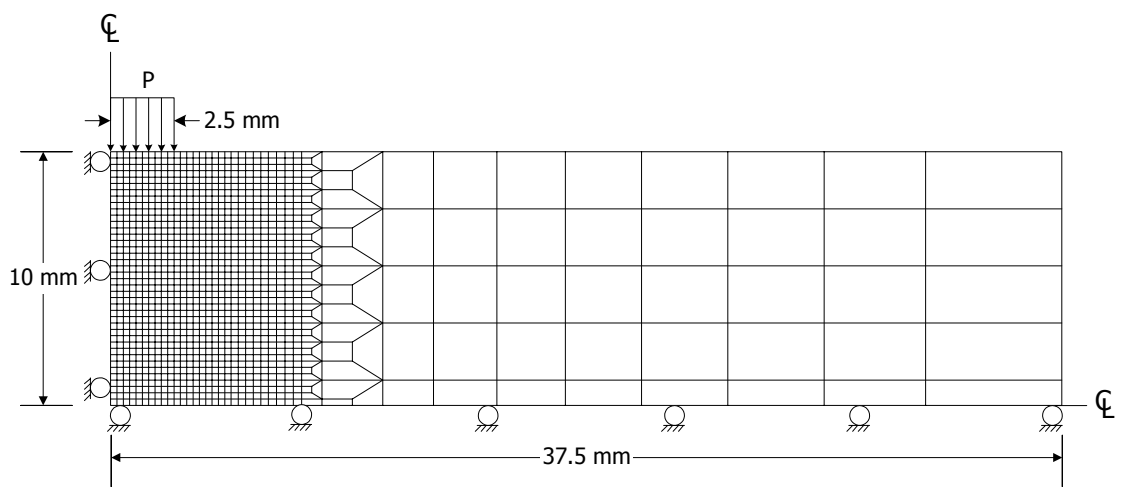


Figure 4.6 Mesh and boundary conditions used in finite element analysis of modified point load test specimen (Model No. 5). It represents 20 mm thick specimen with $t/d = 4$ and $D/d = 15$.

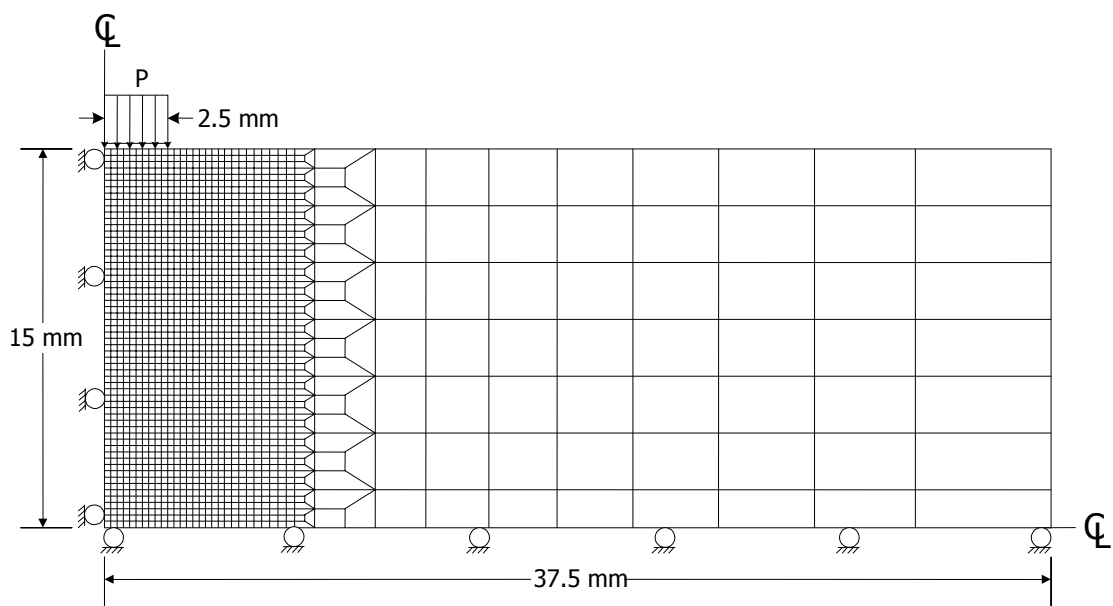


Figure 4.7 Mesh and boundary conditions used in finite element analysis of modified point load test specimen (Model No. 6). It represents 30 mm thick specimen with $t/d = 6$ and $D/d = 15$.

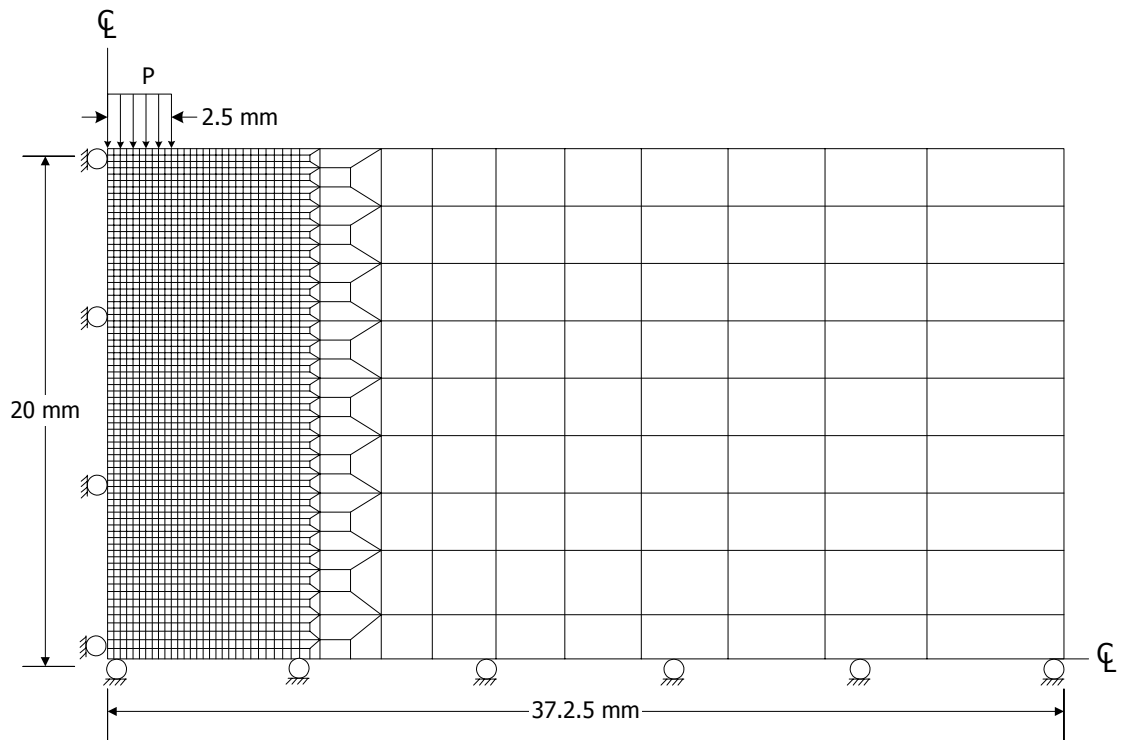


Figure 4.8 Mesh and boundary conditions used in finite element analysis of modified point load test specimen (Model No. 7). It represents 40 mm thick specimen with $t/d = 8$ and $D/d = 15$.

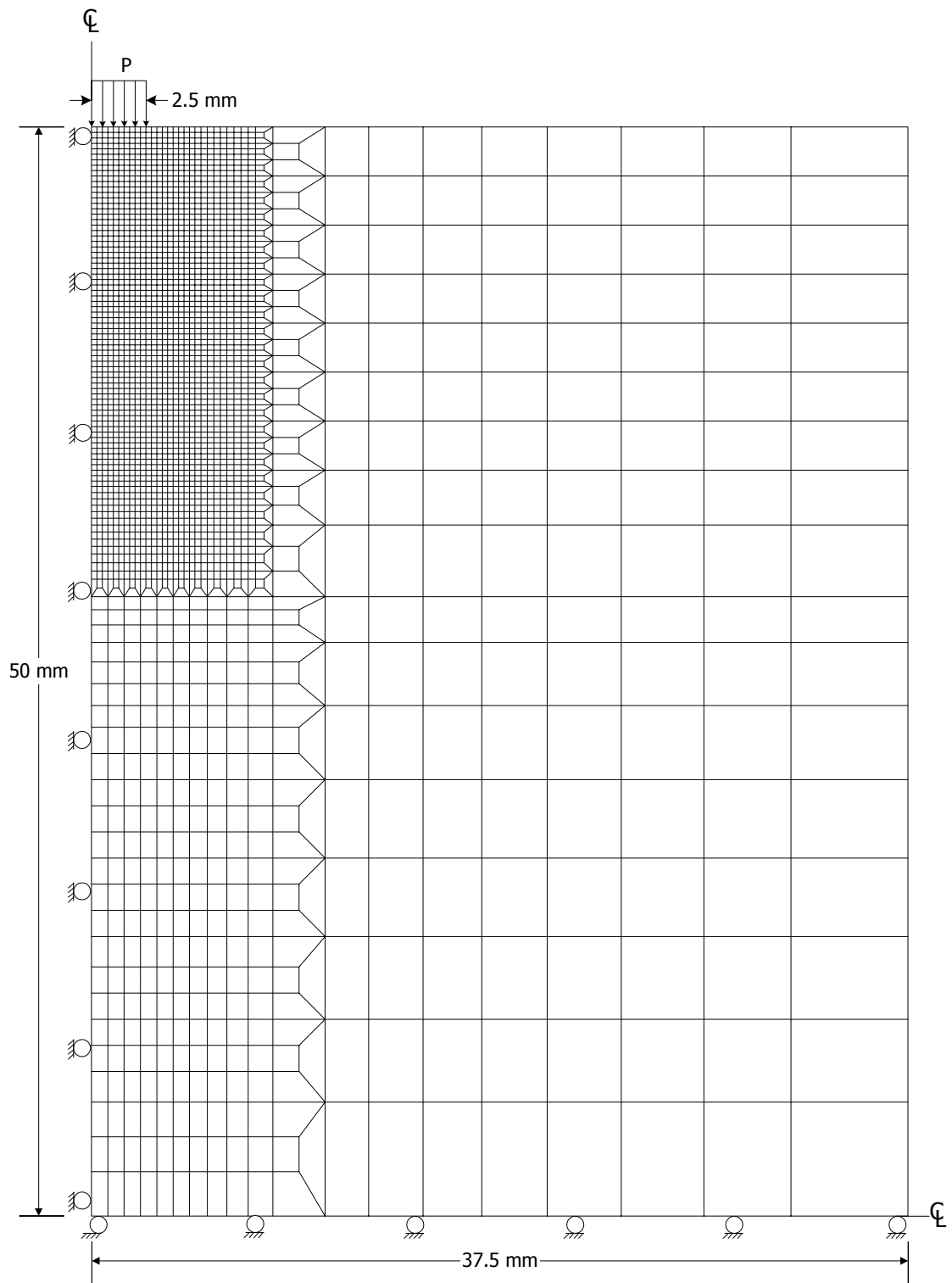


Figure 4.9 Mesh and boundary conditions used in finite element analysis of modified point load test specimen (Model No. 8). It represents 100 mm thick specimen with $t/d = 20$ and $D/d = 15$.

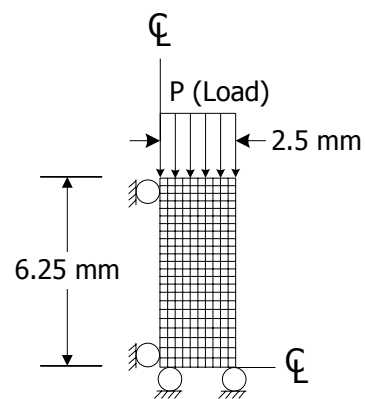


Figure 4.10 Mesh and boundary conditions used in finite element analysis of modified point load test specimen (Model No. 9). It represents 5 mm diameter specimen with $t/d = 2.5$ and $D/d = 1$.

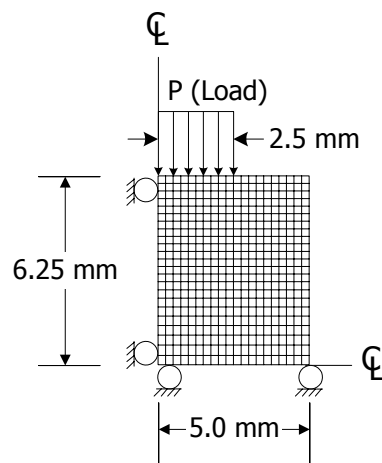


Figure 4.11 Mesh and boundary conditions used in finite element analysis of modified point load test specimen (Model No. 10). It represents 10 mm diameter specimen with $t/d = 2.5$ and $D/d = 2$.

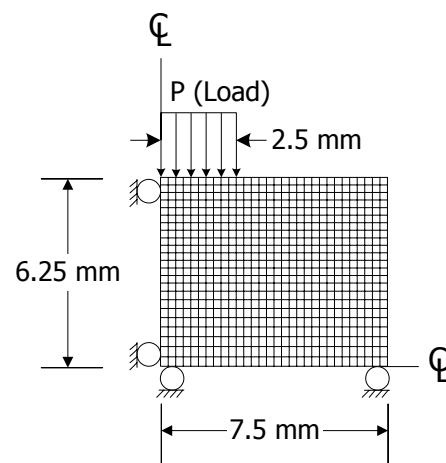


Figure 4.12 Mesh and boundary conditions used in finite element analysis of modified point load test specimen (Model No. 11). It represents 15 mm diameter specimen with $t/d = 2.5$ and $D/d = 3$.

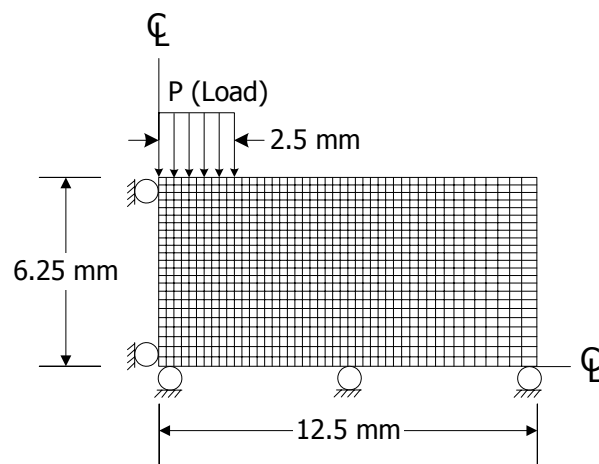


Figure 4.13 Mesh and boundary conditions used in finite element analysis of modified point load test specimen (Model No. 12). It represents 25 mm diameter specimen with $t/d = 2.5$ and $D/d = 5$.

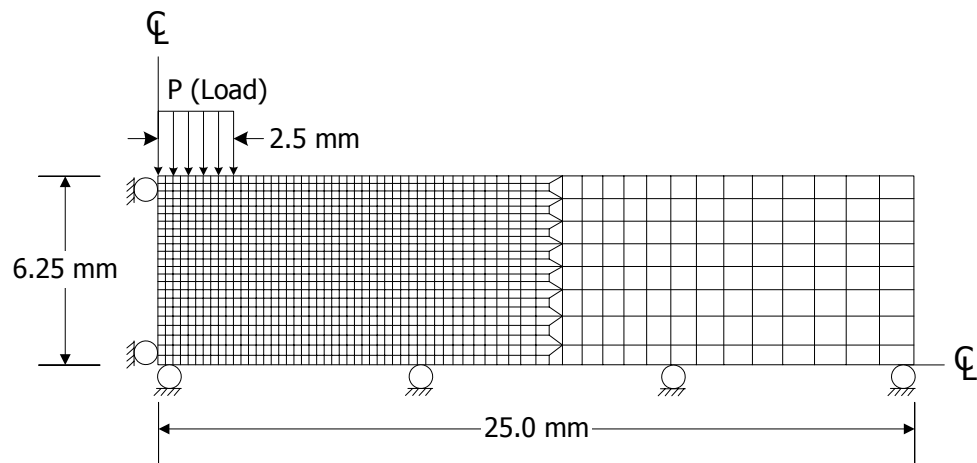


Figure 4.14 Mesh and boundary conditions used in finite element analysis of modified point load test specimen (Model No. 13). It represents 50 mm diameter specimen with $t/d = 2.5$ and $D/d = 10$.

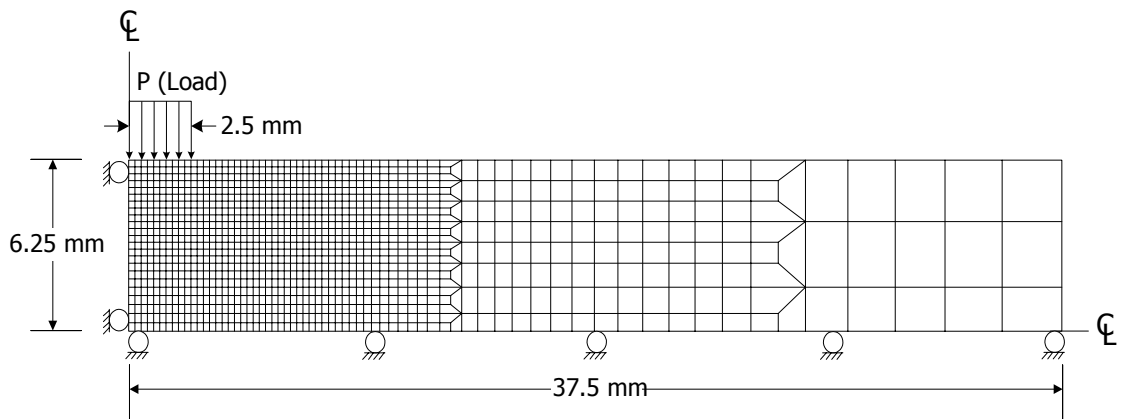


Figure 4.15 Mesh and boundary conditions used in finite element analysis of modified point load test specimen (Model No. 14). It represents 75 mm diameter specimen with $t/d = 2.5$ and $D/d = 15$.

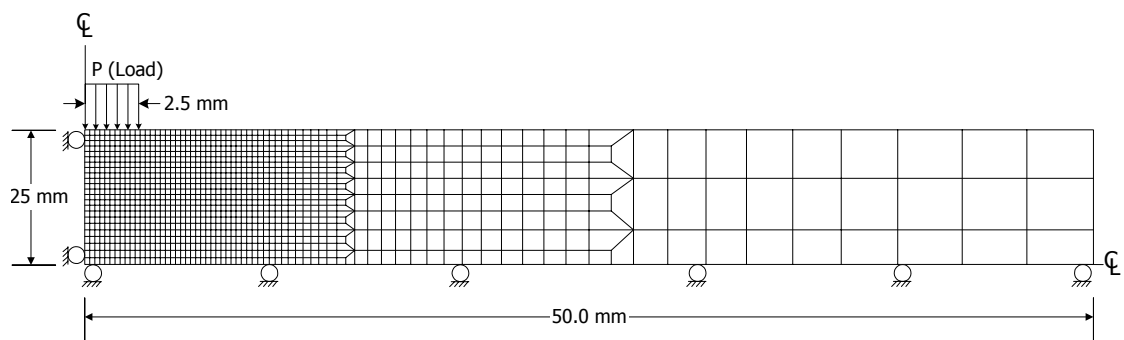


Figure 4.16 Mesh and boundary conditions used in finite element analysis of modified point load test specimen (Model No. 15). It represents 100 mm diameter specimen with $t/d = 2.5$ and $D/d = 20$

Poisson's ratio as 0.25. The specimen diameter (D) and thickness (t) have been varied within the range used in the laboratory experiment, and subsequently their effects on the stress distribution can be assessed. To isolate the impact from the size of loading point, D and t are normalized by the loading diameter (d). The Poisson's ratio has been varied for Model No.4 to investigate the effects of the Poisson's ratio. The values are ranged from 0 to 0.5.

4.4 Modeling Results and Discussions

4.4.1 Effects of Thickness

Figures 4.17 and 4.18 plot the maximum principal stresses (σ_1/P) and the minimum principal stresses (σ_2/P) along the loaded axis for MPL specimen models, respectively. The t/d ratio varying from 1 to 20 with a constant D/d ratio ($D/d = 15$). These stresses are normal to the loaded axis. It is clearly shown that the largest compressive and tensile stress is developed near the loading area. Figure 4.19 shows the distribution of the difference of the maximum and minimum principal stresses ($\sigma_1/P - \sigma_2/P$) along the loaded axis of MPL specimens obtained from finite elements analysis. The maximum value occurs approximately a half distance from the loading point. This point should also be the point where the extension failure initiates. Similar findings have been reported by Wei et al. (1999) for the CPL test specimens. For the t/d is equal or larger than two the magnitude of the largest tensile stress decreases as increasing the t/d ratio. For t/d equals one (very thin specimens), the largest tensile stress decreases. For this case most of the stresses induced along the loaded axis are in compression. This indicates that thin specimens tend to fail under compressive shear failure while thick specimens fail under extension failure. This also agrees with the post-failure observations on the MPL specimens.

4.4.2 Effects of the Poisson's ratio

The distribution of the maximum principal stresses (σ_1/P) and the minimum principal stresses (σ_2/P) along the loaded axis is plotted as a function of distance from the loading point in Figures 4.20 and 4.21, respectively. The Poisson's ratio (ν) varying from 0 to 0.5 with a constant $t/d = 4$ (Model No.4). The effects of the Poisson's ratio only occur on the minimum principal stresses (tension failure). The lower the Poisson's ratio, the larger the tensile stresses. The distribution of the maximum principal stresses has not shown the effects of the Poisson's ratio.

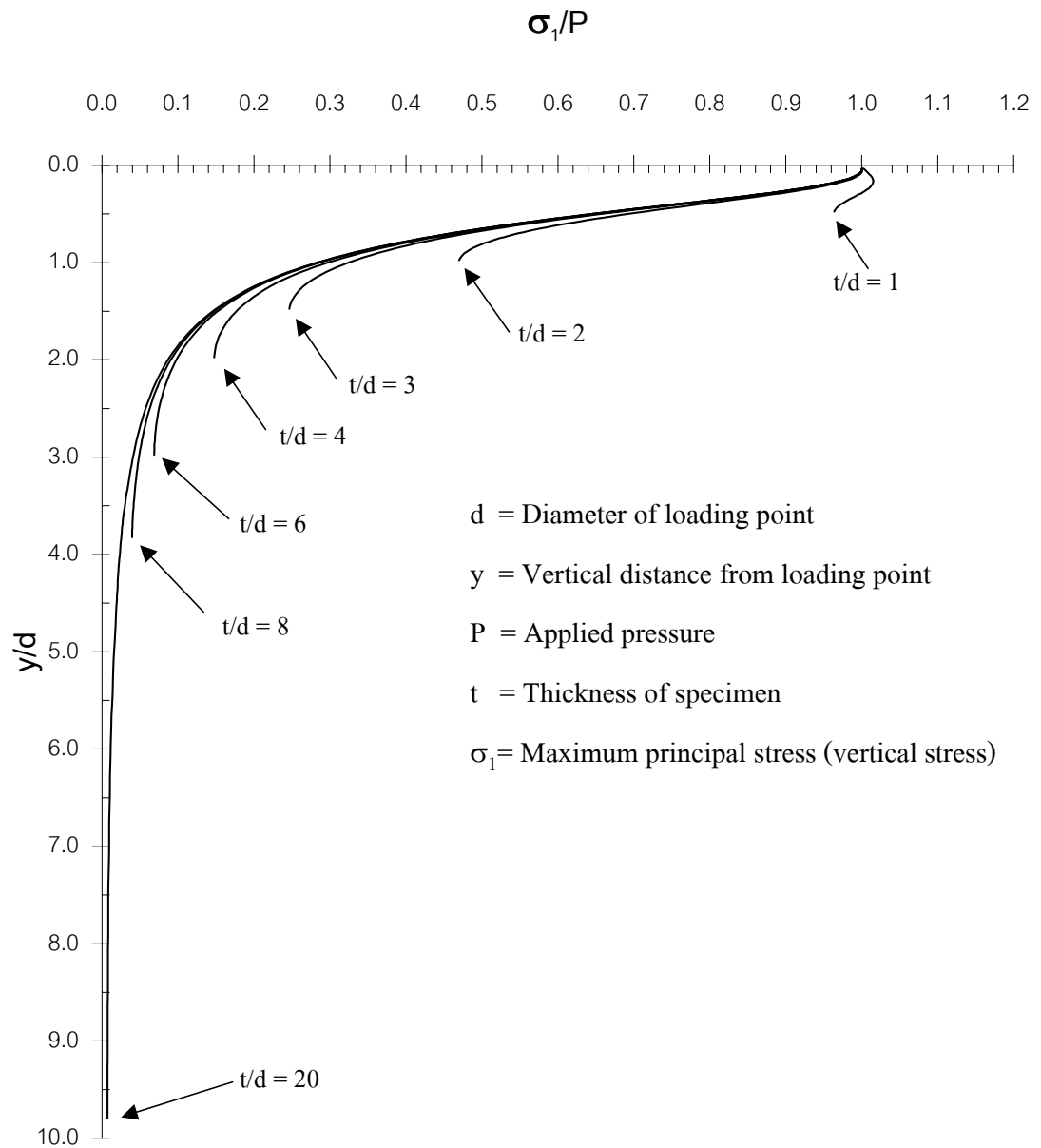


Figure 4.17 Distribution of the maximum principal (σ_1/P) stresses along the loaded axis of MPL specimens obtained from finite elements analysis (Model No. 2 through 8). The t/d varies from 1, 2, 3, 4, 6, 8 to 20 with a constant $D/d = 15$.

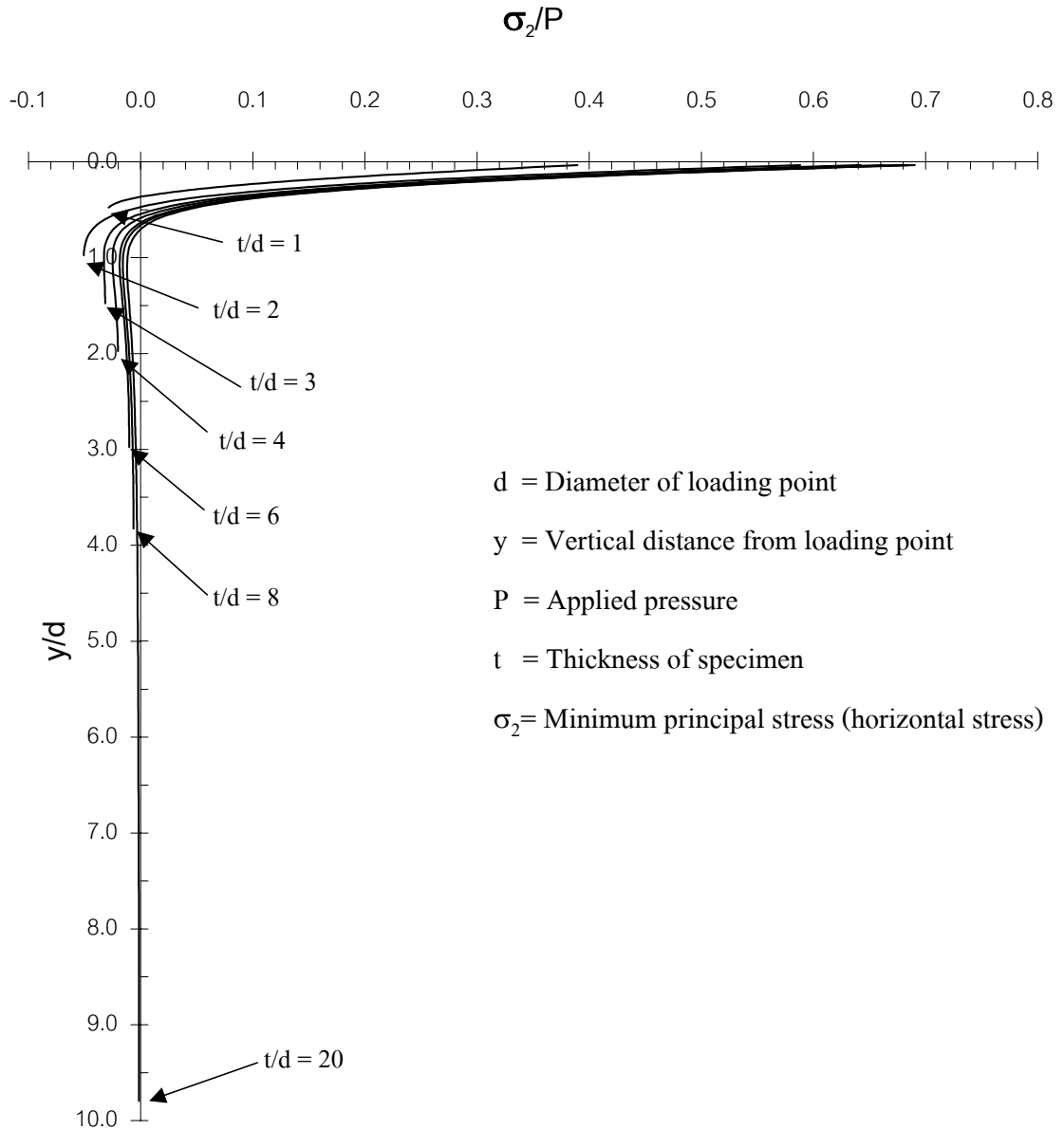


Figure 4.18 Distribution of the minimum principal (σ_2/P) stresses along the loaded axis of MPL specimens obtained from finite element analysis (Model No. 2-8). The t/d varies from 1, 2, 3, 4, 6, 8 to 20 with a constant $D/d = 15$.

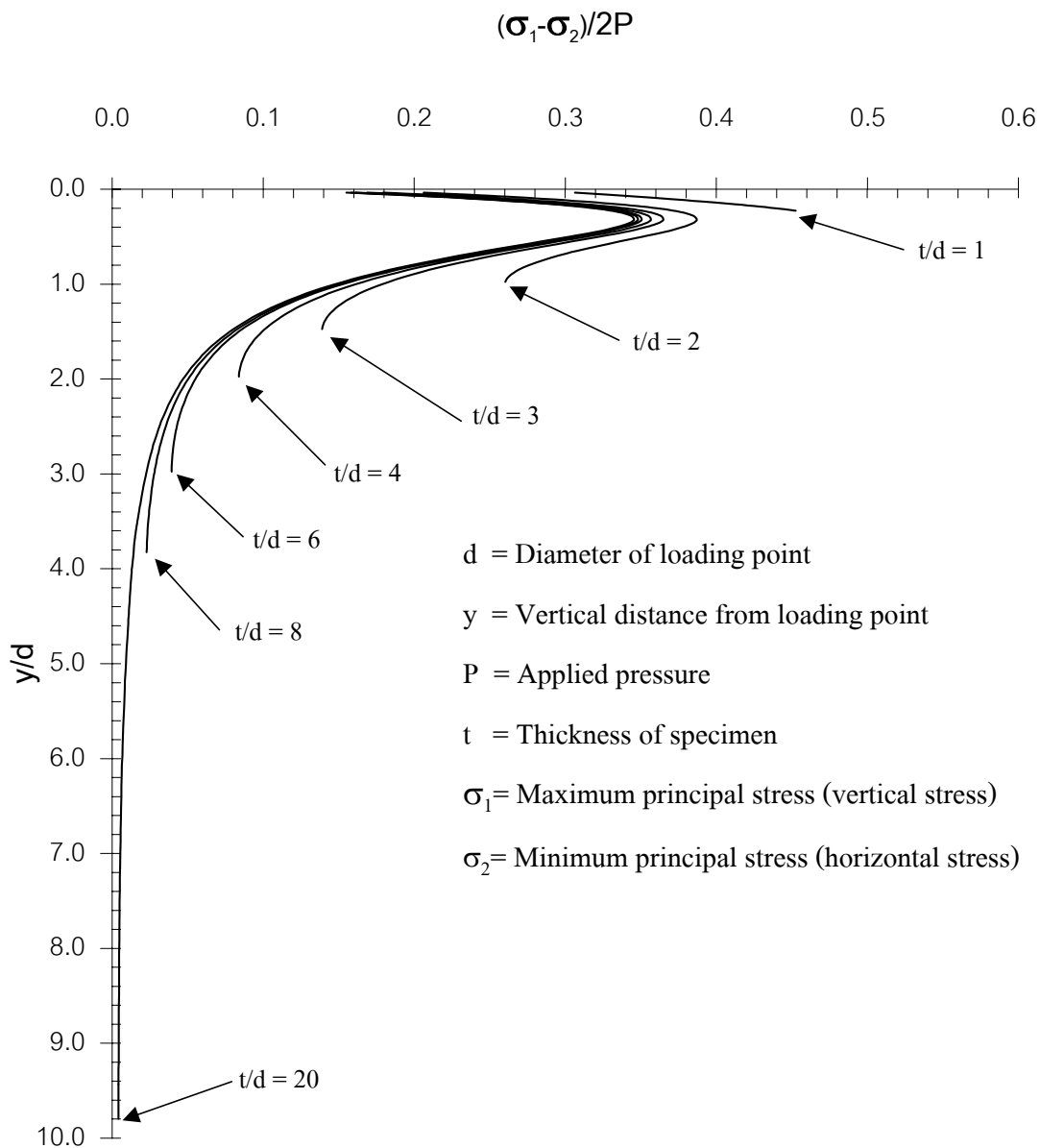


Figure 4.19 Distribution of the difference of the maximum and minimum principal stresses $(\sigma_1/P - \sigma_2/P)$ along the loaded axis of MPL specimens obtained from finite elements analysis (Model No. 2-8). The t/d varies from 1, 2, 3, 4, 6, 8 to 20 with a constant $D/d = 15$.

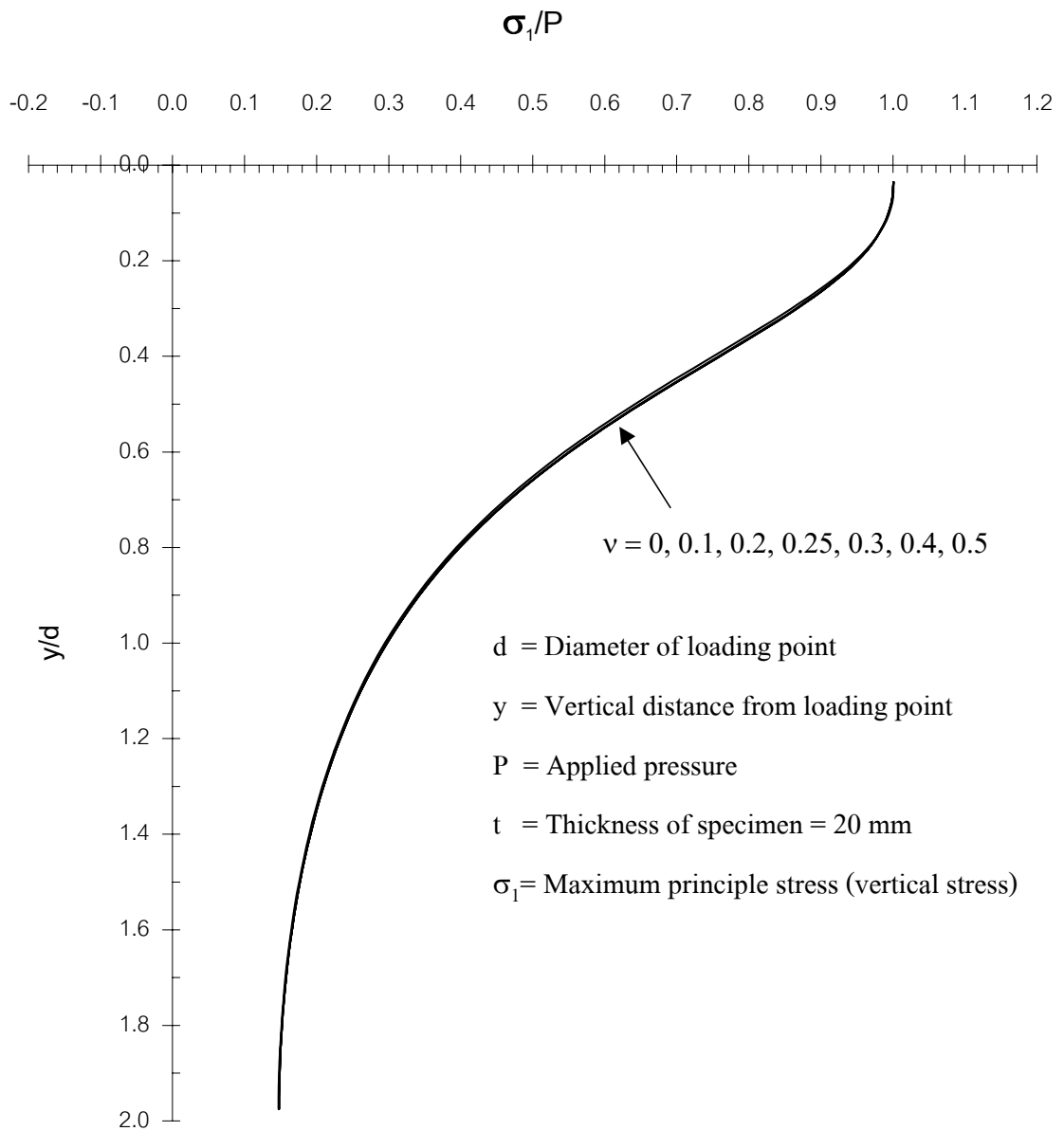


Figure 4.20 Distribution of the maximum principal stresses (σ_1/P) or vertical stresses (σ_x/P) along the loaded axis of MPL specimens using Model No. 5 with $D/d = 15$ and $t/d = 4$. The Poisson's ratio varies from 0 to 0.5. The effects of Poisson's ratio have not been obtained from the simulations.

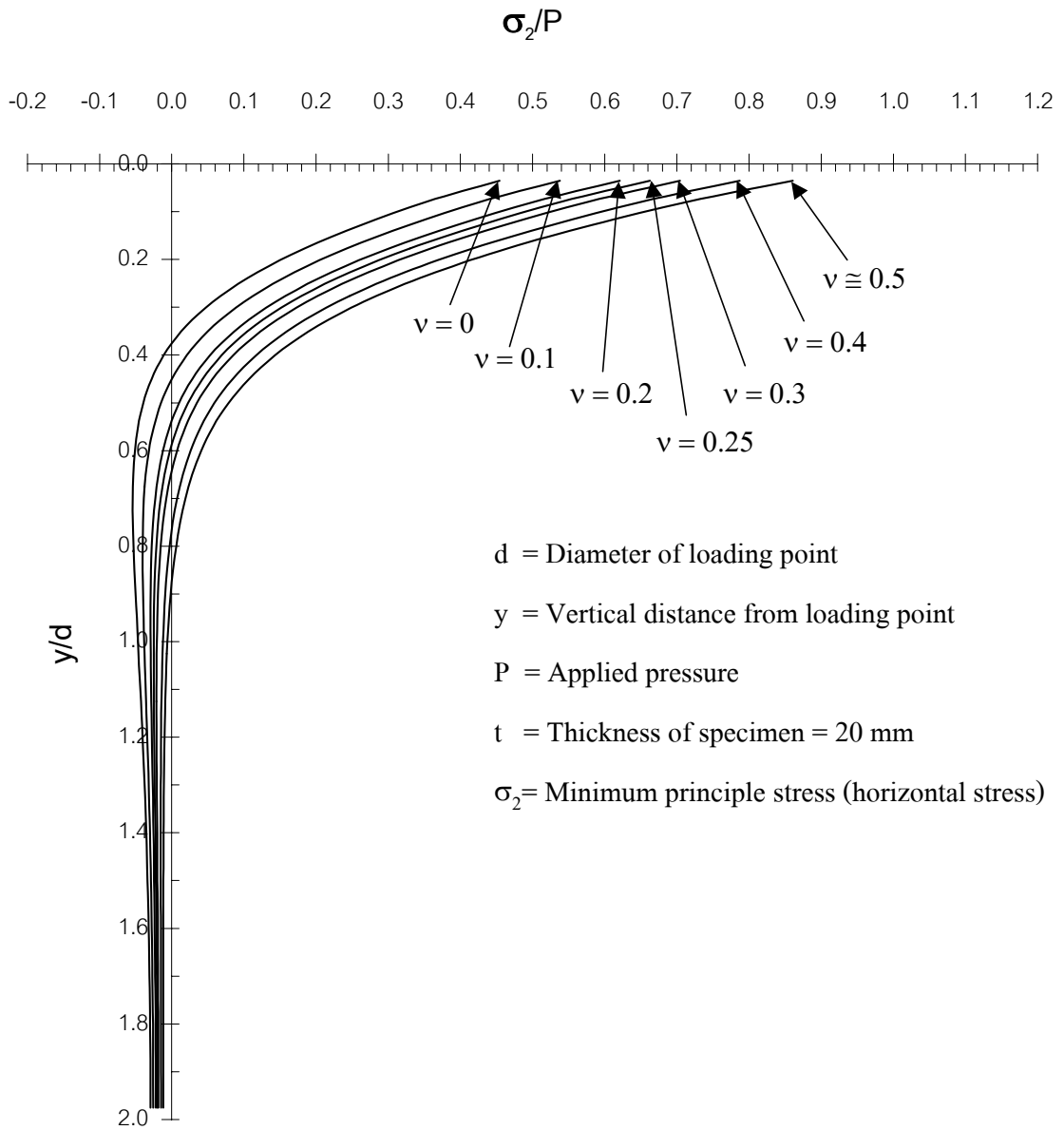


Figure 4.21 Distribution of the minimum principal stresses (σ_2/P) or horizontal stresses (σ_y/P) along the loaded axis of MPL specimens using Model No. 5 with $D/d = 15$ and $t/d = 4$. The Poisson's ratio varies from 0 to 0.5. The effects of Poisson's ratio have been obtained from the simulations.

In practical, most rocks have the Poisson's ratio ranging between 0.2-0.3 with the mean value of 0.25. For the analysis in this study the Poisson's ratio is taken as a constant and equal to 0.25 which represents the nominal value of the rocks.

4.4.3 Effects of Diameter (Width)

Figure 4.22 plots the maximum principal stresses (σ_1/P) along the loaded axis for MPL specimen models obtained from finite element analysis (Model No. 9-15). The D/d ratio varying from 1 to 20 with a constant t/d ratio ($t/d = 2.5$). The values of the σ_1/P at the middle of specimen tend to decrease as the D/d ratio increases. This decrease is clearly shown for $D/d = 1$ through $D/d = 5$. But at the $D/d = 5$ through $D/d = 20$, the values of the σ_1/P does not changed. Figure 4.23 plots the normalized maximum principal stresses (σ_2/P) along the loaded axis. The compressive stresses are developed near the loading area at y/d less than 0.5. The tensile stresses are induced at y/d more than 0.5. The maximum tensile stresses tend to decrease as the D/d ratio increases. For D/d equals one or uniaxial compression test condition, the σ_1/P and σ_2/P are constant throughout the specimen thickness.

4.4.4 Effects of t/d and D/d on P/σ_2

The results obtained from all series of computer simulations are shown in Figure 4.24 and 4.25. The applied stress (P) is normalized by the largest values of the tensile stress (σ_2), and are plotted as a function of t/d and D/d. The stress ratio $-P/\sigma_2$ increases logarithmically with t/d and with D/d. The general relation can be described as follows

$$-P/\sigma_2 = A \ln (t/d) + B \quad (4.1)$$

and
$$-P/\sigma_2 = C \ln (D/d) + D \quad (4.2)$$

where A and B are constants depending upon the rock type and specimen thickness, C and D are constants depending upon the rock type and specimen diameter (as shown in Tables 4.2 and 4.3, respectively).

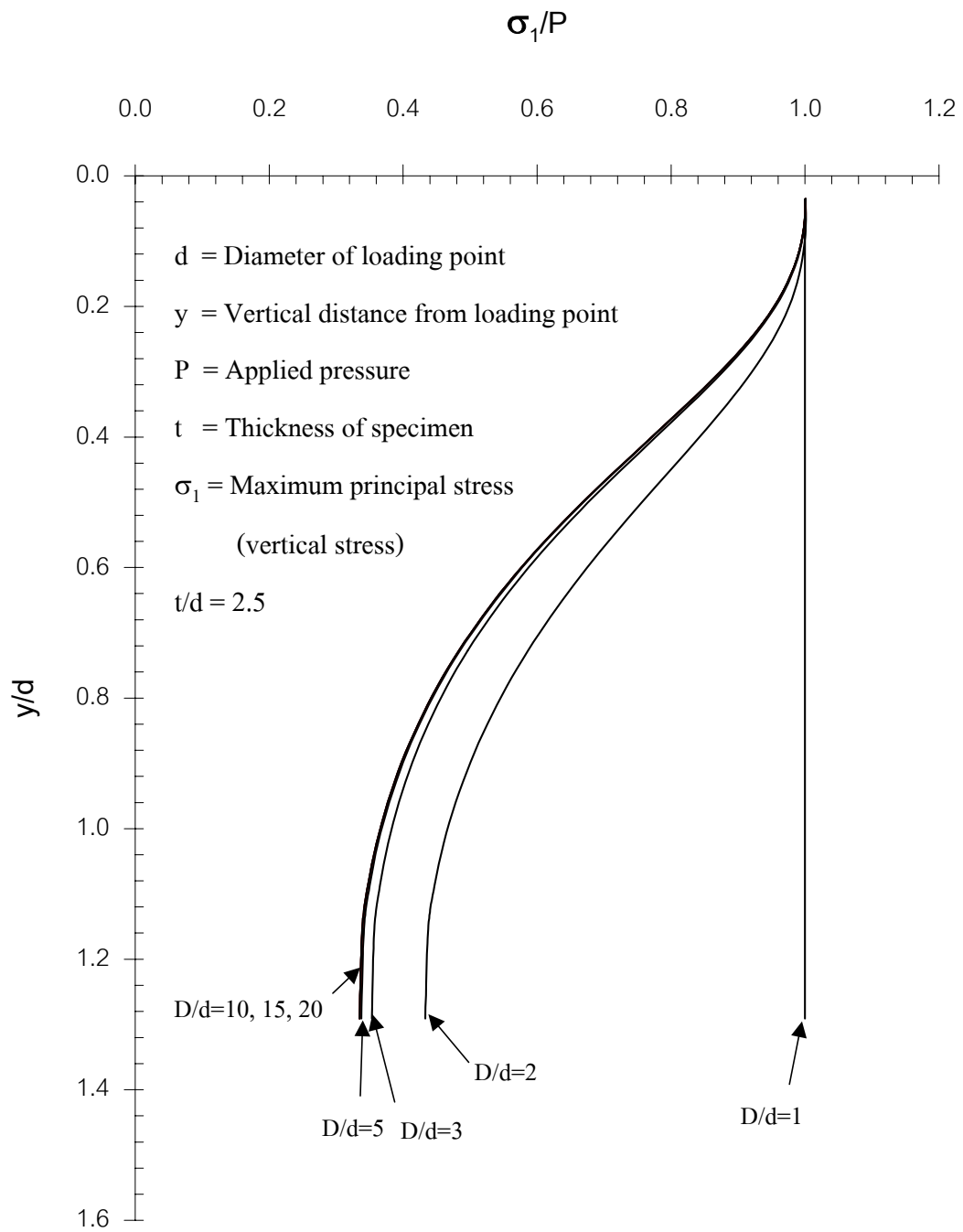


Figure 4.22 Distribution of the maximum principal stresses (σ_1/P) along the loaded axis of MPL specimens obtained from finite elements analysis (Model No. 9-15). The D/d varies from 1, 2, 3, 5, 10, 15 to 20 with a constant $t/d = 2.5$.

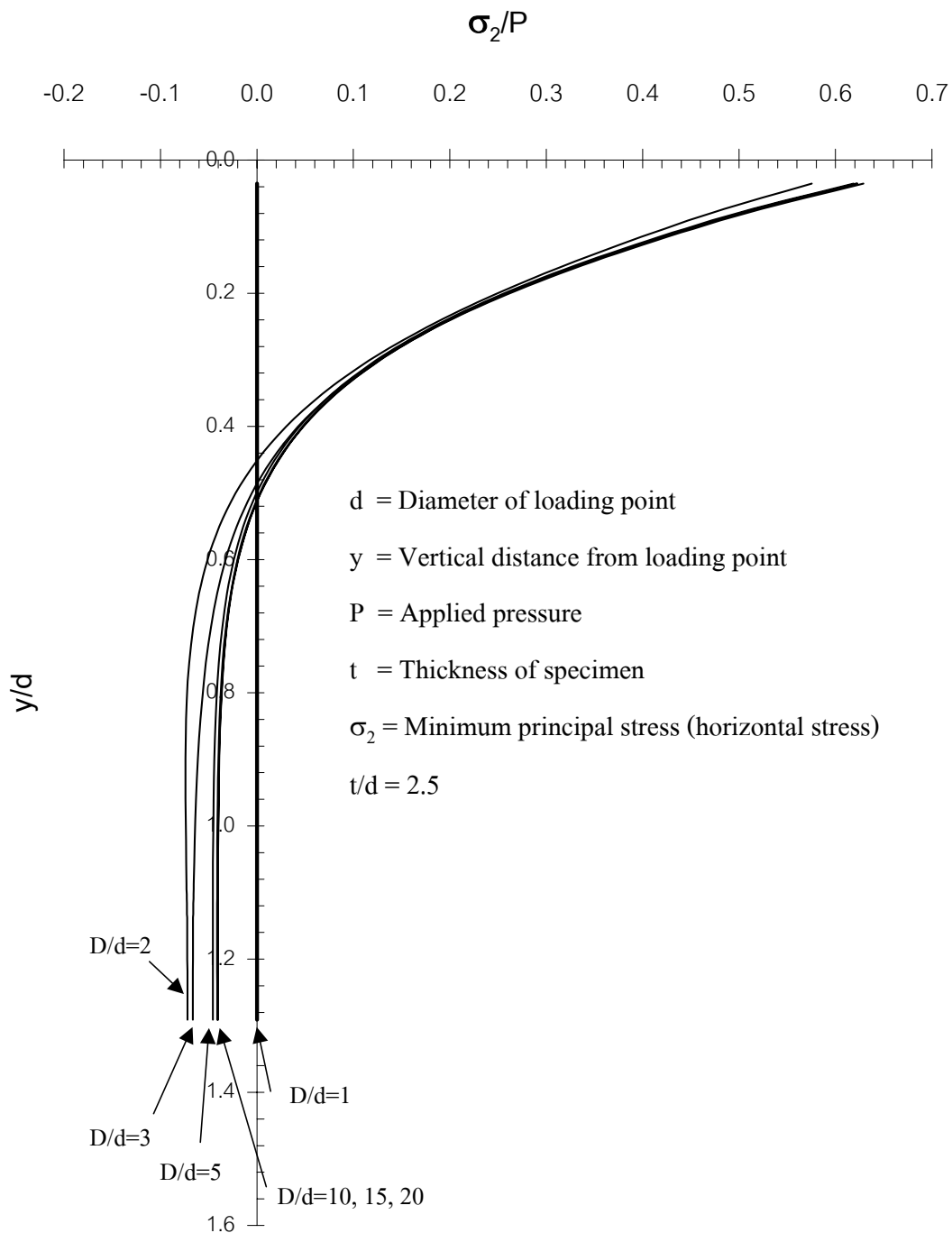


Figure 4.23 Distribution of the minimum principal stresses (σ_2/P) along the loaded axis of MPL specimens obtained from finite elements analysis (Model No. 9-15). The D/d varies from 1, 2, 3, 5, 10, 15 to 20 with a constant $t/d = 2.5$

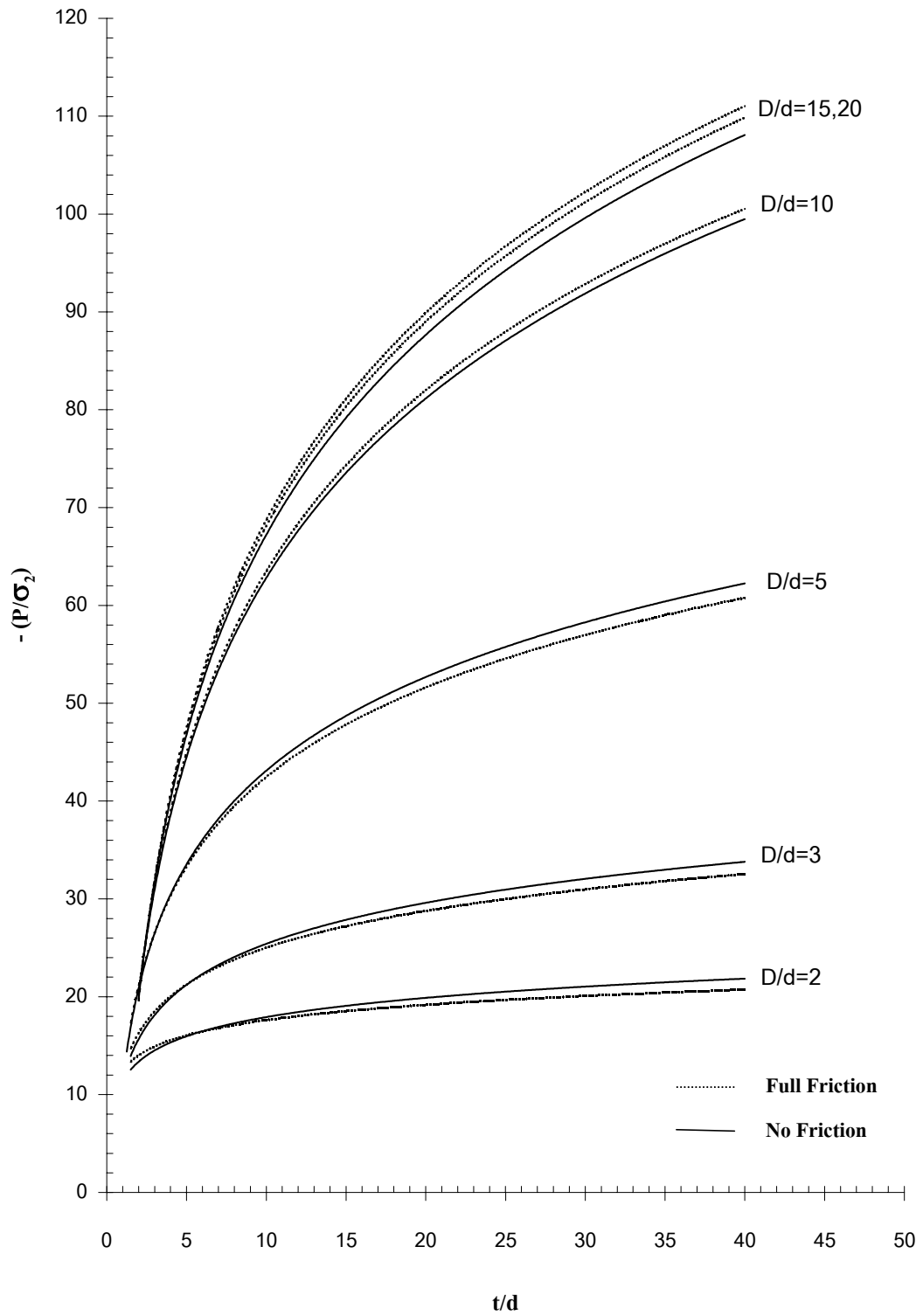


Figure 4.24 Normalized failure stress as a function of t/d , obtained from 57 models.

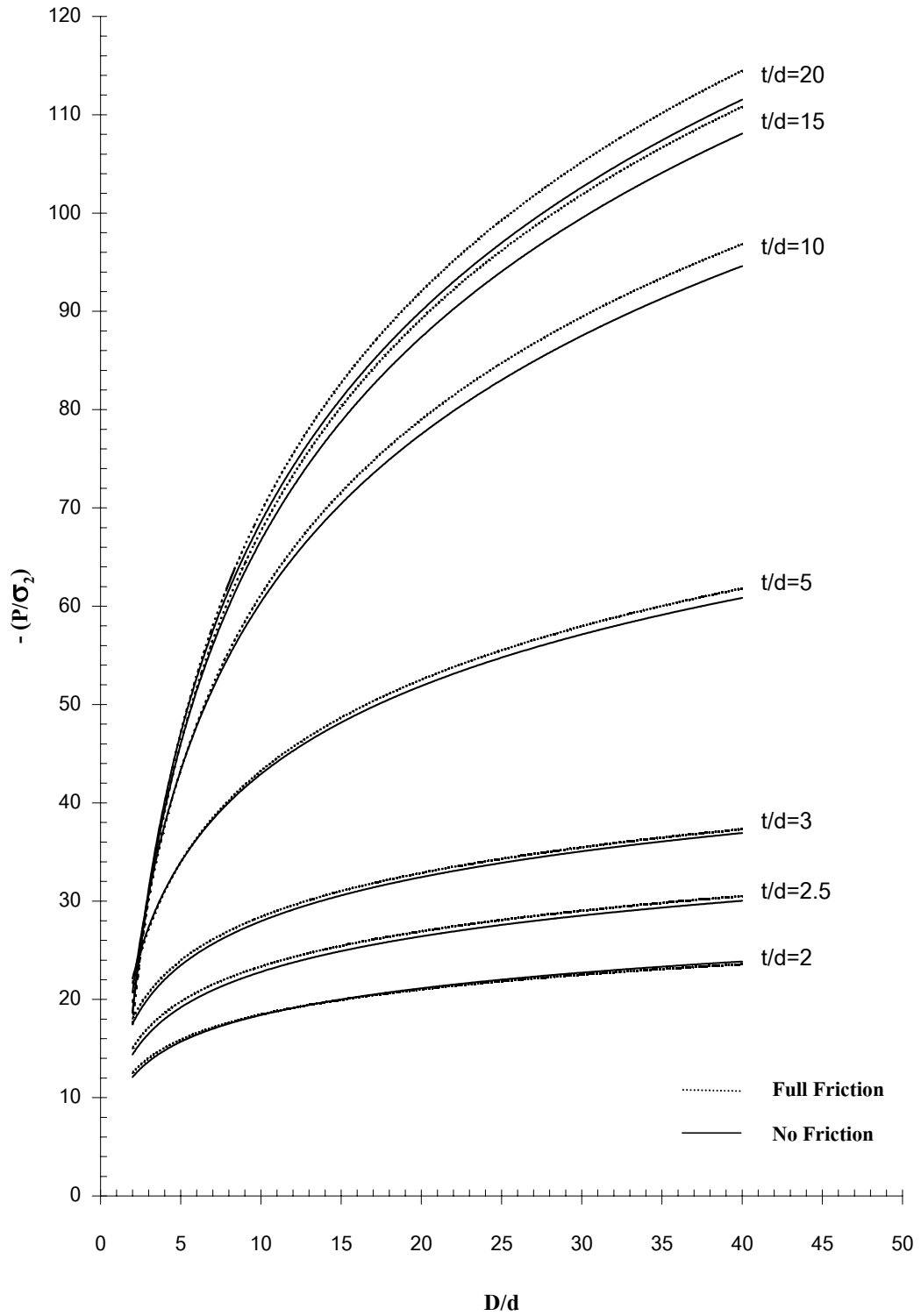


Figure 4.25 Normalized failure stress as a function of D/d , obtained from 57 models.

Table 4.2 Constants in logarithmic relations between $-P/\sigma_2$ and t/d , computed from finite elements analysis.

t/d	No Friction		Full Friction	
	A	B	A	B
2	3.928	9.365	3.691	9.964
2.5	5.219	10.778	5.161	11.468
3	6.474	13.041	6.435	13.586
5	12.928	13.157	13.397	12.387
10	24.665	3.615	25.738	1.881
15	29.862	-2.079	31.145	4.079
20	31.000	-2.821	32.385	4.987

Table 4.3 Constants in logarithmic relations between $-P/\sigma_2$ and D/d , computed from finite elements analysis.

D/d	No Friction		Full Friction	
	C	D	C	D
2	2.834	11.394	2.247	12.439
3	6.046	11.486	5.432	12.502
5	13.809	11.307	13.226	11.986
10	26.455	1.905	26.729	1.935
15	30.118	1.242	29.482	-0.665
20	30.518	-1.538	29.587	-0.992

These curves can be used to correlate the MPL results with the uniaxial compressive strength and tensile strength of the rock in the next chapter.

4.4.5 Effects of the Friction on Loading Platens

Recognizing that the friction at the interface between the loading point and the rock surface may cause the difference in the stress distribution within MPL specimen. To study this effect, the finite element analyses are divided into no-friction cases and full-friction cases. For the full-friction case, the lateral movement is not allowed at the interface. For the no-friction case, the loading area of the rock specimen is allowed to move freely. The minimum principal stresses obtain from the case of full-friction are slightly different (about 2-5 %) from the case of no-friction (Figures 4.24 and 4.25). The actual friction at contact area will be between those two extreme cases. The results of the finite element analysis obtained from two series of the simulations for the difference case studies (no-friction and full-friction at the interface) are relatively small, all analyses in this study therefore assume that no friction occurs at the interface.

CHAPTER V

COMPRESSIVE AND TENSILE STRENGTH PREDICTIONS

The objective of this chapter is to predict the compressive and tensile strength of the rocks by using MPL and CPL tests. The actual uniaxial compressive strength and the tensile strengths of the rocks determined in the previous chapters are compared with the predictions.

5.1 Modified Point Load Predictions

5.1.1 Compressive Strength Prediction

The predictive capability of the modified point load (MPL) test results has been assessed. The MPL test results are used to determine the uniaxial compressive strength of the Saraburi marble. The failure stresses (P) are plotted as a function of specimen diameter (D/d) in Figure 3.14. Extrapolation of a curve fit of the failure stress (P) at $D/d = 1.0$ and $t/d = 2.5$ (uniaxial test condition) yields the uniaxial compressive strength of the Saraburi marble as 63 MPa. This value can be compared with the uniaxial compressive strength at $L/D = 2.5$.

5.1.2 Tensile Strength Prediction

The MPL results determine the rock tensile strength by using the relationship of the failure stresses (P) as a function of specimen thickness (t/d). Extrapolation of the logarithmic curve in Figure 3.13 gives the value of the failure stresses (P) from the experiment equals to 570 MPa (at $t/d = 20$). The $t/d = 20$ is selected because under this dimension ratio the rock fails in tension mode. At $D/d = 5$ and $t/d = 20$, the stress ratio $-P/\sigma_2 = 52$ from the effect of t/d simulation, as shown in Figure 4.25. The tensile strength ($-\sigma_2$) value can therefore be determined as 11 MPa.

5.2 Conventional Point Load Predictions

The ASTM standard recommends a formula relating the CPL index and the uniaxial compressive strength (Broch and Franklin, 1972). The uniaxial compressive strength (σ_c) can be calculated as 24 times the point load strength index (I_s). The CPL strength index of

Saraburi marble determines the uniaxial compressive strength of the rock as 108 MPa (24 x 4.5 MPa). The I_{σ} can not estimate the tensile strength.

5.3 Comparisons and Verifications

The main objective of this section is to compare and verify the theoretical and experimental studies of the proposed MPL test. The comparisons and verifications are made for both compressive strength and tensile strength of the rocks.

The actual compressive strength of the Saraburi marble specimen for L/D ratio = 2.5 (satisfy both ASTM and ISRM) can be calculated from Figure 3.22 as 46.8 MPa. The Brazilian tensile strength of Saraburi marble is determined as 4 MPa. The MPL and CPL predictions of the uniaxial compressive strength are described in previous section. Table 5.1 compares the compressive strength and tensile strength results obtained from different methods. It can be clearly seen that the CPL test overestimates the actual uniaxial compressive strength by a factor of 2.3 (108/46.8). The MPL prediction deviates from the actual value by a factor of 1.4 (63/46.8). The estimation of the uniaxial compressive strength from MPL may be better. The discrepancy is probably due to the non-uniformity of the mechanical response among the marble specimens.

Comparison of the tensile strength results is given in Table 5.2. The MPL tensile strength prediction is significantly higher than the Brazilian tensile strength. This is because the stress gradient along the incipient failure plane of MPL specimens is higher than that of the Brazilian specimens. The effect of the stress gradient on the strength has long been known for the tensile strength test techniques (Jaeger and Cook, 1979). To further demonstrate the effects of the induced stress gradient, additional tensile strength tests have been performed. These include the ring tension test and the four-point bending test. The ring tension test specimen poses the largest tensile stress gradient along the failure plane. It has the largest tensile strength, and it has the tensile strength larger than the MPL test. The four-point bending test and the Brazilian tension test, yield the smaller values. The predicted tensile strength by MPL agrees reasonably well with the results obtained from other methods.

Table 5.1 Comparisons of the compressive strength and tensile strength results.

Rock Type	Uniaxial Compressive Strength (MPa)				Tensile Strength (MPa)	
	Actual σ_c from UCS testing	Standard deviation	CPL prediction	MPL prediction	Brazilian tensile strength, σ_B	MPL prediction
	Saraburi Marble	46.8	17.9	108.0 (disk)	63.0 (disk)	4.0
Saraburi Limestone	49.3	15.1	76.8 (disk)	30.9 (disk)	8.5	17.9
Khao Somphot Limestone	43.2	22.3	124.8 (disk)	48.4 (disk)	7.8	8.9
Khok Kruat Sandstone	21.8	6.8	24.0 (irregular)	10.1 (irregular)	1.5	1.3

Table 5.2 Comparisons of the tensile strength results of Saraburi marble for different test methods.

Test Method	Tensile Strength (MPa)
Brazilian tensile strength test	4.0
Four-point bending test	7.5
Modified point load test	11.0
Ring tensile strength test	14.5

Verification of the proposed concept and results from the Saraburi marble has been made on different rock types. In the verification process, the MPL, CPL, uniaxial compression test and Brazilian tests have been carried out on Saraburi limestone, Khao Somphot limestone and Khok Kruat sandstone. The results are given in Table 5.1. It is clearly seen that the MPL method yields a better prediction of the UCS strength than the CPL method.

CHAPTER VI

DISCUSSIONS

The results from all tests have relatively high standard deviations (about 10–20%). This is because the intrinsic variability or the mechanical non-uniformity among the specimens. This poses some difficulties, particularly in the correlation process. There are some inclusions in the Saraburi marble. The crystals of calcite are large (grain size about 3 to 5 mm), as compared with the loading areas. This could also cause the discrepancy between the prediction and the actual strength results. The impact of the grain size and grain orientation on the mechanisms of failure under the loading points could be one of the significant factors inducing some variation on the strength results. However, these issues are beyond the scope of this study. Future research work on these issues is recommended.

The proposed method of predicting UCS has been developed from Saraburi marble, and has been verified by using different rock types (Saraburi limestone, Khoa Somphot limestone and Khok Kruat sandstone). Comparison of the strength results is given in Table 5.1. For all rock types used in this study, the MPL method yields a better prediction of the UCS strength than does the CPL method. The estimation of the UCS from MPL may be better than does the CPL strength index prediction.

The over prediction by the MPL results may also due to the insufficient data in the range between $D/d = 1$ and $D/d = 5$. Within this range the stress ratio-diameter ratio curves are highly sensitive (high stress gradient) particularly for the low values of thickness ratio (t/d). Therefore, the predictability could be improved by testing more specimens with D/d less than 5.

Despite the intrinsic variability of the marble, the proposed MPL test is a promising method of predicting the compressive strength of the rock. More MPL test data are needed to further define the effects of the specimen thickness (t/d) and diameter (D/d). Additional computer modeling is desirable to obtain the variation of MPL results under a wider range of specimen dimensions. Verification of the proposed concept under a wider range of rock types is also desirable.

The comparisons of tensile strength results obtained from the MPL prediction with those from the Brazilian tension test, the ring tension test and the four-point bending test show notably discrepancies. This is due to the fact that the tensile stress gradient induced along the incipient crack for the MPL specimen is significantly higher than the Brazilian specimen and the four-point bending specimen. But it has stress gradient lower than the ring specimen.

For the finite element analysis in this study the Poisson's ratio is taken as a constant at 0.25 which represents the nominal value of the rocks. The Poisson's ratio has no effect on the magnitude and distribution of the vertical stress along the loading axis. It has some effect on the induced tensile stress (horizontal stress). In practical, most rocks have the Poisson's ratio ranging between 0.2-0.3. The mean value of 0.25 used here is therefore appropriated.

The effects of the friction at the interface between the loading platen and rock surface are studied in the computer simulation. The tensile stresses obtained from the full friction case are slightly lower (by 2-5%) than those from the no-friction case. It is recognized that the actual friction at the interface will be between those two extreme cases. Since the differences are relatively small, all analyses in this study assume that no friction occurs at the interface.

The machine used may have a limitation on the loading required to fail the rock specimens for the MPL testing, particularly in the field. The laboratory test machine normally has the maximum loading capacity of up to 350 kN, which is adequate to fail most rocks even when using the large loading points (e.g., 15 or 20 mm diameter) and large specimens. The equipment used in the field normally has the maximum load as low as 50 kN. This may limit the types of rocks that can be tested. For example, when using $d = 15$ mm with the 50 x 50 mm specimen size, the maximum rock strength that can be tested may be less than 130 MPa.

The investment cost of the MPL testing is significantly lower than the UCS testing. This is because the expensive machines used in the rock sample preparation and testing become unnecessary, particularly when using the MPL test on irregular lumps. The comparisons of the investment cost, the operating time and power, and the estimate unit cost are shown in Tables 6.1 through 6.3, respectively. The investment cost for the UCS testing can be as high as 2.4 million bahts while the MPL testing on irregular lumps need only the point load tester machine which may cost as less 0.19 million bahts. In the complete process of the UCS testing (coring, cutting, grinding and testing), the electric power is normally consumed about 800 watts per tested

specimen while the MPL testing uses human power to operate the point load tester, and therefore does not need electric power during the test. More than 50 percent of energy per specimen are reduced for MPL testing.

In the long run, considering the investment cost and the operating cost, the UCS testing yields a unit cost of about 800 bahts per specimen while the MPL testing yields a unit cost of about 400 bahts per specimen (for testing on disk specimen) and about 50 bahts per specimen (for testing on irregular shape specimens).

Table 6.1 Comparisons of the investment costs between UCS test and MPL test.

Testing Methods	UCS Test	MPL (or CPL) Test	
Investment Cost	core	disk	Irregular shape
Specimen preparations equipment	Drilling machine (700,000 Bahts)		-
	Cutting machine (540,000 Bahts)		-
	Grinding machine (600,000 Bahts)	-	-
Testing equipment	Loading machine(570,000 Bahts)	Point load tester (190,000 Bahts)	
Total capital cost	2,410,000 Bahts	1,430,000 Bahts	190,000 Bahts

Table 6.2 Comparisons of the operating costs between UCS test and MPL test.

Testing Methods	UCS Test	MPL (or CPL) Test	
Operating Cost	core	disk	Irregular shape
Preparations time	40 min/specimen	20 min/specimen	2 min/specimen
Testing time	30 min/specimen	5 min/specimen	5 min/specimen
Total operation time	70 min/specimen	25 min/specimen	7 min/specimen
Electric power used	800 watts/specimen	400 watts/specimen	0 watts/specimen

Table 6.3 Comparisons of the estimate unit costs between UCS test and MPL test.

Testing Methods	UCS Test	MPL (or CPL) Test	
Estimate Unit Cost	core	disk	Irregular shape
	800 Bahts/specimen	400 Bahts/specimen	50 Bahts/specimen

CHAPTER VII

CONCLUSIONS AND FUTURE RESEARCH NEEDS

7.1 Conclusions

The main objective of the present thesis research is to develop a new testing technique, called “modified point load (MPL) test” to obtain a better indicator of the compressive and tensile strengths of intact rocks. The effort involves laboratory tests and finite element analyses. A series of MPL testing, CPL testing, uniaxial compression testing and Brazilian tension testing are performed on cylindrical specimens with various sizes and shapes. Saraburi marble has been primary used as rock samples. The finite element analyses determine the stress distribution along the loaded axis of the MPL test specimens. Comparison is made between the predictive capability of the compressive strength by the CPL index and by the MPL results.

The uniaxial test results indicate that the strengths decrease with increasing length-to-diameter (L/D) ratio. This relationship is described by a power law. The size effects on the uniaxial compressive strength are obscured by the intrinsic variability of the marble. The Brazilian tensile strengths also decrease as the specimen diameters increase. The results from MPL test agree well with those from the finite element analyses. This confirms that the logarithmic relations of stress and specimen shape derived by a series of numerical analyses can be used to correlate the MPL strength with the uniaxial compressive strength of the intact rock.

The simulation results also suggest that Poisson’s ratio of the rock can affect the magnitude and distribution of the horizontal stresses along the loading axis of the MPL specimen. When the Poisson’s ratio approaches 0.5, the induced tensile stress (horizontal stress) tends to be lower and tends to have the maximum value near the middle of the specimen. The Poisson’s ratio has no effect on the magnitude and distribution of the vertical stress along the loading axis.

The simulations are divided into no-friction at the interface between the loading platen and rock surface and full-friction at the interface. The minimum principal stresses obtained from the full-friction case are slightly lower (about 2-5%) than those from the no-friction case. It is recognized that the actual friction at the interface will be between those two extreme cases.

Post-tested observations on the specimens also suggest that shear failure is predominant when the specimen thickness is less than twice the loading diameter while extension failure (fracture) is predominant when the specimens are thicker than three times the loading diameter. This can be postulated that the MPL strength can be correlated with the compressive strength when the MPL specimens are relatively thin, and should be an indicator of the tensile strength when the specimens are significantly larger than the diameter of the loading points.

The UCS prediction from the MPL test has been assessed by presenting the failure stresses as a function of specimen diameter (D/d) with $t/d = 2.5$. Extrapolation of a curve fit of the failure stress at $D/d = 1.0$ (uniaxial test condition) yields the UCS (σ_c) of the rocks. This value can be compared with the UCS at $L/D = 2.5$. The MPL results can also determine the rock tensile strength by using the relationship of the failure stresses as a function of specimen thickness (t/d). Extrapolation of the curve fit of the relation gives the value of the failure stresses from the experiment (at $t/d = 20$). The $t/d = 20$ is selected because under this dimension ratio the rock fails in tension mode. At the same D/d ratio (Figure 4.24), extrapolation of the logarithmic curve gives the value of the stress ratio ($-P/\sigma_2$). The tensile strength ($-\sigma_2$) value can therefore be determined. The MPL results correlate with the uniaxial compressive strength of the rock better than using the CPL strength index. It can also estimate the tensile strength of rock.

7.2 Future Research Needs and Recommendations

The discrepancy remains between the UCS predictions from both methods (MPL and CPL). More MPL test data are needed to further redefine the effects of the specimen thickness (t/d) and diameter (D/d). Additional computer simulations are desirable to obtain the variation of MPL results under a wider range of specimen dimensions. Verification of the MPL proposed concept should be tested under a wider range of rock types.

REFERENCES

- Addinall, E. and Hackett, P. (1964). Tension failure in rock-link material. **Proceeding of the 6th Rock Mechanics Symposium** (pp. 515-538). Missouri: Rolla.
- ASTM D2664-86. Standard test method for triaxial compressive strength of undrained rock core specimens without pore pressure measurements. In **Annual Book of ASTM Standards** (Vol. 04.08). Philadelphia: American Society for Testing and Materials.
- ASTM D2938-86. Standard test method for unconfined compressive strength of intact rock core specimens. In **Annual Book of ASTM Standards** (Vol. 04.08). Philadelphia: American Society for Testing and Materials.
- ASTM D3967-81. Standard test method for splitting tensile strength of intact rock core specimens. In **Annual Book of ASTM Standards** (Vol. 04.08). Philadelphia: American Society for Testing and Materials.
- ASTM D4543-85. Standard test method for preparing rock core specimens and determining dimensional and shape tolerances. In **Annual Book of ASTM Standards** (Vol. 04.08). Philadelphia: American Society for Testing and Materials.
- ASTM D5731-95. Standard test method for determination of the point load strength index of rock. In **Annual Book of ASTM Standards** (Vol. 04.08). Philadelphia: American Society for Testing and Materials.
- Bieniawski, Z.T. (1974). Estimating the strength of rock materials. **J. Inst. Min. Metall.** 7: 123-137.
- Bieniawski, Z.T. (1975). The point-load test in geotechnical practice. **Engng. Geol.** 9: 1-11.
- Broch, E. and Franklin J.A. (1972). The point-load test. **Int. J. Rock Mech. Min. Sci.** 9: 669-697.
- Broch, E. (1983). Estimation of strength anisotropy using the load test. **Int. J. Rock Mech. Min. Sci. & Geomech. Abstr.** 20: 181-187.
- Brook, N. (1977). The use of irregular specimens for rock strength tests. **Int. J. Rock Mech. Min. Sci. & Geomech. Abstr.** 14: 193-202.
- Brook, N. (1985). The Equivalent core diameter method of size and shape correction in point load testing. **Int. J. Rock Mech. Min. Sci. & Geomech. Abstr.** 22: 61-70.
- Brook, N. (1993). The measurement and estimation of basic rock strength. In J. A. Hudson (ed.), **Comprehensive Rock Engineering: Principles, Practices, and Projects** (pp. 41-66).

Oxford: Pergamon Press.

- Brown, E.T. (1981). **Rock Characterization Testing and Monitoring: ISRM Suggested Methods**. New York: International Society for Rock Mechanics, Pergamon Press.
- Butenuth, C. (1997). Comparison of tensile strength values of rocks determined by point load and direct tension tests. **Rock Mech. Rock Engng.** 30: 65-72.
- Carter, B.J., Scott Duncan E.J. and Laitai E.Z. (1991). Fitting strength criteria to intact rock. **J. Geotech. Geol. Eng.** 9: 73-81.
- Chau, K.T. and Wong, R.H.C. (1996). Uniaxial compressive strength and point load strength of rocks. **Int. J. Rock Mech. Min. Sci. & Geomech. Abstr.** 33: 183-188.
- Costin, L.S. (1987). Time-dependent deformation and failure. In: B.K. Atkinson (ed.). **Fracture Mechanics of Rock** (pp. 167-215). London: Academic press.
- Deere, D.U. and Miller, R.P. (1966). Engineering classification and index properties for intact Rock. In **U.S. Air Force Weapons Lab.** (AFWL-TR-65-116). Minnesota: U.S. Air Force Weapons Lab. Rep.
- DMR, (1983). Geological map of Thailand 1:500,000. (1983 edition). Bangkok: Royal Thai Survey Department.
- Evans, I. (1961). The tensile strength of coal. **J. Colliery Eng.** 38: 428-434.
- Forster, I.R. (1983). The influence of core sample geometry on the axial point load test. **Int. J. Rock Mech. Min. Sci. & Geomech. Abstr.** 20: 291-295.
- Fuenkajorn, K. and Daemen, J.J.K. (1986). Shape effect on ring test tensile strength. In **Key to Energy Production: Proceedings of the 27th U.S. Symposium on Rock Mechanics** (pp. 155-163). Tuscaloosa: University of Alabama.
- Fuenkajorn, K. and Daemen, J.J.K. (1991a). **Mechanical Characterization of the Densely Welded Apache Leap Tuff**. NUREG/CR 5688. Washington, D.C.: U.S. Nuclear Regulatory Commission, Rep.
- Fuenkajorn, K. and Daemen, J.J.K. (1991b). **Borehole stability in Densely Welded Tuffs**. NUREG/CR 5687. Washington, D.C.: U.S. Nuclear Regulatory Commission, Rep.
- Fuenkajorn, K. and Daemen, J.J.K. (1991c). An empirical strength criterion for heterogeneous welded tuff. In **ASME Applied Mechanics and Biomechanics Summer Conference**. Columbus: Ohio University.

- Fuenkajorn, K. and Daemen, J.J.K. (1992). An empirical strength criterion for heterogeneous tuff. **Int. J. Engineering Geolog.** 32: 209-223.
- Fuenkajorn, K. and Serata, S. (1993). Numerical simulation of strain-softening and dilation of rock salt. **Int. J. Rock Mech. Min. Sci.** 30: 1303-1306
- Ghosh, A., Fuenkajorn, K. and Daemen, J.J.K. (1995). Tensile strength of welded Apache Leap tuff: investigation for scale effects. In **Proceeding of 35th U.S. Rock Mech. Symposium** (pp. 459-646). Reno: University of Nevada.
- Goodman, R.E. (1989). **Introduction to Rock Mechanics.** 2nd Edition. New York: Wiley.
- Hiramatsu, Y. and Oka, Y. (1966). Determination of the tensile strength of rock by a compression test of an irregular test piece. **Int. J. Rock Mech. Min. Sci.** 3: 89-99.
- Hobbs, D.W. (1964). The tensile strength of rocks. **Int. J. Rock Mech. Min. Sci.** 1: 385-394.
- Hoek, E. (1990). Estimating Mohr-Coulomb friction and cohesion values from the Hoek-Brown failure criterion-technical note. **Int. J. Rock Mech. Min. Sci. Geomech. Abstr.** 27: 227-229.
- Hoek, E. and Brown, E.T. (1980). Empirical strength criterion for rock masses. **J. Geotech. Eng. Div.** 106 (GT9): 1013-1035.
- Horii, H. and Nemat-Nasser, S. (1985). Compression-induced microcrack growth in brittle solids: axial splitting and shear failure. **J. Geophys. Res.** 90: 3105-3125.
- ISRM, (1985). Suggested method for determining point load strength. **Int. J. Rock Mech. Min. Sci. & Geomech. Abstr.** 22: 53-60.
- Jaeger, J.C. and Cook, N.G.W. (1979). **Fundamentals of Rock Mechanics.** London: Chapman and Hall.
- Kaczynski, R.R. (1986). Scale effect during compressive strength of rocks. In **Proceeding of 5th Int. Assoc. Eng. Geol. Congr.** (pp. 371-373).
- Lundborg, N. (1967). The strength-size relation of granite. **Int. J. Rock Mech. Min. Sci.** 4: 269-272.
- Miller, R.P. (1965). **Engineering Classification and Index Properties for Intact Rock.** Ph.D. Dissertation, University of Illinois, Urbana.
- Nimick, F.B. (1988). Empirical relationships between porosity and the mechanical properties of tuff. In **Key Questions in Rock Mechanics** (pp. 741-742). Balkema, Rotterdam.

- Panek, L. A. and Fannon, T. A. (1992). Size and shape effects in point load tests of irregular rock fragments. **J. Rock Mechanics and Rock Engineering**. 25: 109-140.
- Reichmuth, D.R. (1968). Point-load testing of brittle materials to determine tensile strength and relative brittleness. In **Proceeding of 9th U.S. Symp. Rock Mech.** (pp. 134-159). Colorado: University of Colorado.
- Ripperger, E.A. and Davids, N. (1947). Critical Stresses in circular ring. **J. Transaction of American Society of Civil Engineering**. 112: 619-627.
- Serata, S. and Fuenkajorn, K. (1992a). Finite element program 'GEO' for modeling brittle-ductile deterioration of aging earth structures. In **SMRI Paper** (24 pp.). Texas: Solution Mining Research Institute.
- Serata, S. and Fuenkajorn, K. (1992b). Formulation of a constitutive equation for salt. In **Proceeding of 7th International Symposium on Salt** (pp. 483-488). Amsterdam: Elsevier Science publishers.
- Turk, N. and Dearman, W.R. (1986). A correction equation on the influence of length-to-diameter ratio on the uniaxial compressive strength of rocks. **J. Eng. Geol.** 22: 293-300.
- Wei, X.X., Chau, K.T. and Wong, R.H.C. (1999). Analytic solution for axial point load strength test on solid circular cylinders. **J. Engng. Mech.** December: 1349-1357.
- Wiebols, G.A. and Cook, N.G.W. (1968). An energy criterion for the strength of rock in polyaxial compression. **Int. J. Rock Mech. Min. Sci.** 5: 529-549.
- Wijk, G. (1978). Some new theoretical aspects of indirect measurements of the tensile strength of rocks. **Int. J. Rock Mech. Min. Sci. & Geomech. Abstr.** 15: 149-160.
- Wijk, G. (1980). The point load test for the tensile strength of rock. **Geotechnical Testing Journal**. 3: 49-54.

APPENDIX A

SUMMARY OF THE LABORATORY EXPERIMENTAL RESULTS

Table A.1 Summary results of modified point load tests on the circular disks of Saraburi marble.

Sample No.	Average Diameter, D (mm)	Average Thickness, t (mm)	t/d	D/d	Density (g/cm ³)	MPL Strength, P (MPa)
MB-32-4-MPL-1	67.22	38.17	3.8	6.7	2.69	152.8
MB-32-4-MPL-2	67.35	38.60	3.9	6.7	2.68	222.8
MB-33-7-MPL-3	67.50	38.52	3.9	6.8	2.68	401.1
MB-33-7-MPL-4	67.57	39.63	4.0	6.8	2.68	360.3
MB-33-7-MPL-5	67.45	39.20	3.9	6.8	2.69	362.9
MB-37-4-MPL-36	67.52	40.75	4.1	6.8	2.68	394.7
MB-37-4-MPL-37	67.42	41.97	4.2	6.7	2.71	235.6
MB-38-2-MPL-38	67.58	42.65	4.3	6.8	2.67	222.8
MB-38-2-MPL-39	67.33	40.47	4.1	6.7	2.69	241.9
MB-43-4-MPL-40	67.42	41.23	4.1	6.7	2.69	347.6
MB-32-1-MPL-6	67.35	28.98	2.9	6.7	2.66	216.5
MB-32-1-MPL-7	67.18	28.80	2.9	6.7	2.63	203.7
MB-32-1-MPL-8	67.23	29.08	2.9	6.7	2.67	222.8
MB-42-1-MPL-9	67.57	28.87	2.9	6.8	2.67	235.6
MB-32-1-MPL-10	67.38	29.03	2.9	6.7	2.65	203.7
MB-45-4-MPL-41	67.42	29.73	3.0	6.7	2.69	261.0
MB-45-4-MPL-42	67.43	30.23	3.0	6.7	2.69	171.9
MB-45-3-MPL-43	67.43	30.88	3.1	6.7	2.65	197.4
MB-45-6-MPL-44	67.43	31.92	3.2	6.7	2.69	331.0
MB-37-6-MPL-45	67.45	31.25	3.1	6.8	2.67	226.6
MB-42-5-MPL-11	67.43	18.17	1.8	6.7	2.66	178.3
MB-42-5-MPL-12	67.57	19.28	1.9	6.8	2.63	171.9
MB-42-1-MPL-13	67.43	19.30	1.9	6.7	2.63	146.4
MB-42-5-MPL-14	67.50	19.22	1.9	6.8	2.63	133.7
MB-42-5-MPL-15	67.57	19.13	1.9	6.8	2.65	178.3
MB-45-2-MPL-46	67.38	21.20	2.1	6.7	2.57	222.8
MB-45-2-MPL-47	67.38	21.00	2.1	6.7	2.69	149.0
MB-37-6-MPL-48	67.37	20.10	2.0	6.7	2.67	159.2
MB-37-7-MPL-49	67.38	22.10	2.2	6.7	2.68	127.3
MB-45-2-MPL-50	67.43	22.10	2.2	6.7	2.69	248.3
MB-36-4-MPL-16	67.53	14.40	1.4	6.8	2.64	133.7

Table A.1 Summary results of modified point load tests on the circular disk of Saraburi marble
(continued).

Sample No.	Average Diameter, D (mm)	Average Thickness, t (mm)	t/d	D/d	Density (g/cm ³)	MPL Strength, P (MPa)
MB-36-4-MPL-17	67.40	13.33	1.3	6.7	2.64	178.3
MB-42-3-MPL-18	67.43	15.35	1.5	6.7	2.67	191.0
MB-36-4-MPL-19	67.52	13.60	1.4	6.8	2.61	140.1
MB-36-4-MPL-20	67.72	15.00	1.5	6.8	2.64	127.3
MB-37-6-MPL-51	67.42	16.15	1.6	6.7	2.70	121.0
MB-45-6-MPL-52	67.40	14.43	1.4	6.7	2.90	101.9
MB-37-6-MPL-53	67.42	16.18	1.6	6.7	2.64	114.6
MB-45-3-MPL-54	67.40	15.72	1.6	6.7	2.48	184.6
MB-45-6-MPL-55	67.42	16.45	1.7	6.7	2.63	152.8
MB-42-4-MPL-21	67.48	9.38	0.9	6.8	2.64	140.1
MB-42-4-MPL-22	67.42	10.10	1.0	6.7	2.59	70.0
MB-42-5-MPL-23	67.52	9.68	1.0	6.8	2.64	216.5
MB-42-3-MPL-24	67.40	10.13	1.0	6.7	2.66	127.3
MB-42-5-MPL-25	67.40	8.93	0.9	6.7	2.65	146.4
MB-38-6-MPL-56	67.38	11.07	1.1	6.7	2.65	150.2
MB-37-6-MPL-57	67.42	10.28	1.0	6.7	2.60	114.6
MB-42-3-MPL-58	67.40	10.57	1.1	6.7	2.63	89.1
MB-45-3-MPL-59	67.40	10.37	1.0	6.7	2.65	182.1
MB-45-3-MPL-60	67.42	10.62	1.1	6.7	2.74	140.1
MB-42-4-MPL-26	67.70	7.90	0.8	6.8	2.60	152.8
MB-42-3-MPL-27	67.45	7.20	0.7	6.8	2.47	57.3
MB-42-4-MPL-28	67.37	6.63	0.7	6.7	2.69	203.7
MB-42-4-MPL-29	67.38	7.43	0.7	6.7	2.66	121.0
MB-42-4-MPL-30	67.38	8.13	0.8	6.7	2.60	101.9
MB-43-4-MPL-61	67.40	7.43	0.7	6.7	2.64	197.4
MB-43-4-MPL-62	67.47	7.22	0.7	6.8	2.66	171.9
MB-43-4-MPL-63	67.42	7.48	0.8	6.7	2.64	191.0
MB-43-4-MPL-64	67.42	6.97	0.7	6.7	2.55	76.4
MB-43-4-MPL-65	67.45	7.78	0.8	6.8	2.66	165.5
MB-32-6-MPL-31	66.90	5.50	0.6	6.7	2.88	63.7

Table A.1 Summary results of modified point load tests on the circular disk of Saraburi marble
(continued).

Sample No.	Average	Average	t/d	D/d	Density (g/cm ³)	MPL
	Diameter, D (mm)	Thickness, t (mm)				Strength, P (MPa)
MB-32-6-MPL-32	67.33	4.62	0.5	6.7	2.92	121.0
MB-42-6-MPL-33	67.47	6.20	0.6	6.8	2.84	133.7
MB-45-2-MPL-34	67.45	5.95	0.6	6.8	2.75	95.5
MB-45-2-MPL-35	67.38	6.25	0.6	6.7	2.47	89.1
MB-45-6-MPL-66	67.42	5.27	0.5	6.7	2.77	108.2
MB-45-6-MPL-67	67.43	5.12	0.5	6.7	2.57	114.6
MB-45-6-MPL-68	67.42	4.77	0.5	6.7	2.53	63.7
MB-45-6-MPL-69	67.42	5.82	0.6	6.7	2.55	89.1
MB-45-2-MPL-70	67.40	6.02	0.6	6.7	2.63	70.0
MB-36-4-MPL-126	67.40	37.57	7.5	13.5	2.68	626.8
MB-37-1-MPL-127	67.37	40.25	8.1	13.5	2.69	687.9
MB-43-4-MPL-132	67.28	41.03	8.2	13.5	2.73	611.5
MB-45-4-MPL-133	67.48	40.15	8.0	13.5	2.70	662.4
MB-45-4-MPL-137	67.43	37.98	7.6	13.5	2.70	723.6
MB-38-1-MPL-138	67.57	38.60	7.7	13.5	2.65	611.5
MB-37-2-MPL-139	67.40	37.47	7.5	13.5	2.69	738.9
MB-38-4-MPL-102	67.37	41.43	4.1	6.7	2.69	220.4
MB-45-4-MPL-103	67.25	39.25	3.9	6.7	2.72	401.3
MB-38-4-MPL-106	67.38	38.35	3.8	6.7	2.72	248.4
MB-37-2-MPL-107	67.43	39.28	3.9	6.7	2.66	318.5
MB-45-4-MPL-108	67.50	39.20	3.9	6.8	2.72	402.6
MB-37-3-MPL-109	67.38	38.52	3.9	6.7	2.69	324.8
MB-38-4-MPL-110	67.38	38.62	3.9	6.7	2.70	299.4
MB-37-5-MPL-141	67.42	40.18	4.0	6.7	2.73	295.5
MB-37-5-MPL-142	67.40	39.23	3.9	6.7	2.73	377.1
MB-38-2-MPL-112	67.38	38.47	2.6	4.5	2.88	Not failed
MB-37-3-MPL-113	67.27	41.03	2.7	4.5	2.48	215.2
MB-38-3-MPL-114	67.53	37.98	2.5	4.5	2.73	150.0
MB-38-3-MPL-115	67.43	40.58	2.7	4.5	2.69	178.3
MB-45-5-MPL-116	67.38	39.77	2.7	4.5	2.70	172.7

Table A.1 Summary results of modified point load tests on the circular disk of Saraburi marble
(continued).

Sample No.	Average Diameter, D (mm)	Average Thickness, t (mm)	t/d	D/d	Density (g/cm ³)	MPL Strength, P (MPa)
MB-38-1-MPL-117	67.35	38.73	2.6	4.5	2.69	150.0
MB-37-2-MPL-118	67.42	39.40	2.6	4.5	2.69	172.7
MB-45-5-MPL-119	67.38	38.88	2.6	4.5	2.70	186.8
MB-37-1-MPL-120	67.38	38.72	2.6	4.5	2.71	152.9
MB-37-5-MPL-143	67.38	40.40	2.7	4.5	2.70	110.4
MB-37-5-MPL-144	67.50	38.77	2.6	4.5	2.69	198.2
MB-38-3-MPL-128	67.37	38.98	2.0	3.4	2.68	63.7
MB-38-1-MPL-129	67.38	37.67	1.9	3.4	2.68	63.7
MB-45-5-MPL-130	67.43	37.83	1.9	3.4	2.71	159.2
MB-37-3-MPL-136	67.30	39.77	2.0	3.4	2.69	143.3
MB-45-2-MPL-140	67.42	39.77	2.0	3.4	2.69	73.3
MB-38-5-MPL-145	67.45	40.27	2.0	3.4	2.68	76.4
MB-38-5-MPL-146	67.38	38.68	1.9	3.4	2.67	71.7
MB-38-5-MPL-147	67.47	40.47	2.0	3.4	2.68	51.0
MB-37-3-MPL-101	67.27	40.75	1.6	2.7	2.70	65.2
MB-37-1-MPL-104	67.37	37.62	1.5	2.7	2.67	49.3
MB-45-2-MPL-134	67.35	40.42	1.6	2.7	2.70	117.2
MB-37-2-MPL-135	67.48	40.37	1.6	2.7	2.69	81.5
MB-45-1-MPL-148	67.42	39.73	1.6	2.7	2.69	73.4
MB-45-1-MPL-150	67.38	37.73	1.5	2.7	2.70	86.6
MB-38-1-MPL-105	67.40	39.53	1.3	2.3	2.67	38.2
MB-37-3-MPL-111	67.38	37.55	1.3	2.3	2.70	49.5
MB-45-5-MPL-121	67.43	39.92	1.3	2.3	2.69	38.2
MB-38-4-MPL-122	67.42	38.53	1.3	2.3	2.70	42.5
MB-38-3-MPL-131	67.28	39.82	1.3	2.2	2.68	35.4
MB-45-1-MPL-151	67.38	37.72	1.3	2.3	2.66	48.1
MB-37-1-MPL-123	67.28	37.58	0.7	1.3	2.68	Not failed
MB-37-1-MPL-124	67.47	41.53	0.8	1.3	2.68	32.8
MB-37-2-MPL-125	67.38	39.33	0.7	1.3	2.71	6.3
MB-45-1-MPL-149	67.47	39.30	0.7	1.3	2.70	91.7

Table A.2 Summary results of modified point load tests on the square disk of Saraburi marble.

Sample No.	Average Width, D (mm)	Average Thickness, t (mm)	t/d	D/d	Density (g/cm³)	MPL Strength, P (MPa)
MB-58-1-MPL-71	23.0	18.19	1.8	2.3	2.87	91.7
MB-58-2-MPL-72	24.0	18.19	1.8	2.4	2.86	104.4
MB-58-3-MPL-73	25.0	18.19	1.8	2.5	2.76	108.2
MB-58-4-MPL-74	23.0	18.19	1.8	2.3	2.93	118.4
MB-58-5-MPL-75	24.0	18.19	1.8	2.4	2.79	108.2
MB-49-1-MPL-76	47.0	18.19	1.8	4.7	2.77	203.7
MB-49-2-MPL-77	48.0	18.19	1.8	4.8	2.71	178.3
MB-49-3-MPL-78	48.0	18.19	1.8	4.8	2.72	184.6
MB-49-4-MPL-79	49.0	18.19	1.8	4.9	2.59	212.6
MB-52-2-MPL-80	49.0	18.19	1.8	4.9	2.77	235.6
MB-51-1-MPL-81	73.0	18.19	1.8	7.3	2.68	248.3
MB-51-2-MPL-82	74.0	18.19	1.8	7.4	2.68	210.1
MB-51-3-MPL-83	73.0	18.19	1.8	7.3	2.73	227.9
MB-51-4-MPL-84	73.0	18.19	1.8	7.3	2.69	216.5
MB-52-1-MPL-85	74.0	18.19	1.8	7.4	2.80	280.1
MB-49-5-MPL-86	99.0	18.19	1.8	9.9	2.69	263.6
MB-49-6-MPL-87	98.0	18.19	1.8	9.8	2.70	252.1
MB-50-1-MPL-88	99.0	18.19	1.8	9.9	2.81	305.6
MB-50-2-MPL-89	97.0	18.19	1.8	9.7	2.85	311.9
MB-50-3-MPL-90	98.0	18.19	1.8	9.8	2.74	273.8
MB-58-1-MPL-91	124.0	18.19	1.8	12.4	2.83	261.0
MB-59-1-MPL-92	124.0	18.19	1.8	12.4	2.78	241.9
MB-60-1-MPL-93	124.0	18.19	1.8	12.4	2.70	212.6
MB-61-1-MPL-94	125.0	18.19	1.8	12.5	2.53	202.5
MB-62-1-MPL-95	125.0	18.19	1.8	12.5	2.73	249.6
MB-53-1-MPL-96	150.0	18.19	1.8	15.0	2.68	313.2
MB-54-1-MPL-97	150.0	18.19	1.8	15.0	2.91	280.1
MB-55-1-MPL-98	150.0	18.19	1.8	15.0	2.92	210.1
MB-56-1-MPL-99	152.0	18.19	1.8	15.2	2.79	264.8
MB-57-1-MPL-100	150.0	18.19	1.8	15.0	2.68	267.4

Table A.2 Summary results of modified point load tests on the square disk of Saraburi marble
(continued).

Sample No.	Average Width, D (mm)	Average Thickness, t (mm)	t/d	D/d	Density (g/cm ³)	MPL Strength, P (MPa)
MB-63-1-MPL-161	23.0	18.19	3.6	4.6	2.82	397.3
MB-63-2-MPL-162	24.0	18.19	3.6	4.8	2.77	346.3
MB-63-3-MPL-163	23.0	18.19	3.6	4.6	2.85	320.9
MB-63-4-MPL-164	23.0	18.19	3.6	4.6	2.79	346.3
MB-63-5-MPL-165	23.0	18.19	3.6	4.6	2.87	331.0
MB-64-1-MPL-166	45.0	18.19	3.6	9.0	2.98	417.6
MB-64-2-MPL-167	49.0	18.19	3.6	9.8	2.74	422.7
MB-64-3-MPL-168	48.0	18.19	3.6	9.6	2.75	417.6
MB-64-4-MPL-169	48.0	18.19	3.6	9.6	2.72	356.5
MB-64-5-MPL-170	50.0	18.19	3.6	10.0	2.67	356.5
MB-65-3-MPL-171	75.0	18.19	3.6	15.0	2.62	560.2
MB-66-1-MPL-172	76.0	18.19	3.6	15.2	2.64	555.1
MB-66-2-MPL-173	73.0	18.19	3.6	14.6	2.71	560.2
MB-66-3-MPL-174	74.0	18.19	3.6	14.8	2.64	570.4
MB-66-4-MPL-175	74.0	18.19	3.6	14.8	2.68	534.8
MB-67-1-MPL-176	97.0	18.19	3.6	19.4	2.85	555.1
MB-67-2-MPL-177	99.0	18.19	3.6	19.8	2.75	570.4
MB-67-3-MPL-178	100.0	18.19	3.6	20.0	2.72	560.2
MB-68-1-MPL-179	100.0	18.19	3.6	20.0	2.70	611.2
MB-68-2-MPL-180	100.0	18.19	3.6	20.0	2.73	662.1
MB-70-1-MPL-181	137.0	18.19	3.6	27.4	2.58	611.2
MB-71-1-MPL-182	130.0	18.19	3.6	26.0	2.80	611.2
MB-72-1-MPL-183	135.0	18.19	3.6	27.0	2.65	993.1
MB-73-1-MPL-184	138.0	18.19	3.6	27.6	2.64	550.0
MB-74-1-MPL-185	135.0	18.19	3.6	27.0	2.59	611.2
MB-75-1-MPL-186	150.0	18.19	3.6	30.0	2.57	758.9
MB-76-1-MPL-187	150.0	18.19	3.6	30.0	2.60	702.8
MB-77-1-MPL-188	149.0	18.19	3.6	29.8	2.53	677.4
MB-78-1-MPL-189	151.0	18.19	3.6	30.2	2.50	611.2
MB-79-1-MPL-190	150.0	18.19	3.6	30.0	2.65	519.5

Table A.2 Summary results of modified point load tests on the square disk of Saraburi marble
(continued).

Sample No.	Average Width, D (mm)	Average Thickness, t (mm)	t/d	D/d	Density (g/cm ³)	MPL Strength, P (MPa)
MB-63-6-MPL-191	22.0	18.19	0.9	1.1	2.97	57.3
MB-63-7-MPL-192	23.0	18.19	0.9	1.2	2.61	102.2
MB-63-8-MPL-193	23.0	18.19	0.9	1.2	2.86	84.7
MB-63-9-MPL-194	22.0	18.19	0.9	1.1	3.09	86.6
MB-63-10-MPL-195	22.0	18.19	0.9	1.1	2.99	99.3
MB-64-6-MPL-196	47.0	18.19	0.9	2.4	2.79	69.7
MB-64-7-MPL-197	47.0	18.19	0.9	2.4	2.70	78.0
MB-64-8-MPL-198	47.0	18.19	0.9	2.4	2.83	103.8
MB-65-1-MPL-199	49.0	18.19	0.9	2.5	2.70	131.8
MB-65-2-MPL-200	50.0	18.19	0.9	2.5	2.60	84.0
MB-65-4-MPL-201	73.0	18.19	0.9	3.7	2.74	115.2
MB-63-11-MPL-202	72.0	18.19	0.9	3.6	2.76	93.9
MB-63-12-MPL-203	73.0	18.19	0.9	3.7	2.74	93.6
MB-63-13-MPL-204	74.0	18.19	0.9	3.7	2.65	142.6
MB-63-14-MPL-205	73.0	18.19	0.9	3.7	2.69	127.6
MB-68-3-MPL-206	100.0	18.19	0.9	5.0	2.65	103.8
MB-64-9-MPL-207	98.0	18.19	0.9	4.9	2.66	112.1
MB-69-1-MPL-208	100.0	18.19	0.9	5.0	2.75	80.5
MB-69-2-MPL-209	97.0	18.19	0.9	4.9	2.73	51.3
MB-69-3-MPL-210	100.0	18.19	0.9	5.0	2.77	88.5
MB-80-1-MPL-211	130.0	18.19	0.9	6.5	2.79	87.5
MB-81-1-MPL-212	130.0	18.19	0.9	6.5	3.12	135.9
MB-82-1-MPL-213	130.0	18.19	0.9	6.5	3.03	80.9
MB-83-1-MPL-214	129.0	18.19	0.9	6.5	2.62	100.6
MB-84-1-MPL-215	120.0	18.19	0.9	6.0	3.20	79.6
MB-85-1-MPL-216	151.0	18.19	0.9	7.6	2.62	68.4
MB-86-1-MPL-217	150.0	18.19	0.9	7.5	2.59	175.1
MB-87-1-MPL-218	150.0	18.19	0.9	7.5	2.46	181.4
MB-88-1-MPL-219	151.0	18.19	0.9	7.6	2.62	130.5
MB-89-1-MPL-220	150.0	18.19	0.9	7.5	2.99	127.3

Table A.2 Summary results of modified point load tests on the square disk of Saraburi marble
(continued).

Sample No.	Average Width, D (mm)	Average Thickness, t (mm)	t/d	D/d	Density (g/cm ³)	MPL Strength, P (MPa)
MB-90-1-MPL-221	137.0	18.15	2.5	18.8	3.05	389.2
MB-91-1-MPL-222	144.0	18.10	2.5	19.8	2.56	401.2
MB-92-1-MPL-223	153.0	18.10	2.5	21.0	2.34	451.7
MB-93-1-MPL-224	165.0	18.15	2.5	22.7	2.34	530.9
MB-94-1-MPL-225	160.0	18.30	2.5	22.0	2.55	367.6
MB-95-1-MPL-226	100.0	18.00	2.5	13.7	2.58	317.1
MB-95-2-MPL-227	100.0	18.05	2.5	13.7	2.56	331.5
MB-95-3-MPL-228	96.5	18.10	2.5	13.3	2.62	307.5
MB-96-1-MPL-229	100.0	18.10	2.5	13.7	2.53	401.2
MB-96-2-MPL-230	99.0	18.25	2.5	13.6	2.78	446.9
MB-96-3-MPL-231	73.5	18.30	2.5	10.1	2.60	370.0
MB-97-1-MPL-232	71.0	18.20	2.5	9.8	2.79	228.2
MB-97-2-MPL-233	71.0	18.35	2.5	9.8	2.74	259.5
MB-97-3-MPL-234	70.0	18.25	2.5	9.6	2.87	300.3
MB-98-1-MPL-235	69.0	18.05	2.5	9.5	2.72	396.4
MB-98-3-MPL-237	50.0	18.15	2.5	6.9	2.66	331.5
MB-98-4-MPL-238	49.5	18.15	2.5	6.8	2.62	370.0
MB-98-5-MPL-239	50.0	18.20	2.5	6.9	2.55	379.6
MB-98-6-MPL-240	50.0	18.25	2.5	6.9	2.57	353.2
MB-98-7-MPL-241	51.0	18.10	2.5	7.0	2.59	341.1
MB-98-8-MPL-242	48.0	18.15	2.5	6.6	2.71	271.5
MB-99-1-MPL-243	25.0	18.05	2.5	3.4	2.18	221.0
MB-99-2-MPL-244	22.5	18.15	2.5	3.1	3.04	192.2
MB-99-3-MPL-245	21.5	18.20	2.5	3.0	2.94	235.4
MB-99-4-MPL-246	21.5	18.25	2.5	3.0	3.15	163.4
MB-99-5-MPL-247	23.0	18.10	2.5	3.2	2.93	257.1
MB-100-1-MPL-251	16.5	17.90	2.5	2.3	2.54	139.3
MB-100-2-MPL-252	16.8	18.00	2.5	2.3	2.43	103.3
MB-100-3-MPL-253	16.0	17.90	2.5	2.2	2.51	120.1
MB-100-4-MPL-254	15.2	17.95	2.5	2.1	2.51	144.1

Table A.2 Summary results of modified point load tests on the square disk of Saraburi marble
(continued).

Sample No.	Average Width, D (mm)	Average Thickness, t (mm)	t/d	D/d	Density (g/cm³)	MPL Strength, P (MPa)
MB-100-5-MPL-255	16.7	17.95	2.5	2.3	2.53	132.1
MB-101-1-MPL-256	36.6	17.95	2.5	5.0	2.58	297.9
MB-101-2-MPL-257	36.8	17.90	2.5	5.1	2.57	273.9
MB-101-3-MPL-258	35.4	17.95	2.5	4.9	2.61	281.1
MB-101-4-MPL-259	36.1	17.55	2.4	5.0	2.65	281.1
MB-102-1-MPL-260	35.4	18.00	2.5	4.9	2.71	283.5
MB-102-2-MPL-261	51.4	17.75	2.4	7.1	2.72	350.8
MB-103-1-MPL-262	51.4	18.00	2.5	7.1	2.66	223.4
MB-103-2-MPL-263	52.0	17.90	2.5	7.1	2.63	192.2
MB-103-3-MPL-264	51.3	18.05	2.5	7.0	2.68	264.3
MB-103-4-MPL-265	51.1	18.15	2.5	7.0	2.62	324.3

Table A.3 Summary results of uniaxial compressive strength tests of Saraburi marble.

Sample No.	Average Diameter, D (mm)	Average Length, L (mm)	L/D	Density (g/cm³)	Uniaxial Compressive Strength (MPa)
MB-5-3-UN-1	38.48	10.83	0.3	2.64	299.1
MB-2-2-UN-2	38.52	10.65	0.3	2.77	147.6
MB-2-2-UN-3	38.48	11.28	0.3	2.73	203.9
MB-2-2-UN-4	38.50	11.05	0.3	2.74	281.8
MB-2-2-UN-5	38.50	11.13	0.3	2.73	204.0
MB-2-2-UN-6	38.55	10.72	0.3	2.72	284.4
MB-2-2-UN-7	38.50	12.43	0.3	2.65	283.1
MB-2-2-UN-8	38.50	11.18	0.3	2.65	274.6
MB-4-1-UN-9	38.53	13.37	0.4	2.57	194.6
MB-1-1-UN-10	38.50	10.00	0.3	2.56	206.1
MB-4-1-UN-11	38.52	24.18	0.6	2.70	148.6
MB-6-1-UN-12	38.53	22.85	0.6	2.65	82.9
MB-5-3-UN-13	38.60	23.02	0.6	2.68	152.9
MB-2-2-UN-14	38.58	23.05	0.6	2.69	190.3
MB-2-3-UN-15	38.52	23.92	0.6	2.67	91.1
MB-4-2-UN-16	38.53	22.18	0.6	2.68	122.9
MB-1-2-UN-17	38.43	22.62	0.6	2.51	100.9
MB-2-3-UN-18	38.53	22.63	0.6	2.61	119.4
MB-2-1-UN-19	38.50	23.80	0.6	2.61	123.2
MB-1-2-UN-20	38.45	22.93	0.6	2.55	89.0
MB-2-3-UN--21	38.50	36.65	1.0	2.67	61.2
MB-7-1-UN-22	38.48	34.10	0.9	2.64	97.5
MB-10-1-UN-23	38.57	34.32	0.9	2.67	39.0
MB-10-3-UN-24	38.55	38.63	1.0	2.67	52.0
MB-10-2-UN-25	38.58	36.48	1.0	2.64	39.1
MB-1-2-UN-26	38.40	36.07	0.9	2.57	29.4
MB-5-2-UN-27	38.52	36.52	1.0	2.70	83.8
MB-5-2-UN-28	38.50	37.43	1.0	2.36	49.0
MB-1-2-UN-29	38.48	34.77	0.9	2.57	36.3
MB-4-2-UN-30	38.50	33.63	0.9	2.73	134.2

Table A.3 Summary results of uniaxial compressive strength tests of Saraburi marble (continued).

Sample No.	Average Diameter, D (mm)	Average Length, L (mm)	L/D	Density (g/cm ³)	Uniaxial Compressive Strength (MPa)
MB-7-1-UN-31	38.53	49.05	1.3	2.61	72.2
MB-6-1-UN-32	38.50	47.02	1.2	2.66	110.0
MB-9-2-UN-33	38.42	49.70	1.3	2.59	79.9
MB-10-5-UN-34	38.47	49.82	1.3	2.67	72.3
MB-9-1-UN-35	38.43	49.02	1.3	2.55	53.7
MB-6-2-UN-36	38.48	48.08	1.3	2.69	95.5
MB-6-2-UN-37	38.52	48.40	1.3	2.70	126.4
MB-3-1-UN-38	38.55	48.33	1.3	2.62	121.4
MB-3-1-UN-39	38.57	49.47	1.3	2.68	111.2
MB-5-1-UN-40	38.58	51.32	1.3	2.68	49.6
MB-9-1-UN-41	38.53	61.45	1.6	2.63	75.3
MB-8-1-UN-42	38.48	62.70	1.6	2.65	66.6
MB-8-1-UN-43	38.60	59.42	1.5	2.63	104.0
MB-6-1-UN-44	38.50	61.48	1.6	2.69	63.5
MB-10-6-UN-45	38.57	64.13	1.7	2.67	52.3
MB-10-6-UN-46	38.50	62.27	1.6	2.68	67.6
MB-10-5-UN-47	38.53	63.55	1.7	2.49	47.7
MB-10-4-UN-48	38.53	61.25	1.6	2.77	50.8
MB-10-4-UN-49	38.48	60.88	1.6	2.71	36.6
MB-9-2-UN-50	38.48	61.15	1.6	2.67	37.0
MB-20-7-UN-51	38.53	78.75	2.0	2.68	38.6
MB-20-5-UN-52	38.48	76.50	2.0	2.68	43.2
MB-16-6-UN-53	38.55	78.37	2.0	2.69	94.3
MB-21-1-UN-54	38.55	77.95	2.0	2.71	108.6
MB-20-6-UN-55	38.48	78.20	2.0	2.69	44.2
MB-21-2-UN-56	38.57	77.52	2.0	2.73	140.9
MB-15-3-UN-57	38.58	77.73	2.0	2.69	116.7
MB-22-1-UN-58	38.53	78.78	2.0	2.65	75.4
MB-15-2-UN-59	38.53	77.53	2.0	2.70	128.2
MB-15-2-UN-60	38.53	77.83	2.0	2.70	46.3

Table A.3 Summary results of uniaxial compressive strength tests of Saraburi marble
(continued).

Sample No.	Average Diameter, D (mm)	Average Length, L (mm)	L/D	Density (g/cm ³)	Uniaxial Compressive Strength (MPa)
MB-11-3-UN-61	22.87	6.13	0.3	2.60	248.6
MB-12-9-UN-62	22.50	5.15	0.2	2.62	226.0
MB-12-9-UN-63	22.57	5.83	0.3	2.62	196.9
MB-12-9-UN-64	22.57	4.98	0.2	2.56	196.4
MB-20-1-UN-65	21.90	5.90	0.3	2.51	150.3
MB-16-5-UN-66	22.88	4.93	0.2	2.56	119.6
MB-16-5-UN-67	22.88	5.48	0.2	2.54	115.8
MB-16-5-UN-68	22.85	4.43	0.2	2.63	200.6
MB-11-4-UN-69	22.82	5.72	0.3	2.57	201.9
MB-5-5-UN-70	22.58	6.03	0.3	2.56	192.6
MB-11-8-UN-71	22.87	11.53	0.5	2.58	79.9
MB-11-3-UN-72	22.87	10.58	0.5	2.60	66.1
MB-12-5-UN-73	21.57	10.98	0.5	2.62	113.3
MB-12-4-UN-74	21.87	11.55	0.5	2.62	124.2
MB-12-1-UN-75	21.90	13.05	0.6	2.61	80.6
MB-20-2-UN-76	22.65	11.00	0.5	2.60	88.5
MB-5-6-UN-77	22.67	10.87	0.5	2.67	103.9
MB-5-6-UN-78	22.68	11.68	0.5	2.62	135.2
MB-5-7-UN-79	22.72	10.82	0.5	2.63	141.2
MB-6-4-UN-80	22.58	12.03	0.5	2.59	82.4
MB-11-3-UN-81	21.27	15.60	0.7	2.49	56.5
MB-12-1-UN-82	21.83	17.07	0.8	2.61	43.2
MB-12-8-UN-83	22.52	16.77	0.7	2.69	72.0
MB-16-4-UN-84	22.58	18.10	0.8	2.67	35.3
MB-16-5-UN-85	22.87	18.03	0.8	2.66	81.9
MB-16-5-UN-86	22.88	18.17	0.8	2.69	108.4
MB-5-5-UN-87	22.67	15.78	0.7	2.66	93.3
MB-4-4-UN-88	22.52	16.00	0.7	2.66	102.4
MB-5-7-UN-89	22.73	16.62	0.7	2.66	116.2
MB-6-3-UN-90	22.47	16.72	0.7	2.70	107.6

Table A.3 Summary results of uniaxial compressive strength tests of Saraburi marble (continued).

Sample No.	Average Diameter, D (mm)	Average Length, L (mm)	L/D	Density (g/cm ³)	Uniaxial Compressive Strength (MPa)
MB-11-7-UN-91	22.82	23.63	1.0	2.66	51.1
MB-12-2-UN-92	22.68	22.30	1.0	2.43	40.9
MB-12-3-UN-93	22.27	22.17	1.0	2.63	35.8
MB-12-5-UN-94	22.13	22.05	1.0	2.56	60.5
MB-20-3-UN-95	22.72	23.02	1.0	2.66	37.3
MB-11-5-UN-96	22.55	22.75	1.0	2.65	44.1
MB-16-5-UN-97	22.83	21.57	0.9	2.71	66.3
MB-16-1-UN-98	21.27	22.77	1.1	2.68	54.1
MB-20-1-UN-99	22.42	22.25	1.0	2.71	32.6
MB-5-4-UN-100	22.72	22.43	1.0	2.64	75.4
MB-11-6-UN-101	22.88	32.72	1.4	2.65	42.4
MB-11-3-UN-102	22.95	33.10	1.4	2.73	62.7
MB-12-1-UN-103	21.58	32.83	1.5	2.71	60.0
MB-12-5-UN-104	22.05	33.23	1.5	2.64	22.2
MB-12-8-UN-105	22.55	34.17	1.5	2.69	24.9
MB-16-1-UN-106	22.62	33.87	1.5	2.72	51.0
MB-16-3-UN-107	21.57	33.40	1.6	2.73	88.9
MB-16-3-UN-108	22.20	32.30	1.5	2.68	90.1
MB-20-2-UN-109	22.50	32.90	1.5	2.68	53.2
MB-4-3-UN-110	22.97	34.33	1.5	2.61	25.5
MB-11-4-UN-111	23.03	45.43	2.0	2.61	33.4
MB-11-3-UN-112	21.22	45.32	2.1	2.64	54.9
MB-12-6-UN-113	22.83	43.85	1.9	2.66	40.3
MB-12-7-UN-114	22.75	44.23	1.9	2.68	30.9
MB-16-1-UN-115	21.63	45.43	2.1	2.72	44.9
MB-16-2-UN-116	22.60	44.27	2.0	2.71	55.1
MB-16-2-UN-117	22.73	43.83	1.9	2.68	58.3
MB-20-2-UN-118	22.80	43.50	1.9	2.63	29.0
MB-4-4-UN-119	22.80	43.53	1.9	2.64	42.7
MB-6-3-UN-120	22.72	43.22	1.9	2.69	60.7

Table A.3 Summary results of uniaxial compressive strength tests of Saraburi marble (continued).

Sample No.	Average Diameter, D (mm)	Average Length, L (mm)	L/D	Density (g/cm ³)	Uniaxial Compressive Strength (MPa)
MB-25-7-UN-121	53.88	14.48	0.3	2.60	89.1
MB-25-10-UN-122	53.93	13.02	0.2	2.65	80.4
MB-25-8-UN-123	53.90	14.25	0.3	2.64	104.1
MB-25-6-UN-124	53.97	13.30	0.3	2.58	115.9
MB-26-12-UN-125	53.98	14.18	0.3	2.61	86.4
MB-25-11-UN-126	53.90	12.37	0.2	2.61	114.0
MB-25-11-UN-127	53.95	13.08	0.2	2.53	90.9
MB-26-3-UN-128	53.97	14.50	0.3	2.63	95.3
MB-26-4-UN-129	53.83	14.87	0.3	2.69	105.7
MB-26-11-UN-130	53.93	14.18	0.3	2.60	85.4
MB-25-2-UN-131	53.93	29.00	0.5	2.69	36.4
MB-25-2-UN-132	53.93	29.00	0.5	2.69	29.3
MB-25-2-UN-133	53.90	28.73	0.5	2.56	26.7
MB-25-2-UN-134	53.93	27.55	0.5	2.70	78.0
MB-25-11-UN-135	53.97	27.03	0.5	2.67	88.7
MB-25-11-UN-136	53.90	27.32	0.5	2.67	68.5
MB-25-2-UN-137	53.92	27.93	0.5	2.69	77.0
MB-25-9-UN-138	53.95	29.93	0.6	2.67	43.1
MB-25-9-UN-139	53.95	26.87	0.5	2.67	107.3
MB-25-9-UN-140	53.92	26.82	0.5	2.68	62.2
MB-25-6-UN-141	53.93	40.82	0.8	2.68	42.2
MB-25-7-UN-142	53.95	40.35	0.8	2.69	30.8
MB-26-4-UN-143	53.92	41.63	0.8	2.67	48.1
MB-26-3-UN-144	53.98	41.02	0.8	2.67	40.7
MB-26-11-UN-145	54.00	40.38	0.8	2.69	40.2
MB-26-12-UN-146	53.97	39.35	0.7	2.69	26.4
MB-25-8-UN-147	53.95	39.87	0.7	2.66	35.6
MB-25-10-UN-148	54.00	40.37	0.8	2.68	30.0
MB-25-11-UN-149	53.92	39.83	0.7	2.68	29.1
MB-25-11-UN-150	53.93	40.03	0.7	2.69	31.3

Table A.3 Summary results of uniaxial compressive strength tests of Saraburi marble (continued).

Sample No.	Average Diameter, D (mm)	Average Length, L (mm)	L/D	Density (g/cm ³)	Uniaxial Compressive Strength (MPa)
MB-27-6-UN-151	53.93	53.13	1.0	2.69	56.9
MB-27-5-UN-152	53.95	54.57	1.0	2.70	43.9
MB-27-7-UN-153	53.93	53.00	1.0	2.67	32.4
MB-27-2-UN-154	54.00	54.00	1.0	2.67	48.5
MB-27-8-UN-155	53.97	54.42	1.0	2.69	35.2
MB-27-1-UN-156	53.97	53.95	1.0	2.77	49.2
MB-26-6-UN-157	53.87	57.55	1.1	2.65	56.8
MB-27-4-UN-158	53.93	54.88	1.0	2.68	37.4
MB-27-3-UN-159	53.93	53.08	1.0	2.73	34.2
MB-26-5-UN-160	53.95	55.35	1.0	2.70	34.7
MB-26-8-UN-161	53.88	79.98	1.5	2.70	56.8
MB-26-2-UN-162	53.97	81.10	1.5	2.42	51.1
MB-26-10-UN-163	53.92	80.78	1.5	2.70	36.9
MB-26-1-UN-164	53.95	81.17	1.5	2.69	43.9
MB-27-12-UN-165	53.95	82.52	1.5	2.70	34.8
MB-27-11-UN-166	53.98	81.97	1.5	2.69	44.1
MB-26-7-UN-167	53.95	81.72	1.5	2.69	34.6
MB-26-9-UN-168	53.92	79.87	1.5	2.70	54.0
MB-27-9-UN-169	53.95	80.35	1.5	2.69	89.4
MB-27-10-UN-170	53.95	81.23	1.5	1.07	54.9
MB-27-12-UN-171	53.95	101.12	1.9	2.67	29.1
MB-26-1-UN-172	53.93	101.07	1.9	2.70	59.4
MB-27-11-UN-173	53.95	101.10	1.9	2.70	50.2
MB-27-9-UN-174	53.92	100.75	1.9	2.71	41.9
MB-27-10-UN-175	53.95	100.32	1.9	2.70	44.4
MB-26-9-UN-176	53.97	101.38	1.9	2.69	41.8
MB-26-2-UN-177	53.95	100.58	1.9	2.69	83.6
MB-26-8-UN-178	53.93	101.43	1.9	2.69	74.0
MB-25-7-UN-179	53.92	103.07	1.9	2.65	54.6
MB-25-6-UN-180	53.98	99.03	1.8	2.70	31.8

Table A.3 Summary results of uniaxial compressive strength tests of Saraburi marble (continued).

Sample No.	Average Diameter, D (mm)	Average Length, L (mm)	L/D	Density (g/cm ³)	Uniaxial Compressive Strength (MPa)
MB-42-6-UN-181	67.47	17.32	0.3	2.69	274.6
MB-36-6-UN-182	67.20	16.37	0.2	2.65	281.4
MB-33-8-UN-183	67.48	18.40	0.3	2.64	241.8
MB-30-4-UN-184	67.38	18.98	0.3	2.66	174.6
MB-33-4-UN-185	67.63	16.32	0.2	2.65	269.5
MB-36-3-UN-186	67.40	15.45	0.2	2.67	271.2
MB-36-2-UN-187	67.48	18.45	0.3	2.69	166.0
MB-42-2-UN-188	67.37	19.42	0.3	2.66	168.5
MB-36-1-UN-189	67.52	18.72	0.3	2.65	213.5
MB-29-3-UN-190	67.38	17.72	0.3	2.63	214.7
MB-32-2-UN-191	67.37	33.27	0.5	2.68	57.6
MB-33-6-UN-192	67.38	32.07	0.5	2.67	94.0
MB-30-6-UN-193	67.43	32.90	0.5	2.71	98.9
MB-33-6-UN-194	67.42	33.55	0.5	2.68	88.8
MB-32-3-UN-195	67.45	34.45	0.5	2.73	91.4
MB-32-2-UN-196	67.25	33.10	0.5	2.68	75.4
MB-32-2-UN-197	67.27	32.47	0.5	2.69	62.5
MB-42-3-UN-198	67.38	33.98	0.5	2.68	70.7
MB-32-3-UN-199	67.27	33.90	0.5	2.67	76.3
MB-33-6-UN-200	67.43	33.98	0.5	2.69	87.0
MB-34-6-UN-201	67.52	50.53	0.8	2.69	48.5
MB-34-2-UN-202	67.38	50.22	0.8	2.70	48.7
MB-36-5-UN-203	67.55	50.20	0.7	2.69	41.6
MB-30-1-UN-204	67.35	50.40	0.8	2.71	49.6
MB-30-4-UN-205	67.62	49.02	0.7	2.70	50.3
MB-34-1-UN-206	67.38	50.18	0.7	2.69	32.1
MB-34-5-UN-207	67.55	51.42	0.8	2.69	38.5
MB-33-5-UN-208	67.38	50.40	0.8	2.70	34.2
MB-30-2-UN-209	67.43	50.67	0.8	2.68	59.9
MB-30-3-UN-210	67.62	50.58	0.8	2.70	48.1

Table A.3 Summary results of uniaxial compressive strength tests of Saraburi marble (continued).

Sample No.	Average Diameter, D (mm)	Average Length, L (mm)	L/D	Density (g/cm ³)	Uniaxial Compressive Strength (MPa)
MB-29-8-UN-211	67.35	65.45	1.0	2.65	68.5
MB-33-3-UN-212	67.32	67.00	1.0	2.70	46.1
MB-33-3-UN-213	67.47	66.08	1.0	2.69	47.0
MB-34-3-UN-214	67.47	65.55	1.0	2.70	42.9
MB-34-3-UN-215	67.42	64.40	1.0	2.71	82.1
MB-34-3-UN-216	67.43	67.18	1.0	2.70	33.8
MB-33-3-UN-217	67.45	65.37	1.0	2.71	60.3
MB-29-8-UN-218	67.47	65.85	1.0	2.69	42.1
MB-29-8-UN-219	67.38	66.20	1.0	2.68	42.3
MB-30-5-UN-220	67.45	68.00	1.0	2.70	72.0
MB-29-5-UN-221	67.38	100.88	1.5	2.70	62.5
MB-30-5-UN-222	67.35	101.45	1.5	2.71	50.0
MB-29-5-UN-223	67.28	98.47	1.5	2.70	58.1
MB-29-7-UN-224	67.43	100.37	1.5	2.70	50.2
MB-29-7-UN-225	67.38	99.00	1.5	2.70	74.6
MB-29-6-UN-226	67.33	102.40	1.5	2.70	53.2
MB-29-6-UN-227	67.42	96.95	1.4	2.70	60.6
MB-29-4-UN-228	67.27	98.60	1.5	2.70	72.4
MB-29-4-UN-229	67.32	100.45	1.5	2.70	37.3
MB-30-6-UN-230	67.35	100.55	1.5	2.70	34.1
MB-34-2-UN-231	67.40	134.12	2.0	2.74	22.2
MB-36-5-UN-232	67.43	133.17	2.0	2.71	37.2
MB-34-6-UN-233	67.42	133.28	2.0	2.73	45.6
MB-30-1-UN-234	67.43	133.03	2.0	2.74	51.1
MB-30-4-UN-235	67.40	132.07	2.0	2.74	69.5
MB-30-3-UN-236	67.37	132.73	2.0	2.73	46.2
MB-30-2-UN-237	67.42	132.00	2.0	2.73	52.8
MB-34-5-UN-238	67.33	132.00	2.0	2.74	39.0
MB-33-5-UN-239	67.45	132.03	2.0	2.72	31.0
MB-34-1-UN-240	67.40	133.28	2.0	2.75	44.3

Table A.3 Summary results of uniaxial compressive strength tests of Saraburi marble (continued).

Sample No.	Average Diameter, D (mm)	Average Length, L (mm)	L/D	Density (g/cm ³)	Uniaxial Compressive Strength (MPa)
MB-29-3-UN-241	67.22	166.48	2.5	2.73	55.4
MB-39-6-UN-242	67.42	165.47	2.5	2.76	69.5
MB-42-6-UN-243	67.37	167.03	2.5	2.73	64.0
MB-36-1-UN-244	67.48	165.00	2.5	2.74	36.6
MB-34-4-UN-245	67.57	168.17	2.5	2.71	57.8
MB-36-2-UN-246	67.47	166.43	2.5	2.75	44.8
MB-33-4-UN-247	67.43	168.43	2.5	2.72	66.9
MB-36-3-UN-248	67.47	167.43	2.5	2.72	38.5
MB-33-8-UN-249	67.45	166.25	2.5	2.74	63.8
MB-42-2-UN-250	67.53	167.07	2.5	2.73	27.4
MB-27-1-UN-251	53.97	128.52	2.4	2.71	40.1
MB-27-4-UN-252	53.97	128.62	2.4	2.72	56.9
MB-26-6-UN-253	53.97	129.50	2.4	2.69	86.4
MB-27-2-UN-254	53.97	129.47	2.4	2.71	69.3
MB-27-5-UN-255	53.97	129.03	2.4	2.72	67.4
MB-27-7-UN-256	53.98	128.87	2.4	2.72	54.5
MB-26-5-UN-257	53.93	128.67	2.4	2.72	61.9
MB-27-6-UN-258	54.03	128.93	2.4	2.71	63.8
MB-27-8-UN-259	53.98	129.32	2.4	2.71	49.4
MB-27-3-UN-260	54.03	128.50	2.4	2.71	64.4
MB-28-1-UN-261	38.55	96.27	2.5	2.69	27.0
MB-28-6-UN-262	38.55	96.53	2.5	2.69	35.7
MB-28-3-UN-263	38.57	95.10	2.5	2.69	19.4
MB-28-7-UN-264	38.57	95.30	2.5	2.69	14.7
MB-28-2-UN-265	38.55	97.40	2.5	2.69	22.7
MB-28-5-UN-266	38.55	97.15	2.5	2.68	63.5
MB-28-10-UN-267	38.53	97.32	2.5	2.69	83.9
MB-28-4-UN-268	38.55	96.13	2.5	2.68	28.4
MB-28-9-UN-269	38.53	97.37	2.5	2.68	36.1
MB-28-8-UN-270	38.57	96.03	2.5	2.70	36.5

Table A.3 Summary results of uniaxial compressive strength tests of Saraburi marble
(continued).

Sample No.	Average Diameter, D (mm)	Average Length, L (mm)	L/D	Density (g/cm³)	Uniaxial Compressive Strength (MPa)
MB-28-14-UN-271	23.00	55.42	2.4	2.66	48.4
MB-28-11-UN-272	22.58	54.18	2.4	2.61	32.8
MB-28-11-UN-273	22.03	55.05	2.5	2.70	32.7
MB-28-13-UN-274	22.60	54.82	2.4	2.72	54.3
MB-28-12-UN-275	22.72	54.50	2.4	2.68	28.3
MB-28-12-UN-276	22.33	56.30	2.5	2.74	33.8
MB-28-13-UN-277	22.77	54.07	2.4	2.71	32.8
MB-28-11-UN-278	22.75	52.92	2.3	2.71	29.0
MB-28-11-UN-279	22.73	54.97	2.4	2.54	35.6
MB-28-11-UN-280	22.35	54.72	2.5	2.69	37.3

Table A.4 Summary results of Brazilian tensile strength tests on Saraburi marble.

Sample No.	Average Diameter, D (mm)	Average Thickness, t (mm)	t/D	Density (g/cm³)	Brazilian Tensile Strength (MPa)
MB-20-3-BZ-1	22.80	11.57	0.5	2.65	4.3
MB-20-3-BZ-2	22.78	11.20	0.5	2.45	3.9
MB-20-3-BZ-3	22.72	11.60	0.5	2.64	4.0
MB-16-4-BZ-4	22.58	10.83	0.5	2.67	6.9
MB-16-4-BZ-5	22.82	10.48	0.5	2.71	7.0
MB-16-4-BZ-6	22.80	11.92	0.5	2.65	4.8
MB-12-2-BZ-7	21.22	11.02	0.5	2.71	4.8
MB-11-5-BZ-8	22.75	11.22	0.5	2.65	4.2
MB-12-2-BZ-9	21.02	10.42	0.5	2.72	6.0
MB-11-5-BZ-10	22.77	11.60	0.5	2.66	5.2
MB-20-6-BZ-11	38.48	18.00	0.5	2.67	5.6
MB-15-1-BZ-12	38.50	20.38	0.5	2.69	5.6
MB-26-7-BZ-13	38.50	20.83	0.5	2.61	5.5
MB-21-3-BZ-14	38.50	18.97	0.5	2.69	5.6
MB-22-1-BZ-15	38.53	18.60	0.5	2.49	3.9
MB-22-1-BZ-16	38.52	17.97	0.5	2.62	3.4
MB-15-3-BZ-17	38.50	19.98	0.5	2.69	5.4
MB-20-5-BZ-18	38.50	19.35	0.5	2.66	4.4
MB-16-6-BZ-19	38.55	19.18	0.5	2.68	3.2
MB-21-3-BZ-20	38.48	17.45	0.5	2.66	6.1
MB-25-7-BZ-21	53.92	27.92	0.5	2.66	5.2
MB-25-6-BZ-22	54.00	26.38	0.5	2.65	3.7
MB-26-3-BZ-23	53.95	27.02	0.5	2.67	2.4
MB-25-8-BZ-24	53.97	27.98	0.5	2.62	4.3
MB-25-9-BZ-25	53.98	28.02	0.5	2.67	3.0
MB-25-10-BZ-26	54.00	26.72	0.5	2.59	3.2
MB-26-4-BZ-27	53.92	26.60	0.5	2.68	3.3
MB-26-11-BZ-28	53.95	28.13	0.5	2.67	3.7
MB-26-12-BZ-29	53.95	26.90	0.5	2.67	3.9
MB-25-2-BZ-30	53.97	29.08	0.5	2.65	3.1

Table A.4 Summary results of Brazilian tensile strength tests on Saraburi marble (continued).

Sample No.	Average Diameter, D (mm)	Average Thickness, t (mm)	t/D	Density (g/cm ³)	Brazilian Tensile Strength (MPa)
MB-32-2-BZ-31	67.30	33.40	0.5	2.66	3.8
MB-30-6-BZ-32	67.57	33.23	0.5	2.69	4.7
MB-42-3-BZ-33	67.52	36.57	0.5	2.54	4.5
MB-32-3-BZ-34	67.28	33.30	0.5	2.66	2.8
MB-32-3-BZ-35	67.28	34.53	0.5	2.70	3.7
MB-42-3-BZ-36	67.53	35.47	0.5	2.66	2.4
MB-33-6-BZ-37	67.50	33.40	0.5	2.68	3.2
MB-32-3BZ-38	67.27	34.88	0.5	2.68	3.9
MB-32-3-BZ-39	67.27	34.40	0.5	2.68	4.0
MB-32-2-BZ-40	67.33	31.73	0.5	2.65	2.7

Table A.5 Summary results of triaxial compressive strength tests on Saraburi marble.

Sample No.	Average Diameter, D (mm)	Average Length, L (mm)	L/D	Failure Load (kN)	Confining Pressure, σ_3 (MPa)	Axial Stress at Failure, σ_1 (MPa)
MB-25-8-TR-6	53.9	100.7	1.9	174	1.7	76.2
MB-26-11-TR-1	53.9	100.8	1.9	250	3.4	109.5
MB-26-7-TR-4	54.1	100.1	1.9	274	6.9	119.8
MB-25-10-TR-5	54.0	102.8	1.9	284	13.8	124.4
MB-26-12-TR-3	54.0	100.3	1.9	386	20.7	169.1

Table A.6 Summary results of conventional point load tests on Saraburi marble.

Sample No.	Average	Average	t/D	Density (g/cm ³)	Failure Load (kN)	I _s =	I _s =
	Diameter, D (mm)	Thickness, t (mm)				P/t ² (MPa)	P/Dt (MPa)
MB-44-6-CPL-1	67.40	40.63	0.6	2.70	12.0	7.3	4.4
MB-44-6-CPL-2	67.37	41.02	0.6	2.70	10.8	6.4	3.9
MB-44-5-CPL-3	67.60	40.38	0.6	2.69	13.3	8.2	4.9
MB-44-6-CPL-4	67.37	39.30	0.6	2.69	10.5	6.8	4.0
MB-44-6-CPL-5	67.40	40.93	0.6	2.71	12.9	7.7	4.7
MB-44-5-CPL-6	67.38	31.35	0.5	2.71	9.6	9.8	4.5
MB-44-2-CPL-7	67.37	31.18	0.5	2.71	9.5	9.8	4.5
MB-44-2-CPL-8	67.42	31.82	0.5	2.71	13.8	13.6	6.4
MB-44-2-CPL-9	67.43	31.22	0.5	2.70	10.9	11.2	5.2
MB-44-5-CPL-10	67.42	32.03	0.5	2.65	11.3	11.0	5.2
MB-44-2-CPL-11	67.42	20.95	0.3	2.67	6.0	13.7	4.3
MB-44-5-CPL-12	67.38	20.62	0.3	2.71	5.0	11.8	3.6
MB-44-5-CPL-13	67.38	21.35	0.3	2.68	5.7	12.5	4.0
MB-44-2-CPL-14	67.33	21.47	0.3	2.70	6.6	14.3	4.6
MB-44-6-CPL-15	67.32	21.35	0.3	2.70	5.0	11.0	3.5
MB-44-2-CPL-16	67.38	15.12	0.2	2.68	5.5	24.1	5.4
MB-43-3-CPL-17	67.57	17.83	0.3	2.60	4.2	13.1	3.4
MB-43-3-CPL-18	67.48	16.63	0.3	2.62	3.8	13.7	3.4
MB-43-3-CPL-19	67.40	16.10	0.2	2.59	3.9	14.9	3.6
MB-43-3-CPL-20	67.45	16.12	0.2	2.60	3.7	14.1	3.4
MB-43-3-CPL-21	67.38	11.12	0.2	2.60	3.1	25.1	4.1
MB-43-3-CPL-22	67.48	10.92	0.2	2.59	3.2	26.9	4.3
MB-43-3-CPL-23	67.38	10.92	0.2	2.62	3.1	26.0	4.2
MB-43-3-CPL-24	67.47	10.58	0.2	2.66	3.3	29.0	4.6
MB-44-3-CPL-25	67.37	10.80	0.2	2.65	2.8	23.6	3.8
MB-44-4-CPL-26	67.85	7.58	0.1	2.55	1.8	31.3	3.5
MB-43-3-CPL-27	67.38	8.05	0.1	2.53	2.5	39.2	4.7
MB-44-2-CPL-28	67.38	8.33	0.1	2.64	3.1	43.9	5.4
MB-43-3-CPL-29	67.35	7.75	0.1	2.57	2.0	33.3	3.8
MB-43-3-CPL-30	67.40	8.23	0.1	2.50	1.9	28.0	3.4

Table A.6 Summary results of conventional point load tests on Saraburi marble (continued).

Sample No.	Average	Average	t/D	Density (g/cm ³)	Failure Load (kN)	I _s =	I _s =
	Diameter, D (mm)	Thickness, t (mm)				P/t ² (MPa)	P/Dt (MPa)
MB-44-3-CPL-31	67.43	5.78	0.1	2.57	1.8	52.3	4.5
MB-43-3-CPL-32	67.38	6.03	0.1	2.65	2.3	63.2	5.7
MB-44-4-CPL-33	67.43	5.68	0.1	2.59	1.9	58.8	5.0
MB-43-3-CPL-34	67.37	5.58	0.1	2.46	1.3	41.7	3.5
MB-44-5-CPL-35	67.32	5.57	0.1	2.75	1.8	56.5	4.7
MB-33-7-CPL-36	67.43	37.25	0.6	2.72	13.6	9.8	5.4
MB-32-4-CPL-37	67.27	39.02	0.6	2.68	9.9	6.5	3.8
MB-32-4-CPL-38	67.47	39.48	0.6	2.67	9.8	6.3	3.7
MB-32-4-CPL-39	67.15	36.67	0.6	2.69	9.0	6.7	3.7
MB-33-7-CPL-40	67.42	39.07	0.6	2.67	12.0	7.9	4.6
MB-32-1-CPL-41	67.32	29.53	0.4	2.70	8.0	9.2	4.0
MB-42-1-CPL-42	67.43	27.57	0.4	2.73	7.8	10.3	4.2
MB-42-1-CPL-43	67.45	28.72	0.4	2.69	7.0	8.5	3.6
MB-42-1-CPL-44	67.42	29.28	0.4	2.68	7.2	8.4	3.7
MB-32-1-CPL-45	67.02	29.32	0.4	2.66	6.5	7.6	3.3
MB-42-5-CPL-46	67.50	19.40	0.3	2.67	6.0	15.9	4.6
MB-42-5-CPL-47	67.42	17.08	0.3	2.69	5.0	17.1	4.3
MB-42-1-CPL-48	67.40	18.63	0.3	2.71	5.0	14.4	4.0
MB-42-1-CPL-49	67.38	17.68	0.3	2.66	4.8	15.4	4.0
MB-42-5-CPL-50	67.43	17.72	0.3	2.69	5.2	16.6	4.4
MB-36-4-CPL-51	67.43	16.68	0.3	2.48	5.5	19.8	4.9
MB-36-4-CPL-52	67.47	14.85	0.2	2.62	4.8	21.8	4.8
MB-36-4-CPL-53	67.48	14.57	0.2	2.68	5.4	25.5	5.5
MB-36-4-CPL-54	67.53	14.88	0.2	2.68	5.0	22.6	5.0
MB-36-4-CPL-55	67.47	16.10	0.2	2.53	5.7	22.0	5.3
MB-42-4-CPL-56	67.50	10.27	0.2	2.61	3.8	36.1	5.5
MB-42-4-CPL-57	67.42	10.92	0.2	2.66	3.1	26.0	4.2
MB-42-3-CPL-58	67.48	10.52	0.2	2.62	2.9	25.8	4.0
MB-42-4-CPL-59	67.40	10.75	0.2	2.62	3.7	32.0	5.1
MB-42-4-CPL-60	67.53	9.85	0.2	2.65	3.4	35.0	5.1

Table A.6 Summary results of conventional point load tests on Saraburi marble (continued).

Sample No.	Average	Average	t/D	Density (g/cm ³)	Failure Load (kN)	I _s =	I _s =
	Diameter, D (mm)	Thickness, t (mm)				P/t ² (MPa)	P/Dt (MPa)
MB-42-4-CPL-61	67.40	8.18	0.1	2.60	2.1	31.4	3.8
MB-42-4-CPL-62	67.40	7.03	0.1	2.65	2.5	50.5	5.3
MB-42-4-CPL-63	67.42	7.60	0.1	2.60	2.6	44.2	5.0
MB-42-4-CPL-64	67.43	8.17	0.1	2.64	2.7	40.5	4.9
MB-42-4-CPL-65	67.38	7.90	0.1	2.63	2.8	44.9	5.3
MB-32-6-CPL-66	67.30	5.77	0.1	2.63	1.7	51.1	4.4
MB-42-4-CPL-67	67.38	5.98	0.1	2.67	1.9	52.2	4.6
MB-32-6-CPL-68	67.37	5.23	0.1	2.55	1.5	54.8	4.3
MB-32-6-CPL-69	67.32	5.68	0.1	2.62	1.6	49.5	4.2
MB-32-6-CPL-70	67.32	5.62	0.1	2.63	1.7	53.9	4.5

Table A.7 Summary results of Ring tensile strength tests on Saraburi marble.

Sample No.	External	Internal	Thickness, t (mm)	t/D ₁	Failure	σ _R (MPa)
	Diameter, D ₁ (mm)	Diameter, D ₂ (mm)			Load, P (kN)	
MB-39-2-RT-1	92.5	30.9	45.7	0.5	9.1	14.1
MB-39-2-RT-2	92.6	30.1	46.4	0.5	9.5	14.1
MB-39-1-RT-3	92.4	30.4	45.2	0.5	9.8	15.2
MB-39-1-RT-4	92.4	29.9	48.1	0.5	11.0	15.8
MB-39-1-RT-5	92.3	30.9	47.9	0.5	9.2	13.6

Table A.8 Summary results of Four point bending tests on Saraburi marble.

Sample No.	Width, b (mm)	Thickness, h (mm)	Length, L (mm)	Spacing, l (mm)	Failure Load (kN)	σ_{bending} (MPa)
MB-1-BD-1	100.3	18.2	320	80.0	2.0	7.1
MB-2-BD-2	101.4	18.6	310	80.0	2.1	7.2
MB-3-BD-3	102.3	18.4	290	80.0	1.4	4.9
MB-4-BD-4	101.0	17.9	300	80.0	2.3	8.4
MB-5-BD-5	100.5	18.2	305	80.0	2.2	7.8
MB-6-BD-6	102.0	18.4	300	80.0	2.2	7.5
MB-7-BD-7	101.4	17.3	305	80.0	2.0	7.8
MB-8-BD-8	101.6	18.2	300	80.0	2.2	7.7
MB-9-BD-9	99.8	18.1	300	80.0	2.5	9.1
MB-10-BD-10	100.4	18.0	302	80.0	2.2	7.7

Table A.9 Summary verification results of uniaxial compressive strength tests on different rock types.

Sample No.	Average Diameter, D (mm)	Average Length, L (mm)	L/D	Density (g/cm³)	Uniaxial Compressive Strength (MPa)
LS-48-1-UN-1	38.10	94.40	2.7	2.48	83.3
LS-51-1-UN-2	38.05	95.05	2.7	2.50	54.8
LS-53-1-UN-3	38.20	95.45	2.7	2.50	65.1
LS-61-1-UN-4	38.10	94.60	2.7	2.48	41.1
LS-46-1-UN-5	38.15	110.21	2.8	2.89	44.9
LS-54-1-UN-6	38.40	110.20	2.8	2.87	43.9
LS-42-1-UN-7	38.45	110.35	2.8	2.87	36.7
LS-38-1-UN-8	38.35	110.20	2.8	2.87	24.7
SL-3-9-UN-1	53.87	126.83	2.4	2.72	46.1
SL-3-2-UN-2	53.88	126.83	2.4	2.75	24.1
SL-3-3-UN-3	49.25	126.83	2.6	3.24	94.5
SL-3-10-UN-4	53.87	126.83	2.4	2.72	26.3
SL-1-1-UN-5	53.90	126.83	2.4	2.73	32.9
SL-2-3-UN-6	53.88	126.83	2.4	2.73	21.9
SL-2-4-UN-7	53.80	126.83	2.4	2.73	30.8
SL-3-8-UN-8	53.85	126.83	2.4	2.72	57.1
SL-1-2-UN-9	53.90	126.83	2.4	2.71	39.5
SL-3-7-UN-10	53.92	126.83	2.4	2.62	59.1
SS-3-7-UN-1	53.88	125.67	2.3	2.38	23.3
SS-3-1-UN-2	53.90	128.00	2.4	2.36	24.1
SS-3-8-UN-3	53.88	127.33	2.4	2.37	25.4
SS-4-1-UN-4	53.62	128.33	2.4	2.25	13.7
SS-4-2-UN-5	53.67	128.00	2.4	2.23	10.6
SS-6-4-UN-6	53.83	127.00	2.4	2.42	28.1
SS-6-5-UN-7	53.82	127.50	2.4	2.42	27.3

Table A.10 Summary verification results of Brazilian tensile strength tests on different rock types.

Sample No.	Average Diameter, D (mm)	Average Thickness, t (mm)	t/D	Density (g/cm ³)	Brazilian Tensile Strength (MPa)
LS-16-2-BZ-1	54.00	25.76	0.5	2.66	4.4
LS-16-2-BZ-2	53.93	26.67	0.5	2.64	7.1
LS-16-2-BZ-3	53.90	24.70	0.5	2.67	10.0
LS-16-2-BZ-4	54.00	25.57	0.5	2.66	10.6
LS-16-2-BZ-5	53.86	24.63	0.5	2.67	10.1
LS-09-1-BZ-6	53.93	26.23	0.5	2.68	6.2
LS-09-1-BZ-7	54.10	25.13	0.5	2.65	10.3
LS-09-1-BZ-8	53.90	25.76	0.5	2.65	5.5
LS-14-1-BZ-9	53.90	23.70	0.4	2.68	8.5
LS-19-1-BZ-10	53.80	26.70	0.5	2.64	12.0
SL-2-5-BZ-1	53.90	25.45	0.5	2.67	8.3
SL-2-3-BZ-2	53.87	25.48	0.5	2.68	8.1
SL-3-11-BZ-3	53.88	25.85	0.5	2.77	8.4
SL-2-5-BZ-4	53.92	26.10	0.5	2.67	6.8
SL-3-11-BZ-5	53.92	25.78	0.5	2.66	9.1
SL-3-4-BZ-6	53.87	25.98	0.5	2.65	7.4
SL-2-6-BZ-7	53.87	25.67	0.5	2.68	8.8
SL-3-6-BZ-8	53.92	25.58	0.5	2.67	8.5
SL-3-6-BZ-9	53.83	25.23	0.5	2.68	5.7
SL-2-5-BZ-10	53.90	25.63	0.5	2.68	7.2
SS-3-4-BZ-1	53.93	26.48	0.5	2.33	1.9
SS-3-5-BZ-2	53.85	24.37	0.5	2.34	1.0
SS-3-5-BZ-3	53.95	26.38	0.5	2.31	1.4
SS-3-5-BZ-4	53.92	24.77	0.5	2.29	1.3
SS-3-5-BZ-5	54.00	25.48	0.5	2.28	1.6

Table A.11 Summary verification results of conventional point load tests on different rock types.

Sample No.	Average Diameter, D (mm)	Average Thickness, t (mm)	t/D	Density (g/cm ³)	Failure Load (kN)	$I_s = P/Dt$ (MPa)	$\sigma_s = 24I_s$ (MPa)
LS-CPL-IR-1	48.80	13.05	0.3	-	1.0	1.6	37.7
LS-CPL-IR-2	65.00	13.08	0.2	-	0.7	0.8	19.8
LS-CPL-IR-3	72.00	20.58	0.3	-	6.9	4.7	111.8
LS-CPL-IR-4	50.73	16.15	0.3	-	2.9	3.5	85.0
LS-CPL-IR-5	48.15	24.95	0.5	-	7.1	5.9	141.8
LS-CPL-IR-9	86.53	26.08	0.3	-	4.8	2.1	51.1
LS-CPL-IR-10	86.23	14.08	0.2	-	3.6	3.0	71.2
LS-CPL-IR-11	82.05	25.08	0.3	-	5.5	2.7	64.2
LS-CPL-IR-12	58.90	23.70	0.4	-	4.1	2.9	70.5
LS-CPL-IR-13	52.05	17.73	0.3	-	1.8	2.0	46.8
LS-CPL-IR-14	62.48	19.30	0.3	-	3.5	2.9	69.7
LS-CPL-IR-15	72.13	22.65	0.3	-	10.3	6.3	151.3
LS-CPL-IR-16	42.08	18.50	0.4	-	3.5	4.5	107.9
LS-CPL-IR-17	48.55	18.98	0.4	-	3.3	3.6	86.0
LS-CPL-IR-21	85.70	31.35	0.4	-	3.5	1.3	31.3
LS-CPL-IR-25	49.23	19.23	0.4	-	2.5	2.6	63.4
LS-CPL-IR-27	62.75	22.43	0.4	-	3.6	2.6	61.4
LS-CPL-IR-30	38.23	18.23	0.5	-	3.3	4.7	113.7
SL-CPL-IR-1	119.00	47.03	0.4	-	20.8	3.7	89.2
SL-CPL-IR-2	115.98	24.03	0.2	-	10.5	3.8	90.4
SL-CPL-IR-3	38.73	18.35	0.5	-	5.8	8.2	195.9
SL-CPL-IR-4	31.65	9.95	0.3	-	3.7	11.8	282.0
SL-CPL-IR-5	40.27	17.05	0.4	-	4.6	6.7	160.8
SL-CPL-IR-6	49.65	22.08	0.4	-	8.0	7.3	175.2
SL-CPL-IR-7	85.83	22.80	0.3	-	6.2	3.2	76.0
SL-CPL-IR-8	73.48	28.30	0.4	-	6.0	2.9	69.3
SL-CPL-IR-9	61.55	21.20	0.3	-	7.2	5.5	132.4
SL-CPL-IR-10	79.70	37.38	0.5	-	14.0	4.7	112.8
SL-CPL-IR-11	73.05	39.98	0.6	-	13.6	4.7	111.8
SL-CPL-IR-12	174.00	32.63	0.2	-	9.0	1.6	38.1

Table A.11 Summary verification results of conventional point load tests on different rock types (continued).

Sample No.	Average Diameter, D (mm)	Average Thickness, t (mm)	t/D	Density (g/cm ³)	Failure Load (kN)	$I_s = P/Dt$ (MPa)	$\sigma_s = 24I_s$ (MPa)
SL-CPL-IR-13	89.05	45.48	0.5	-	12.8	3.2	75.9
SL-CPL-IR-14	63.15	16.45	0.3	-	4.4	4.2	101.7
SL-CPL-IR-15	44.55	19.43	0.4	-	4.5	5.2	124.8
SL-CPL-IR-16	66.78	38.43	0.6	-	11.2	4.4	104.8
SL-CPL-IR-17	47.20	12.33	0.3	-	4.0	6.9	165.0
SL-CPL-IR-18	60.95	15.50	0.3	-	3.7	3.9	94.0
SL-CPL-IR-19	72.05	47.20	0.7	-	16.2	4.8	114.3
SL-CPL-IR-20	38.78	13.00	0.3	-	2.8	5.6	133.3
SL-CPL-IR-21	32.63	10.35	0.3	-	1.9	5.6	135.0
SL-CPL-IR-22	27.93	12.68	0.5	-	3.9	11.0	264.4
SL-CPL-IR-23	45.53	13.45	0.3	-	3.2	5.2	125.4
SL-CPL-IR-24	44.35	14.08	0.3	-	4.2	6.7	161.5
SL-CPL-IR-25	118.50	50.98	0.4	-	19.3	3.2	76.7
SL-CPL-IR-26	153.60	29.80	0.2	-	14.0	3.1	73.4
SL-CPL-IR-27	75.08	37.50	0.5	-	17.7	6.3	150.9
SL-CPL-IR-28	49.60	24.73	0.5	-	6.6	5.4	129.2
SL-CPL-IR-29	86.93	44.08	0.5	-	15.0	3.9	94.0
SL-CPL-IR-30	60.18	28.23	0.5	-	7.8	4.6	110.2
SS-3-6-CPL-1	53.88	26.35	0.5	2.34	2.0	1.4	33.8
SS-3-6-CPL-2	53.97	26.10	0.5	2.35	1.9	1.4	32.4
SS-3-6-CPL-3	53.78	23.83	0.4	2.35	1.6	1.3	30.3
SS-4-3-CPL-4	53.83	26.58	0.5	2.20	0.7	0.5	10.9
SS-4-3-CPL-5	53.90	23.33	0.4	2.20	0.5	0.4	10.3

Table A.12 Summary verification results of modified point load tests on different rock types.

Sample No.	Average Diameter, D (mm)	Average Thickness, t (mm)	t/d	D/d	Density (g/cm³)	MPL Strength, P (MPa)
LS-21-1-MPL-1	22.18	24.98	2.5	2.2	2.58	171.9
LS-21-2-MPL-2	22.62	24.80	2.5	2.3	2.53	143.9
LS-22-2-MPL-3	22.25	24.50	2.5	2.2	2.67	137.5
LS-28-1-MPL-4	22.53	24.20	2.4	2.3	2.53	149.0
LS-28-2-MPL-5	22.77	25.27	2.5	2.3	2.54	96.8
LS-35-1-MPL-6	38.53	27.68	2.8	3.9	2.63	215.2
LS-35-2-MPL-7	38.40	26.35	2.6	3.8	2.70	211.4
LS-35-3-MPL-8	38.42	25.75	2.6	3.8	2.76	210.1
LS-36-1-MPL-9	38.27	26.25	2.6	3.8	2.75	151.5
LS-36-2-MPL-10	38.47	26.10	2.6	3.9	2.77	271.2
LS-49-1-MPL-11	53.88	26.40	2.6	5.4	2.57	269.9
LS-49-2-MPL-12	53.95	25.98	2.6	5.4	2.69	309.4
LS-49-3-MPL-13	53.92	26.10	2.6	5.4	2.65	273.8
LS-49-4-MPL-14	53.98	25.40	2.5	5.4	2.70	471.1
LS-1-1-MPL-15	53.95	24.95	2.5	5.4	2.67	182.1
LS-26-1-MPL-16	65.90	25.88	2.6	6.6	2.81	143.9
LS-26-2-MPL-17	67.23	26.53	2.7	6.7	2.74	345.1
LS-26-3-MPL-18	67.42	24.48	2.5	6.7	2.69	354.0
LS-26-4-MPL-19	67.65	25.08	2.5	6.8	2.70	402.3
LS-31-1-MPL-20	92.60	28.23	2.8	9.3	2.66	333.6
LS-31-2-MPL-21	92.60	26.62	2.7	9.3	2.69	382.0
LS-47-1-MPL-22	92.55	27.63	2.8	9.3	2.70	273.8
LS-47-2-MPL-23	92.22	25.85	2.6	9.2	2.72	443.1
LS-57-1-MPL-24	22.40	57.90	2.9	1.1	2.66	62.1
LS-23-5-MPL-25	21.85	56.78	2.8	1.1	2.64	70.7
LS-28-3-MPL-26	22.50	58.07	2.9	1.1	2.66	41.4
LS-23-1-MPL-27	22.35	57.22	2.9	1.1	2.69	62.4

Table A.12 Summary verification results of modified point load tests on different rock types
(continued).

Sample No.	Average Diameter, D (mm)	Average Thickness, t (mm)	t/d	D/d	Density (g/cm³)	MPL Strength, P (MPa)
SL-MPL-IR-21	44.01	51.30	2.6	51.3	-	74.2
SL-MPL-IR-23	57.50	53.93	2.7	53.9	-	119.4
SL-MPL-IR-11	33.65	26.85	2.7	26.9	-	124.8
SL-MPL-IR-27	58.55	51.40	3.4	51.4	-	115.5
SL-MPL-IR-31	104.00	50.85	2.5	50.9	-	117.8
SL-MPL-IR-18	55.50	39.65	4.0	39.7	-	252.2
SL-MPL-IR-22	88.40	46.80	3.1	46.8	-	116.0
SL-MPL-IR-25	90.75	45.20	3.0	45.2	-	189.6
SL-MPL-IR-19	63.80	33.88	3.4	33.9	-	169.4
SL-MPL-IR-9	97.25	44.13	2.9	44.1	-	82.1
SL-MPL-IR-1	69.45	30.00	3.0	30.0	-	276.4
SL-MPL-IR-3	70.60	28.65	2.9	28.7	-	242.0
SL-MPL-IR-30	112.00	43.05	2.9	43.1	-	181.7
SL-MPL-IR-8	78.40	30.38	3.0	30.4	-	184.7
SL-MPL-IR-17	124.00	39.35	2.6	39.4	-	62.3
SL-MPL-IR-44	51.10	11.28	2.3	11.3	-	152.8
SL-MPL-IR-51	60.10	14.25	2.9	14.3	-	239.4
SS-5-1-MPL-1	22.90	26.93	2.7	2.3	2.18	29.5
SS-5-1-MPL-2	23.00	25.23	2.5	2.3	2.29	24.2
SS-5-1-MPL-3	23.03	24.45	2.5	2.3	2.26	12.1
SS-5-1-MPL-4	22.92	25.08	2.5	2.3	2.28	29.7
SS-5-1-MPL-5	23.05	26.37	2.6	2.3	2.22	30.3
SS-3-2-MPL-6	54.03	26.57	2.7	5.4	2.28	57.0
SS-3-3-MPL-7	54.22	28.30	2.8	5.4	2.27	50.7
SS-3-3-MPL-8	54.05	26.72	2.7	5.4	2.32	67.5
SS-3-4-MPL-9	54.08	28.07	2.8	5.4	2.31	66.0
SS-3-4-MPL-10	54.08	26.48	2.7	5.4	2.32	69.4
SS-6-2-MPL-21	67.50	25.72	2.6	6.8	2.37	89.1
SS-6-2-MPL-22	67.37	25.70	2.6	6.7	2.38	122.2
SS-6-2-MPL-23	67.38	23.47	2.4	6.7	2.36	104.4

Table A.12 Summary verification results of modified point load tests on different rock types
(continued).

Sample No.	Average Diameter, D (mm)	Average Thickness, t (mm)	t/d	D/d	Density (g/cm³)	MPL Strength, P (MPa)
SS-6-2-4-MPL-24	67.42	25.03	2.5	6.7	2.34	95.5
SS-6-2-5-MPL-25	67.43	25.08	2.5	6.7	2.39	82.8
SS-6-1-1-MPL-26	92.95	27.65	2.8	9.3	2.36	114.6
SS-6-1-2-MPL-27	92.67	26.10	2.6	9.3	2.37	114.6
SS-6-1-3-MPL-28	92.80	26.23	2.6	9.3	2.36	93.0
SS-6-1-4-MPL-29	92.63	26.57	2.7	9.3	2.37	117.1
SS-6-3-1-MPL-30	93.13	26.27	2.6	9.3	2.37	121.0

APPENDIX B

ROCK SAMPLE DESIGNATION CODING SYSTEM

MB – 34 – 3 – UN – 216

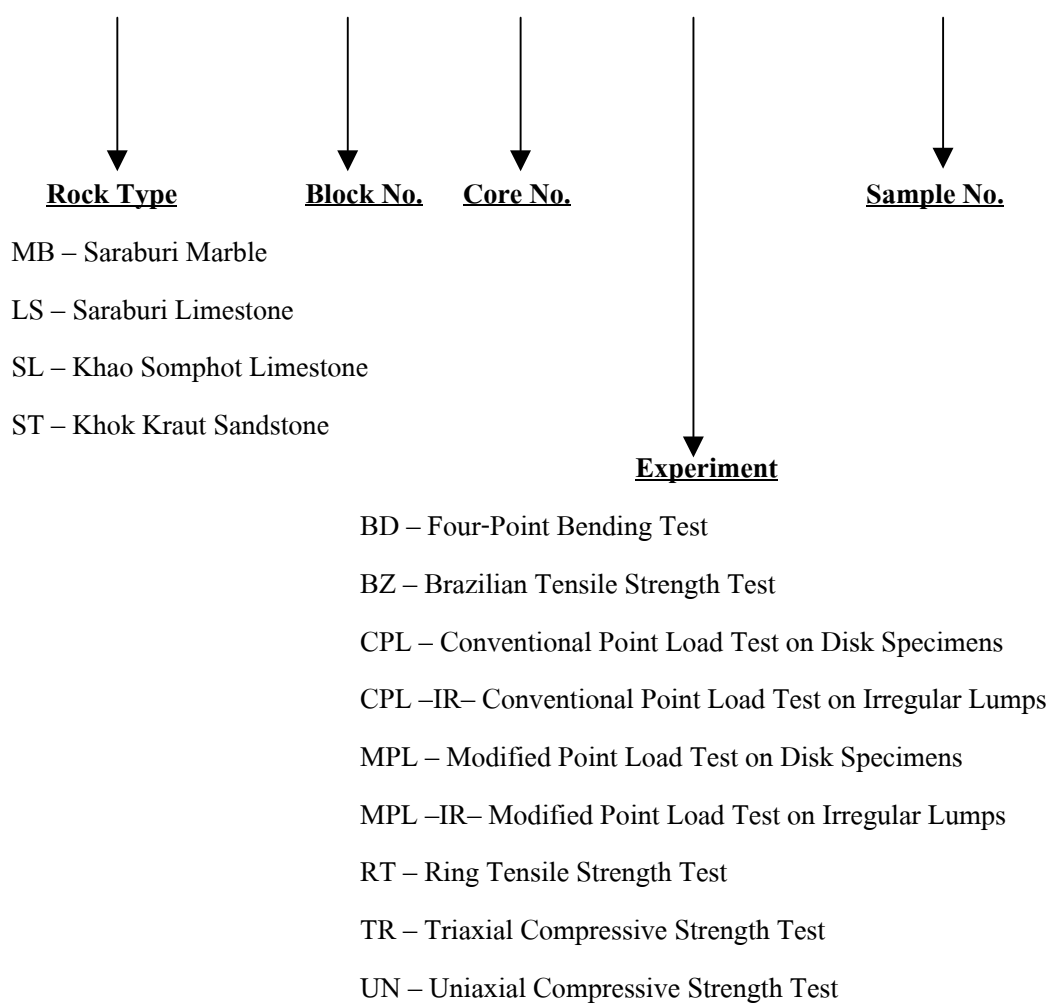


Figure B.1 Rock Sample designation coding system.

CURRICULUM VITAE

Mr. Prachya Tepnarong was born on September 14, 1978 in Kanchanaburi province, Thailand. He received his Bachelor's Degree in Engineering (Geological Engineering Program) from Suranaree University of Technology in 1999. He continued with his graduate studies in the Geological Engineering Program, Institute of Engineering, Suranaree University of Technology.